

T 1495

PREDICTION OF SURFACE SHAPES FROM
A SINGLE SEISMIC TRACE

By

Jonathan Bork

ProQuest Number: 10796027

All rights reserved

INFORMATION TO ALL USERS

The quality of this reproduction is dependent upon the quality of the copy submitted.

In the unlikely event that the author did not send a complete manuscript and there are missing pages, these will be noted. Also, if material had to be removed, a note will indicate the deletion.



ProQuest 10796027

Published by ProQuest LLC (2019). Copyright of the Dissertation is held by the Author.

All rights reserved.

This work is protected against unauthorized copying under Title 17, United States Code
Microform Edition © ProQuest LLC.

ProQuest LLC.
789 East Eisenhower Parkway
P.O. Box 1346
Ann Arbor, MI 48106 – 1346

A Thesis submitted to the Faculty and the Board of Trustees of the Colorado School of Mines in partial fulfillment of the requirements for the degree of Doctor of Philosophy.

Signed: Jonathan Bork
Jonathan Bork

Golden, Colorado

Date: 4/13, 1973

ARTHUR LAKES LIBRARY
COLORADO SCHOOL OF MINES
GOLDEN, COLORADO

Approved: J. E. White
J. E. White
Thesis Advisor

R. C. Holmer
R. C. Holmer
Head of Department

Golden, Colorado

Date: April 13, 1973

ABSTRACT

Reflected-diffracted energy from curved surfaces is numerically generated from Kirchhoff's integral formula. This diffraction integral, when put into a surface-dependent, time convolution form, is susceptible to inversion.

A single trace is used to reconstruct several three-dimensional surfaces of geologic interest in a three-stage procedure. First, the shot pulse is removed from the trace by deconvolution. Secondly, a Volterra integral equation of the first kind is solved for the apparent slopes of the surface. Finally, the numerical solution of the resulting first order differential equation completes the prediction of the surface.

Reasonable reconstructions obtained by the above method suggest that a diffraction model yields a more complete picture of the physical composition of a single trace than the classical ray-path theory.

ARTHUR LAKES LIBRARY
COLORADO SCHOOL OF MINES
GOLDEN, COLORADO

CONTENTS

	Page
ABSTRACT	iii
CONTENTS	iv
LIST OF FIGURES	vi
LIST OF TABLES	ix
ACKNOWLEDGMENTS	x
INTRODUCTION	1
MATHEMATICAL DEVELOPMENT OF THE FORWARD SOLUTION . .	6
APPLICATION OF KIRCHHOFF'S INTEGRAL FORMULA TO THREE-DIMENSIONAL MODEL STUDIES	17
A SURFACE-DEPENDENT FORM OF THE DIFFRACTION INTEGRAL	20
THE INVERSE PROCEDURE	41
Mathematical Development	41
P(t) For a Flat Plane	45
Exact Inverse For a Flat Plane	47
NUMERICAL PROCEDURE	49
Numerical Integration	49
Prediction of S	52
Introduction	52
Prediction of the First Point	55
Prediction For the General Case	58
RESULTS OF NUMERICAL PREDICTION	59
Model A--Flat Plane	61
Model B--Anticline	64
Model C--Syncline	69
Model D--Normal Fault	73
Model E--Composite	75
COMPOSITION OF P(t)	80

	Page
CONCLUSIONS	83
APPENDIX A - DERIVATION OF THE FULL-SPACE GREEN'S FUNCTION	85
APPENDIX B - DELTA FUNCTION RELATIONSHIPS	91
Case I - Two One-Dimensional Delta Functions	91
Case II - Two-Dimensional Delta Functions	92
APPENDIX C - PROOF OF THE π IDENTITY	95
APPENDIX D - DERIVATION OF HILTERMAN'S DIFFRACTION ALGORITHM	98
BIBLIOGRAPHY	102

LIST OF FIGURES

Figure	Page
1. Retarded time relationships	13
2. Schematic diagram of S'	18
3. Vector locations of the observation point, source point and the surface, S	22
4. s-y coordinate system on S	26
5. Angular relationship between \vec{R} and \vec{n}'	28
6. Intersection of spherical wave with S	31
7. Description of progressing C* and one-way time nomenclature	35
8. Trigonometric relationships of \vec{n}_s , \vec{n}' and \vec{T}	37
9. Region of integration in equation 39	44
10. Angular relationships for a flat plane	46
11. Reconstruction of S using the Modified Euler Method	53
12a. Geometry of initial prediction	54
12b. Expansion of 12a	54
13. Determination of m_1	55
14a. Estimated versus true slope for a concave surface	56
14b. Estimated versus true slope for a convex surface	56
15. Iterative improvement of x_1, z_1	57
16. Ricker wavelet	60
17. Amplitude spectrum of the Ricker wavelet	61
18. Dimensions of model A	62
19. Computed versus true $\tan_R(\alpha(t_1))$ for model A	63

Figure	Page
20. Inverse of model A	64
21. Dimensions of model B	65
22a. Synthetic trace of model B	66
22b. Deconvolved trace of model B	66
23. Computed versus true $\tan_R(\alpha(t))$ for model B . .	67
24. Inverse of model B	68
25. Dimensions of model C	69
26a. Synthetic trace of model C	70
26b. Deconvolved trace of model C	70
27. Computed versus true $\tan_R(\alpha(t_1))$ for model C . .	71
28. Inverse of model C	72
29. Dimensions of model D	73
30a. Synthetic trace of model D	74
30b. Deconvolved trace of model D	74
31. Inverse of model D	75
32. Dimensions of model E	76
33a. Synthetic trace for shot point 1	77
33b. Synthetic trace for shot point 2	77
33c. Synthetic trace for shot point 3	77
34a. Deconvolved trace for shot point 1	78
34b. Deconvolved trace for shot point 2	78
34c. Deconvolved trace for shot point 3	78
35. Inverse of model E	79
36a. Faulted surface	82

Figure	Page
36b. Surface factor-- $t^2P(t)$	82
A1. The complex path of integration.	88

LIST OF TABLES

Table	Page
1. Summary of experimental scale factors and units.	59

ACKNOWLEDGMENTS

The author extends his sincere gratitude to Dr. J. E. White for his continued guidance and critical review of the manuscript. Appreciation is also expressed to Professors John C. Hollister, George T. Meredith, John V. Kline, Richard H. DeVoto and Frank Hadsell for monitoring the progress of this work.

Financial assistance from N.D.E.A., Texaco, Mobil and C.S.M. is gratefully acknowledged.

Special thanks are due my wife, Mary, for proof-reading and typing the thesis and for her constant encouragement throught the duration of the research.

INTRODUCTION

Making geological sense from geophysical data is of primary importance to the exploration geophysicist. Problems of this type are usually classified as inverse problems. In order for the exploration seismologist to accomplish such a task a basic understanding of wave propagation and the phenomena a reflections and diffractions is clearly essential. Logically the study of these phenomena must rest ultimately on the solution of boundary value problems involving the scalar or the vector wave equations.

In boundary value problems we are concerned with finding the solution to some ordinary or partial differential equation (P.D.E.) with prescribed boundary and/or initial conditions. However, the diversity of the earth demands solutions to the vector wave equation which, unfortunately, are extremely difficult to find. Consequently, one has to resort to the simpler but still useful problem of determining the solution to the scalar wave equation in a fluid medium (acoustics problem).

The forward problem is basically a matter of determining the solution to the scalar wave equation given the properties of the medium, the boundaries within which the solution is desired, and the boundary

and initial conditions. Initial conditions may constrain the solution to satisfy initial position as well as initial velocity data. A further complication may be the inclusion of a forcing or source function distributed in both space and time, giving one an inhomogeneous equation to solve. However the solution, if found, would represent a pressure wave traveling through a fluid medium.

Interest has increased in the above problem as evidenced by the papers of Hilterman (1970), Trorey (1970), Peterson (1969), and Fontanel and Grau (1969) as well as others. Peterson (1969) has pointed out the utility of considering a seismogram as an acoustical hologram and using inverse mapping to reconstruct a down-going wave which converges on a diffracting point. In this technique a reflector is considered as a series of point diffractors, and with the use of several 12 or 24-trace records, the reflecting surface may be reconstructed on a point-by-point basis. Schneider (1971) gives a brief account of such methods.

Inverse problems differ from forward problems in that the solution to the differential equation at some or, perhaps, many locations is known a priori. One attempts, then, to determine some of the data which in the forward case was assumed as given. For example, one may try to determine some or all of the following: the forcing function,

the boundary conditions, the boundary shape, initial velocity or initial position data, or perhaps some constants in the partial differential equation. In some cases the partial differential equation itself is desired. Perdreauville and Goodson (1966), Collins and Khatri (1969), Carpenter, Wozny and Goodson (1971) and Seinfeld and Chen (1971) have discussed this problem, usually called a systems identification problem.

Inverse problems usually have an indeterminate form since the known data is rarely sufficient to solve for the unknown parameters (Roy, 1962). However, simplified geometrical considerations as well as more field data will sometimes permit a unique solution.

For the exploration seismologist the solutions to the wave equation (vector) are the collection of seismic traces. The work of the interpreter involves the inverse problem of determining the geometrical configuration of the sub-surface layers, along with certain properties of the media such as velocity, density, lithology etc. Redundancy in his field data results in the well known common-depth-point stack.

Perhaps the most familiar inverse problem in seismology is deconvolution whereby one attempts to recover the forcing function (wavelet) of the downward-traveling wave from the known seismic trace. After its determination, an attempt is made to recover the reflection

coefficients of the subsurface layers through inverse filtering. Frequently (Roy, 1962) the measured response can be put in terms of integrals; in the case of deconvolution, a convolution integral. Therefore, generally speaking, an inverse problem requires the solution of an integral equation.

Deconvolution and several other processes are based on the horizontally-layered earth model. It is well known, however, that the response of a single geophone contains information from reflectors and diffractors of a three-dimensional nature. Consequently, a more complete model of the composition of a single trace has to incorporate the curvature and lateral extent of reflecting-diffracting surfaces.

The inversion problem of this study is to recover (predict), after certain assumptions have been made, the shape of a three-dimensional surface with cylindrical symmetry from a single seismic trace. The trace will be numerically generated using Kirchhoff's integral formula (also called Kirchhoff's diffraction formula or Kirchhoff's integral representation) and an acoustical model. Since Kirchhoff's integral formula yields good synthetic results (Hilterman, 1970; Trorey, 1970), it will be used as the mathematical basis for the inverse problem.

The deterministic model of this study consists of

a point source located in a fluid medium (air) overlying a rigid half space. The boundary between the media has a shape of geologic interest. Although the boundaries are three-dimensional, they have cylindrical symmetry in a direction perpendicular to the shot line. The lone receiver is located at the shot point, and the velocity is assumed to be constant.

MATHEMATICAL DEVELOPMENT OF THE FORWARD SOLUTION

There are several avenues available for the solution of the three-dimensional, inhomogeneous, scalar wave equation. One very powerful technique is the Green's function approach, which ultimately yields a solution in terms of integrals involving:

- 1) a forcing function term integrated over space (V), where V may be all space or an enclosed volume, and also with respect to time, t ,
- 2) a term involving the initial velocity and initial position data of the medium integrated over V for $t = 0$ (or any other initial time, say \bar{t}_0), and
- 3) a boundary term integrated over the enclosing surface, S , where S encompasses V , and also with respect to time.

Green's functions are defined to be solutions to the original differential equation (including the same initial and boundary conditions) with the forcing function replaced by impulsive delta functions. The solution to the P.D.E. with an impulsive input but neglecting the boundary conditions is called the fundamental solution. It corresponds to the Green's function in a full space. If the Green's function can be determined then the solution of

the P.D.E. may be written as a combination of generalized superposition integrals.

It is useful to sketch the mathematical representation of the general (forward) solution to the three-dimensional, inhomogeneous, scalar wave equation through the use of the fundamental solution. Kirchhoff's integral formula will appear as the boundary term (number 3 above) in the final expression.

Parts of the following derivation may be found in Morse and Feshbach (1953), Jackson (1962), Good and Nelson (1971) and Duff and Naylor (1966). We start with the three-dimensional, inhomogeneous, scalar wave equation and with the identical equation with an impulsive source located at $\vec{R} = \vec{R}'$ and $t = \tau$:

$$\nabla'^2 u(\vec{R}; \tau) - \frac{1}{c^2} \frac{\partial^2 u(\vec{R}; \tau)}{\partial \tau^2} = -4\pi f(\vec{R}; \tau) \quad (1)$$

and

$$\nabla'^2 G(\vec{R}, t | \vec{R}', \tau) - \frac{1}{c^2} \frac{\partial G(\vec{R}, t | \vec{R}', \tau)}{\partial \tau^2} = -4\pi \delta(\vec{R} - \vec{R}') \delta(t - \tau) \quad (2)$$

The vector \vec{R} locates the observation point and \vec{R}' denotes the source point with $\vec{R} - \vec{R}'$ being the vector between them. The prime on the Laplacian operator denotes spatial derivatives with respect to the source variables x' , y' , z' and c denotes the velocity (a constant). The solution to (2) -- G -- denotes the fundamental solution, and t and τ stand

for the time variables at the observation point and source point, respectively. The forcing function $f(\vec{R}', \tau)$ will be considered identically zero outside V . The derivatives may be taken with respect to source variables since reciprocity exists between the source and observation variables (Morse and Feshbach, 1953). This is due to the fact that the variables occur in combinations of $\vec{R} - \vec{R}'$ and $t - \tau$, and the derivatives are taken twice (minus signs cancel).

If we multiply (1) by G and (2) by u , then subtract (2) from (1), and integrate the result over V and with respect to time, we get

$$\int_{\bar{t}_0}^{t^*} d\tau \int_{V'} \{G \nabla'^2 u - u \nabla'^2 G\} dV' - \frac{1}{c^2} \int_{\bar{t}_0}^{t^*} d\tau \int_{V'} \left\{ G \frac{\partial^2 u}{\partial \tau^2} - u \frac{\partial^2 G}{\partial \tau^2} \right\} dV' \quad (3)$$

$$= -4\pi \int_{\bar{t}_0}^{t^*} d\tau \int_{V'} \left\{ G f(\vec{R}', \tau) - \delta(\vec{R} - \vec{R}') \delta(t - \tau) u(\vec{R}', \tau) \right\} dV'$$

We have used the prime on V to indicate integration with respect to source variables. In accordance with Morse and Feshbach, the upper limit has been placed at t^* , i.e. slightly greater than t , and \bar{t}_0 indicates the initial time. After using Green's theorem on the first term, the substitution property of the delta function in the third term, and upon using the identity,

$$\left\{ G \frac{\partial^2 u}{\partial r^2} - u \frac{\partial^2 G}{\partial r^2} \right\} = \frac{\partial}{\partial r} \left\{ G \frac{\partial u}{\partial r} - u \frac{\partial G}{\partial r} \right\}$$

in the second term (with the time differentiation vanishing upon integration by τ), we get

$$\int_{\bar{t}_0}^{\tau^+} d\tau \oint_{S'} \left\{ G \frac{\partial u}{\partial n'} - u \frac{\partial G}{\partial n'} \right\} dS' - \frac{1}{c^2} \int_{V'} \left\{ G \frac{\partial u}{\partial \tau} - u \frac{\partial G}{\partial \tau} \right\} dV' \quad (4)$$

$$+ 4\pi \int_{\bar{t}_0}^{\tau^+} d\tau \int_{V'} G f dV' = 4\pi u(\vec{R}, t).$$

The integral \oint denotes an integration over the surface enclosing V and the $\partial/\partial n'$ denotes the directional derivative in the outward normal direction, i.e. $\partial u/\partial n' = \nabla u \cdot \vec{n}'$. The closed surface S is as yet unspecified.

The solution to equation 2 -- the fundamental solution, G -- is derived in Appendix A and is equal to

$$G(\vec{R}, t | \vec{R}', \tau) = \frac{c \delta(c(t-\tau) - |\vec{R} - \vec{R}'|)}{|\vec{R} - \vec{R}'|} = \frac{\delta((t-\tau) - \frac{|\vec{R} - \vec{R}'|}{c})}{|\vec{R} - \vec{R}'|}$$

where $|\vec{R} - \vec{R}'| = \sqrt{(x-x')^2 + (y-y')^2 + (z-z')^2}$ and $\delta(\)$

is the four-dimensional Dirac delta function (three space and one time variable). The c may be brought into the argument of the delta function if desired since $\delta(at) = 1/|a| \delta(t)$. G may be considered as a spherical wave emanating from \vec{R}' and emitted at time τ where $1/|\vec{R} - \vec{R}'|$ stands for spherical divergence.

Substituting G into (4) and transposing the 4π

yields

$$\begin{aligned}
 & \frac{1}{4\pi} \int_{\bar{t}_0}^{t^*} d\tau \oint_{S'} \left\{ \frac{c \delta(c(t-\tau) - |\bar{R} - \bar{R}'|)}{|\bar{R} - \bar{R}'|} \frac{\partial u}{\partial n'} - u \frac{\partial \left(\frac{c \delta(c(t-\tau) - |\bar{R} - \bar{R}'|)}{|\bar{R} - \bar{R}'|} \right)}{\partial n'} \right\} dS' \\
 & - \frac{1}{4\pi c^2} \int_{V'} \left\{ \frac{c \delta(c(t-\tau) - |\bar{R} - \bar{R}'|)}{|\bar{R} - \bar{R}'|} \frac{\partial u}{\partial \tau} - u \frac{\partial \left(\frac{c \delta(c(t-\tau) - |\bar{R} - \bar{R}'|)}{|\bar{R} - \bar{R}'|} \right)}{\partial \tau} \right\} \Bigg|_{\tau = \bar{t}_0}^{\tau = t^*} \\
 & + c \int_{\bar{t}_0}^{t^*} d\tau \int_{V'} \frac{\delta(c(t-\tau) - |\bar{R} - \bar{R}'|)}{|\bar{R} - \bar{R}'|} f(\bar{R}', \tau) dV' = u(\bar{R}, t). \quad (5)
 \end{aligned}$$

Expanding the normal derivative in term one, integrating term three with respect to τ , and recognizing that term two will be zero at the upper limit; equation (5) becomes

$$\begin{aligned}
 & \frac{1}{4\pi} \int_{\bar{t}_0}^{t^*} d\tau \oint_{S'} \left\{ \frac{\overset{(a)}{\delta(c(t-\tau) - |\bar{R} - \bar{R}'|)}}{|\bar{R} - \bar{R}'|} \frac{\partial u}{\partial n'} - \frac{\overset{(b)}{c \cdot u \partial \delta(c(t-\tau) - |\bar{R} - \bar{R}'|)}}{|\bar{R} - \bar{R}'| \partial n'} \right. \\
 & \left. - \overset{(c)}{c \cdot u \delta(c(t-\tau) - |\bar{R} - \bar{R}'|)} \frac{\partial (1/|\bar{R} - \bar{R}'|)}{\partial n'} \right\} dS' + \frac{1}{4\pi c} \int_{V'} \left\{ \frac{\overset{(d)}{\delta(c(t-\tau) - |\bar{R} - \bar{R}'|)} \frac{\partial u}{\partial \tau}}{|\bar{R} - \bar{R}'|} \right. \\
 & \left. - \frac{\overset{(e)}{u}}{|\bar{R} - \bar{R}'|} \frac{\partial \delta(c(t-\tau) - |\bar{R} - \bar{R}'|)}{\partial \tau} \right\} \Bigg|_{\tau = \bar{t}_0}^{\tau = t^*} dV' + \int_{V'} \frac{\overset{(f)}{f(\bar{R}', t - \frac{|\bar{R} - \bar{R}'|}{c})}}{|\bar{R} - \bar{R}'|} dV' \\
 & = u(\bar{R}, t). \quad (6)
 \end{aligned}$$

The normal derivative of the delta function in (6b) may be expanded through use of the chain rule

$$\begin{aligned}
 \frac{\partial \delta(c(t-\tau) - |\bar{R} - \bar{R}'|)}{\partial n'} &= \frac{\partial \delta(c(t-\tau) - |\bar{R} - \bar{R}'|)}{\partial (c(t-\tau) - |\bar{R} - \bar{R}'|)} \frac{\partial (c(t-\tau) - |\bar{R} - \bar{R}'|)}{\partial n'} \\
 &= \delta'(c(t-\tau) - |\bar{R} - \bar{R}'|) \frac{\partial (-|\bar{R} - \bar{R}'|)}{\partial n'} = -\delta'(c(t-\tau) - |\bar{R} - \bar{R}'|) \frac{\partial |\bar{R} - \bar{R}'|}{\partial n'},
 \end{aligned}$$

and upon integrating (6a) and (6c) with respect to time, we get

$$\begin{aligned} & \frac{1}{4\pi} \oint_{S'} \left\{ \frac{\partial u(\vec{R}', t - \frac{|\vec{R}-\vec{R}'|}{c})}{\partial n'} \frac{1}{|\vec{R}-\vec{R}'|} + \int_{\bar{t}_0}^{t^+} \frac{d\tau}{|\vec{R}-\vec{R}'|} \frac{c \cdot u \delta'(c(t-\tau) - |\vec{R}-\vec{R}'|)}{\partial n'} \right. \\ & \left. + \frac{u(\vec{R}', t - \frac{|\vec{R}-\vec{R}'|}{c})}{|\vec{R}-\vec{R}'|^2} \frac{\partial(|\vec{R}-\vec{R}'|)}{\partial n'} \right\} dS' + \frac{1}{4\pi c} \int_{V'} \left\{ \frac{\delta(c(t-\tau) - |\vec{R}-\vec{R}'|)}{|\vec{R}-\vec{R}'|} \frac{\partial u}{\partial \tau} \right. \\ & \left. - \frac{u}{|\vec{R}-\vec{R}'|} \frac{\partial \delta(c(t-\tau) - |\vec{R}-\vec{R}'|)}{\partial \tau} \right\} \Bigg|_{\tau=\bar{t}_0} dV' + \int_{V'} \frac{f(\vec{R}', t - \frac{|\vec{R}-\vec{R}'|}{c})}{|\vec{R}-\vec{R}'|} dV' = U(\vec{R}, t). \end{aligned} \quad (7)$$

Now since

$$\begin{aligned} \frac{\partial \delta(c(t-\tau) - |\vec{R}-\vec{R}'|)}{\partial (c(t-\tau) - |\vec{R}-\vec{R}'|)} &= \frac{\partial \delta(c(t-\tau) - |\vec{R}-\vec{R}'|)}{\partial (c(t-\tau))} = \frac{1/c \partial \delta((t-\tau) - \frac{|\vec{R}-\vec{R}'|}{c})}{c \partial (t-\tau)} \\ &= -\frac{1}{c^2} \frac{\partial \delta((t-\tau) - \frac{|\vec{R}-\vec{R}'|}{c})}{\partial \tau}, \end{aligned}$$

we can rewrite (7) as

$$\begin{aligned} & \frac{1}{4\pi} \oint_{S'} \left\{ \frac{\partial u(\vec{R}', t - \frac{|\vec{R}-\vec{R}'|}{c})}{\partial n'} \frac{1}{|\vec{R}-\vec{R}'|} + c \int_{\bar{t}_0}^{t^+} \frac{d\tau}{|\vec{R}-\vec{R}'|} \left(-\frac{1}{c^2} \frac{\partial \delta(t-\tau - \frac{|\vec{R}-\vec{R}'|}{c})}{\partial \tau} \right) \frac{\partial |\vec{R}-\vec{R}'|}{\partial n'} \right. \\ & \left. + \frac{u(\vec{R}', t - \frac{|\vec{R}-\vec{R}'|}{c})}{|\vec{R}-\vec{R}'|^2} \frac{\partial |\vec{R}-\vec{R}'|}{\partial n'} \right\} dS' + \frac{1}{4\pi c} \int_{V'} \left\{ \frac{\delta(t-\tau - \frac{|\vec{R}-\vec{R}'|}{c})}{|\vec{R}-\vec{R}'|} \frac{\partial u}{\partial \tau} \right\} \cdot c \Bigg|_{\tau=\bar{t}_0} \\ & - \frac{u}{|\vec{R}-\vec{R}'|} \frac{\partial \delta(c(t-\tau) - |\vec{R}-\vec{R}'|)}{\partial \tau} \Bigg|_{\tau=\bar{t}_0} \left. \right\} dV' + \int_{V'} \frac{f(\vec{R}', t - \frac{|\vec{R}-\vec{R}'|}{c})}{|\vec{R}-\vec{R}'|} dV' = U(\vec{R}, t). \end{aligned} \quad (8)$$

Since $\int \delta'(t) f(t) dt = -\int \delta(t) f'(t) dt$,

we can write (8) as

$$\begin{aligned}
 & \frac{1}{4\pi} \oint_S \left\{ \frac{\partial u(\vec{R}', t - \frac{|\vec{R} - \vec{R}'|}{c})}{\partial n'} \frac{1}{|\vec{R} - \vec{R}'|} + \frac{\partial u(\vec{R}', t - \frac{|\vec{R} - \vec{R}'|}{c})}{\partial \tau} \frac{1}{c|\vec{R} - \vec{R}'|} \frac{\partial |\vec{R} - \vec{R}'|}{\partial n'} \right. \\
 & \left. + \frac{u(\vec{R}', t - \frac{|\vec{R} - \vec{R}'|}{c})}{|\vec{R} - \vec{R}'|^2} \frac{\partial |\vec{R} - \vec{R}'|}{\partial n'} \right\} dS' + \frac{1}{4\pi c} \int_{V'} \left\{ \frac{\delta(t - \tau - \frac{|\vec{R} - \vec{R}'|}{c})}{|\vec{R} - \vec{R}'|} \frac{\partial u}{\partial \tau} \right\}_{\tau = \bar{t}_0} c \quad (9) \\
 & - \frac{u}{|\vec{R} - \vec{R}'|} \frac{\partial \delta(c(t - \tau) - |\vec{R} - \vec{R}'|)}{\partial \tau} \Big|_{\tau = \bar{t}_0} \Big\} dV' + \int_{V'} \frac{f(\vec{R}', t - \frac{|\vec{R} - \vec{R}'|}{c})}{|\vec{R} - \vec{R}'|} dV' \\
 & = U(\vec{R}, t).
 \end{aligned}$$

Now using $\frac{\partial \delta(c(t - \tau) - |\vec{R} - \vec{R}'|)}{\partial \tau} = - \frac{\partial \delta(c(t - \tau) - |\vec{R} - \vec{R}'|)}{\partial t}$
 in term two and since $\tau = t - |\vec{R} - \vec{R}'|/c$, then $d\tau = dt$,
 and hence we may change the τ -derivative in term one to
 a t -derivative, resulting in

$$\begin{aligned}
 & \frac{1}{4\pi} \oint_S \left\{ \frac{[\partial u / \partial n']}{|\vec{R} - \vec{R}'|} + \frac{[\partial u / \partial t]}{c|\vec{R} - \vec{R}'|} \frac{\partial |\vec{R} - \vec{R}'|}{\partial n'} + \frac{[u]}{|\vec{R} - \vec{R}'|^2} \frac{\partial |\vec{R} - \vec{R}'|}{\partial n'} \right\} dS' \\
 & + \frac{1}{4\pi c} \int_{V'} \frac{\delta(c(t - \tau) - |\vec{R} - \vec{R}'|)}{|\vec{R} - \vec{R}'|} \frac{\partial u}{\partial \tau} \Big|_{\tau = \bar{t}_0} dV' + \frac{1}{4\pi c} \frac{\partial}{\partial t} \int_{V'} \frac{\delta(c(t - \tau) - |\vec{R} - \vec{R}'|)}{|\vec{R} - \vec{R}'|} u \Big|_{\tau = \bar{t}_0} dV' \\
 & + \int_{V'} \frac{[f]}{|\vec{R} - \vec{R}'|} dV' = U(\vec{R}, t). \quad (10)
 \end{aligned}$$

The bracketed terms in (10) denote retarded expressions, which are necessary when a change in the source characteristics require a finite amount of time to travel

from the source location to the observation point. If the source function is changing with time τ and the field at the observation point is changing with time t , then assuming causality, $\tau < t$. In potential theory if the field at the observation point (denoted by \vec{R}) is called $\phi(\vec{R}, t)$ and the source function is $\psi(\vec{R}', \tau)$, we could write

$$\phi(\vec{R}, t) = \int_{Vol.} \frac{\psi(\vec{R}', \tau) dV_0}{|\vec{R} - \vec{R}'|}$$

where dV_0 indicates an integration over the source variables. However, for a point source we can write

$$\phi(\vec{R}, t) = \frac{\psi(\vec{R}', \tau)}{|\vec{R} - \vec{R}'|}.$$

Since the distance between \vec{R} and \vec{R}' is $|\vec{R} - \vec{R}'|$ and the velocity is c , the time necessary to travel from \vec{R}' to \vec{R} must be $|\vec{R} - \vec{R}'|/c$, so $t - \tau = |\vec{R} - \vec{R}'|/c$. Consequently, $\tau = t - \frac{|\vec{R} - \vec{R}'|}{c}$ (Figure 1). That is, if we record an

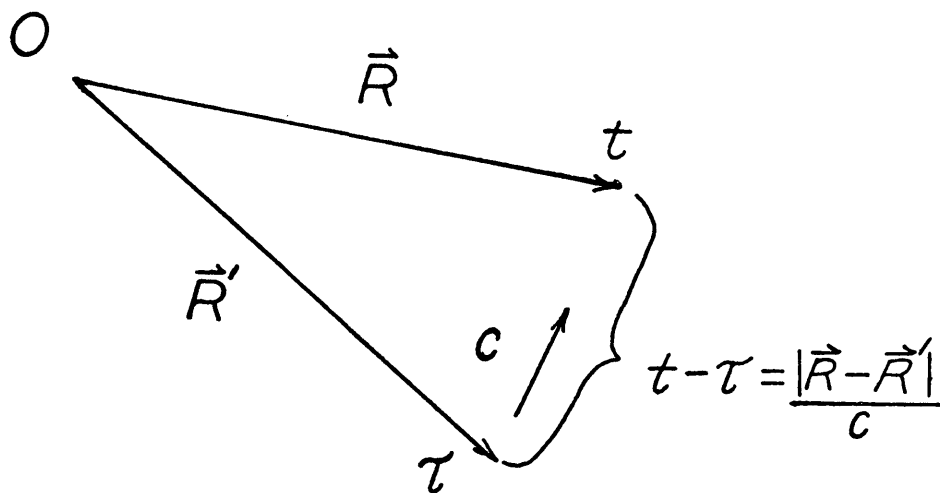


Figure 1. Retarded time relationships.

event at \vec{R} at time t , then this same event must have been at \vec{R}' at a time $t - \frac{|\vec{R} - \vec{R}'|}{c}$ earlier.

Mathematically, it is the substitution property of the delta function, when integrated over τ , that gives us the retarded argument $t - \frac{|\vec{R} - \vec{R}'|}{c}$. Hence the delta functions in the preceding expression can be viewed as a mathematical means of transporting the energy from \vec{R}' to \vec{R} . What this means in equation 10 is that if we desire the value of u at time t for some specified \vec{R} , we must add up (integrate) those portions of the potentials at times τ for various \vec{R}' 's such that the event could reach \vec{R} at time t . Generally the volume contributing to u at \vec{R} , for time t , will be a sphere centered about \vec{R}' . The final form of $u(\vec{R}, t)$ can be written as

$$\begin{aligned}
 u(\vec{R}, t) = & \int_{R=ct} \frac{[f]}{|\vec{R} - \vec{R}'|} dV_s + \frac{1}{4\pi} \int_{S'} \left\{ \frac{[\partial u / \partial n']}{|\vec{R} - \vec{R}'|} + \frac{[\partial u / \partial t]}{c|\vec{R} - \vec{R}'|} \frac{\partial |\vec{R} - \vec{R}'|}{\partial n'} \right. \\
 & \left. + \frac{[u]}{|\vec{R} - \vec{R}'|^2} \frac{\partial |\vec{R} - \vec{R}'|}{\partial n'} \right\} dS' + \frac{1}{4\pi c} \int_{R=ct} \frac{(\partial u / \partial \tau)_{\tau=\bar{t}_0}}{|\vec{R} - \vec{R}'|} dS'_s + \frac{1}{4\pi c} \frac{\partial}{\partial t} \int_{R=ct} \frac{u|_{\tau=\bar{t}_0}}{|\vec{R} - \vec{R}'|} dS'_s
 \end{aligned} \tag{11}$$

This represents the general solution to the inhomogeneous, three-dimensional, scalar wave equation. Term 11a represents the direct transmission of a spherical wave from the source to the observation point, while terms 11b, 11c, and 11d represent the boundary terms in the

solution; that is, the transmission of a wave from an excited boundary. Integrals 11e and 11f represent wave transmission to the observation point either from the medium being initially in motion (11e) or from an initial impulse applied at time $t = \bar{t}_0$ (11f).

The terms dV_S and dS_S indicate that the volume of (11a) and the areas of (11e) and (11f) belong to that of a sphere with radius ct . The integral representation (11) is not a solution to equation 1 unless the boundary conditions and initial conditions are known, and they may not be arbitrarily prescribed (Jackson, 1962). It will be a solution to equation 1 if G is the Green's function satisfying equation 2 as well as the boundary conditions and initial conditions given with equation 1.

Sometimes (11e) and (11f) are written as (Duff and Naylor, 1966)

$$\frac{1}{4\pi c} \int_{R=ct} \frac{(\partial u / \partial \tau) \Big|_{\tau=\bar{t}_0}}{|\bar{R}-\bar{R}'|} dS'_S + \frac{1}{4\pi c} \frac{\partial}{\partial t} \int_{R=ct} \frac{u \Big|_{\tau=\bar{t}_0}}{|\bar{R}-\bar{R}'|} dS'_S = t M_{ct} u_c + \frac{\partial}{\partial t} \left[t M_{ct} u \right] \quad (12)$$

where M_{ct} denotes the mean value over a sphere of radius ct of the quantity following it.

If the initial conditions are equal to zero (media initially at rest) and if the forcing function is zero (or the observation point and source point coincide), then integrals 11a, 11e, and 11f vanish and we are left

with Kirchhoff's diffraction formula,

$$u(\vec{R}, t) = \frac{1}{4\pi} \oint_{S'} \left\{ \frac{[\partial u / \partial n']}{|\vec{R} - \vec{R}'|} + \frac{[\partial u / \partial t] \partial |\vec{R} - \vec{R}'|}{c |\vec{R} - \vec{R}'| \partial n'} + \frac{[u]}{|\vec{R} - \vec{R}'|^2} \frac{\partial |\vec{R} - \vec{R}'|}{\partial n'} \right\} dS' \quad (13)$$

Kirchhoff's diffraction formula is a mathematical expression of Huygen's principle; for example, if S' were a wavefront, then (13) could be used to compute a new wavefront at a later time. The directional derivatives are directivity functions, which state that the energy that propagates from \vec{R}' (on S') to \vec{R} is modified by the cosine of the angle that $\vec{R} - \vec{R}'$ makes with the normal to S' . For example, if $\vec{R} - \vec{R}'$ is perpendicular to the normal to S' ,

$$\frac{\partial |\vec{R} - \vec{R}'|}{\partial n'} = \cos(\vec{R} - \vec{R}', \vec{n}') = \cos(0) = 1;$$

if on the other hand $\vec{R} - \vec{R}'$ is tangent to S' then

$$\frac{\partial |\vec{R} - \vec{R}'|}{\partial n'} = \cos(\vec{R} - \vec{R}', \vec{n}') = \cos(\pi/2) = 0.$$

APPLICATION OF KIRCHHOFF'S INTEGRAL FORMULA
TO THREE-DIMENSIONAL MODEL STUDIES

Since we are dealing with an acoustics problem with a rigid boundary, the $\partial u / \partial n'$ term in equation 13 will be identically zero (Morse and Feshbach, 1953). This means that the fluid flow must be tangential to S' . With this boundary condition imposed (13) becomes

$$u(\vec{R}, t) = \frac{1}{4\pi} \oint \left\{ \frac{[\partial u / \partial t]}{c|\vec{R}-\vec{R}'|} \frac{\partial |\vec{R}-\vec{R}'|}{\partial n'} + \frac{[u]}{|\vec{R}-\vec{R}'|^2} \frac{\partial |\vec{R}-\vec{R}'|}{\partial n'} \right\} dS' \quad (14)$$

This is the equation used by Hilterman (1970) to calculate synthetic seismic traces when the shape and location of S' were known, along with $[\partial u / \partial t]$ and $[u]$ on S' . Basically, this is a matter of exciting the boundary S' with a spherically expanding wave emanating from a point source. Once the boundary is excited, we can forget about the source inside S' and treat the calculation of $u(\vec{R}, t)$ strictly as a boundary term; that is, we may use (14).

This is analogous to a similar problem dealt with in optics. In this case the disturbance from a point source (or a collection of point sources) impinges upon an aperture in an opaque screen (Goodman, 1968). With an integral similar to (14) one integrates over the excitation in the aperture to yield the field on the opposite side of the

aperture. Once the aperture is excited one need not know the source function, only the value of the disturbance in the aperture.

The surface S' previously regarded as a general, closed surface must now be defined. For the purposes of calculation, S' is taken to be the reflecting-diffracting surface of interest (e.g. an anticline flanked by horizontal planes stretching to infinity) capped by a hemispherical dome; the radius of which tends toward infinity (Figure 2).

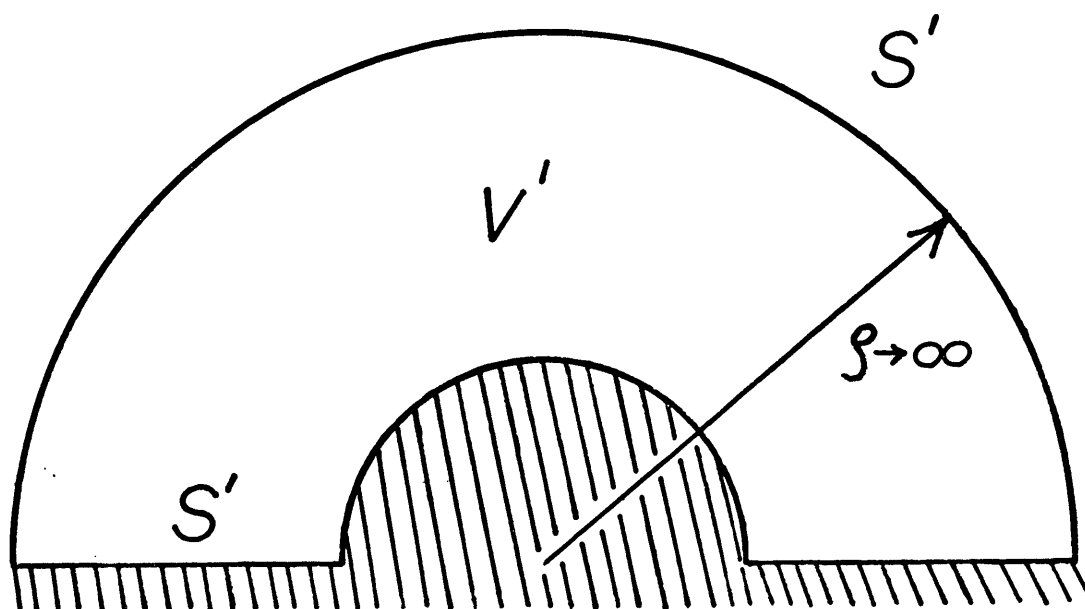


Figure 2. Schematic diagram of S' .

Normally the integration over the hemisphere is ignored as contributing nothing. This may be safely done if the disturbances (waves) in V satisfy Sommerfeld's radiation condition, i.e. if the disturbances in V vanish at least as fast as a diverging spherical wave (Goodman, 1968). For convenience the origin of the coordinate system is chosen inside S' , with the source-observation point located at the origin. Hilterman (1970) produced synthetic seismograms by exciting the surface with a spherically spreading wave sent from the observation-source point. The additional approximation is made that the pressure excitation on S' , $[u] = u_s$ may be approximated as twice the incident pressure. This is directly due to the rigid boundary.

The approximation that the pressure on S' is equal to twice the incident pressure is a good one provided any portion of S' subtends a small solid angle on any other point of S' (Hilterman, 1970). This means that for surfaces with large and rapid fluctuations the approximation breaks down due to doubly reflected-diffracted energy. Ignoring the double-reflections the results will be very good. Appendix D contains a brief account of the numerical procedure.

A SURFACE-DEPENDENT FORM OF THE DIFFRACTION INTEGRAL

To expedite the solution of the inverse problem, it is necessary to put the diffraction integral, equation 14, in a more convenient form. Several notational changes will be made as listed below:

- 1) $s(t)$ = synthetic seismic trace,
- 2) $f(t')\delta(\vec{R}-\vec{R}')$ = forcing function from a point source,
- 3) t' = source time at the point, 0
- 4) τ' = arrival time of the spherical wave at S
- 5) τ = departure time of reflected-diffracted wave at S
- 6) t = arrival time at the observation point,
- 7) \vec{R}' = source point location,
- 8) \vec{R} = arbitrary point on S, and
- 9) \vec{R}'' = observation point location.

Starting with equation 4, setting the initial conditions equal to zero, and applying the boundary condition

$$\partial u / \partial n' = 0, \text{ we get}$$

$$S(t) = -\frac{1}{4\pi} \int_{\vec{R}_0}^{\vec{R}_+} d\tau \oint_S u_s \frac{\partial G}{\partial n'} dS \quad (15)$$

where u_s is the pressure excitation on S. Using the full-space Green's function $G_1 = c \delta(c(\tau'-t') - |\vec{R}-\vec{R}'|) / |\vec{R}-\vec{R}'|$,

we can transport the energy from the source point \vec{R}' to the surface S. A direct transmission term similar to (11a) is necessary to accomplish this,

$$u_s(\vec{R}, \tau') = 2c \int_{\vec{t}_0}^{\tau'_+} dt' \int_{V'} \frac{f(t') \delta(\vec{R} - \vec{R}') \delta(c(\tau' - t') - |\vec{R} - \vec{R}'|)}{|\vec{R} - \vec{R}'|} dV', \quad (16)$$

where due to the perfect rigidity of S we have multiplied the results by two, and where $dV' = dx'dy'dz' =$ source variables. Once again \vec{t}_0 denotes the initial time and τ'_+ denotes a slightly greater time than the arrival time τ' . If we locate the source position at the origin, then

$$\begin{aligned} \vec{R}' = \vec{0} \quad \text{and (16) becomes} \\ u_s(\vec{R}, \tau') &= 2c \int_{\vec{t}_0}^{\tau'_+} f(t') dt' \int_V \frac{\delta(\vec{R}') \delta(c(\tau' - t') - |\vec{R} - \vec{R}'|)}{|\vec{R} - \vec{R}'|} dV' \\ &= 2c \int_{\vec{t}_0}^{\tau'_+} \frac{f(t') \delta(c(\tau' - t') - |\vec{R}|)}{|\vec{R}|} dt'. \end{aligned} \quad (17)$$

Substitution into (15) yields

$$s(t) = \frac{-c}{2\pi} \int_{\vec{t}_0}^{\tau'_+} d\tau \oint_S \left[\int_{\vec{t}_0}^{\tau'_+} \frac{f(t') \delta(c(\tau' - t') - R)}{R} \right] \frac{\partial G}{\partial n'} dS \quad (18)$$

where $R = |\vec{R}|$.

Selection of $G = \frac{c \delta(c(t - \tau) - |\vec{R}'' - \vec{R}'|)}{|\vec{R}'' - \vec{R}'|}$ will trans-

port the energy from S back to the observation point so that (18) becomes

$$S(t) = \frac{-c}{2\pi} \int_{\underline{t}_0}^{\tau_+} d\tau \int_S \left\{ \int_{\underline{t}_0}^{\tau_+} \frac{f(t') \delta(c|\tau-t'-R)}{R} dt' \right\}. \quad (19)$$

$$\frac{\partial}{\partial n'} \left(\frac{c \delta(c(t-\tau) - |\vec{R}'' - \vec{R}|)}{|\vec{R}'' - \vec{R}|} \right) dS.$$

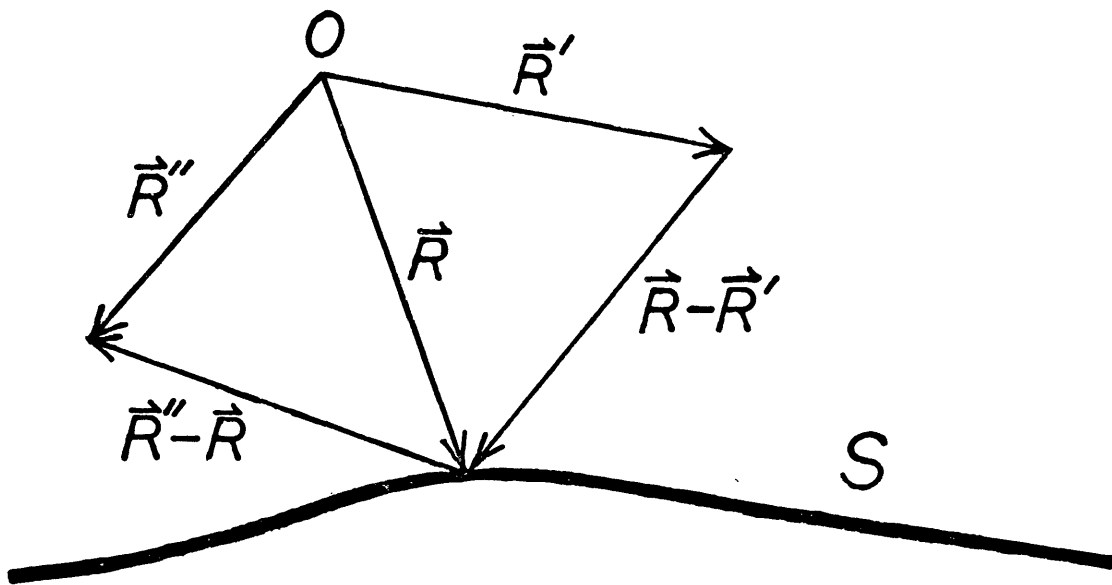


Figure 3. Vector locations of the observation point, source point and the surface, S.

Here S will no longer stand for a closed surface for the reasons discussed on p. 19. If we set the observation point \vec{R}'' at the origin, 0, then $|\vec{R}'' - \vec{R}| = R$. Expanding the normal derivative in (19) we get

$$\begin{aligned}
 S(t) &= \frac{-c^2}{2\pi} \int_{\vec{t}_0}^{t_+} d\tau \int_S \left\{ \int_{\vec{t}_0}^{\tau'} \frac{f(t') \delta(c(\tau - t') - R)}{R} \right\} \left\{ \delta(c(t - \tau) - R) \frac{\partial(1/R)}{\partial n'} \right. \\
 &+ \left. \frac{1}{R} \frac{\partial \delta(c(t - \tau) - R)}{\partial n'} \right\} dS = \frac{c^2}{2\pi} \int_{\vec{t}_0}^{t_+} d\tau \int_S \left\{ \int_{\vec{t}_0}^{\tau'} \frac{f(t') \delta(c(\tau - t') - R)}{R} dt' \right\} \\
 &\cdot \frac{\delta(c(t - \tau) - R)}{R^2} \frac{\partial R}{\partial n'} dS - \frac{c^2}{2\pi} \int_{\vec{t}_0}^{t_+} d\tau \int_S \left\{ \int_{\vec{t}_0}^{\tau'} \frac{f(t') \delta(c(\tau - t') - R)}{R} dt' \right\} \\
 &\cdot \frac{1}{R} \frac{\partial \delta(c(t - \tau) - R)}{\partial n'} dS. \tag{20}
 \end{aligned}$$

Upon using the chain rule

$$\frac{\partial \delta(c(t - \tau) - R)}{\partial n'} = \frac{\partial \delta(c(t - \tau) - R)}{\partial (c(t - \tau) - R)} \frac{\partial (c(t - \tau) - R)}{\partial n'} = - \int' (c(t - \tau) - R) \frac{\partial R}{\partial n'}$$

in the second term, noting that $\tau' = \tau$ (arrival time and departure time at S are the same), and interchanging time integrations in both terms, we arrive at

$$\begin{aligned}
S(t) = & \frac{c^2}{2\pi} \int_{\bar{t}_0}^{\bar{t}_+} f(t') dt' \int_S \frac{1}{R^3} \frac{\partial R}{\partial n'} dS \int_{\bar{t}_0}^{\bar{t}_+} \delta(c(\tau-t')-R) \delta(c(t-\tau)-R) d\tau \\
& + \frac{c^2}{2\pi} \int_{\bar{t}_0}^{\bar{t}_+} f(t') dt' \int_S \frac{1}{R^2} \frac{\partial R}{\partial n'} dS \int_{\bar{t}_0}^{\bar{t}_+} \delta(c(\tau-t')-R) \delta'(c(t-\tau)-R) d\tau. \quad (21)
\end{aligned}$$

Only when the arguments of the delta functions are simultaneously zero will the last integral in term one have a meaning. Solving the system of linear equations

$$\begin{cases} c\bar{t} - ct' - R = 0 \\ -c\bar{t} + ct - R = 0 \end{cases} \quad \text{simultaneously, we get}$$

$c(t - t') - 2R = 0$, and consequently (21) becomes

$$\begin{aligned}
S(t) = & \frac{c}{2\pi} \int_{\bar{t}_0}^{\bar{t}_+} f(t') dt' \int_S \frac{\delta(c(t-t')-2R)}{R^3} \frac{\partial R}{\partial n'} dS \\
& + \frac{c^2}{2\pi} \int_{\bar{t}_0}^{\bar{t}_+} f(t') dt' \int_S \frac{1}{R^2} \frac{\partial R}{\partial n'} dS \int_{\bar{t}_0}^{\bar{t}_+} \delta(c(\tau-t')-R) \delta'(c(t-\tau)-R) d\tau. \quad (22)
\end{aligned}$$

An additional c appears in the denominator of term one from a delta function relationship which is derived in Appendix B. Since

$$\frac{\partial \delta(c(t-\tau)-R)}{\partial t} = \frac{\partial \delta(c(t-\tau)-R)}{\partial (c(t-\tau)-R)} \frac{\partial (c(t-\tau)-R)}{\partial t}$$

$$= c \delta'(c(t-\tau)-R)$$

then

$$\delta'(c(t-\tau)-R) = \frac{1}{c} \frac{\partial \delta(c(t-\tau)-R)}{\partial t}.$$

Therefore, since the last integral in (22) is integrated with respect to \mathcal{V} , we may bring the t -differentiation outside the integral, yielding the two delta functions encountered in equation 21. Performing this operation yields

$$s(t) = \frac{c}{2\pi} \int_{\tau_0}^{\tau_+} f(t') dt' \int_S \frac{\delta(c(t-t')-2R)}{R^3} \frac{\partial R}{\partial n'} dS$$

$$+ \frac{1}{2\pi} \int_{\tau_0}^{\tau_+} f(t') dt' \frac{\partial}{\partial t} \int_S \frac{\delta(c(t-t')-2R)}{R^2} \frac{\partial R}{\partial n'} dS,$$

and noting that the t -derivative in the last term may also be taken with respect to $(t-t')$, we obtain

$$s(t) = \frac{c}{2\pi} \int_{\tau_0}^{\tau_+} f(t') dt' \int_S \frac{\delta(c(t-t')-2R)}{R^3} \frac{\partial R}{\partial n'} dS$$

$$+ \frac{1}{2\pi} \int_{\tau_0}^{\tau_+} f(t') dt' \frac{d}{d(t-t')} \int_S \frac{\delta(c(t-t')-2R)}{R^2} \frac{\partial R}{\partial n'} dS. \quad (23)$$

At this point it is useful to make a coordinate transformation. In general a surface may be represented parametrically through the use of two variables, w and v , by $x = x(w,v)$, $y = y(w,v)$ and $z = z(w,v)$, or in vectorial form by $\vec{R} = \vec{R}(w,v) = x(w,v)\vec{i} + y(w,v)\vec{j} + z(w,v)\vec{k}$.

As w and v vary, \vec{R} will generate the surface. In this problem, however, the surface S is assumed to have cylindrical symmetry parallel to the y -axis, and hence S takes on the simpler form, $\vec{R} = \vec{R}(w,v) = x(w)\vec{i} + y\vec{j} + z(w)\vec{k}$. Allowing $w = s =$ arc length along a cross section of S cut by the $y = 0$ plane, we get

$$\vec{R} = \vec{R}(s,y) = x(s)\vec{i} + y\vec{j} + z(s)\vec{k} \quad (24)$$

which is the vectorial representation of S . The $s = 0$ point on Γ is defined to be the initial point of contact of the spherical wavefront with S . In Figure 4 the s - y coordinate system on S is indicated. If $x(s)$ and $z(s)$ could be determined, the inverse problem would be solved.

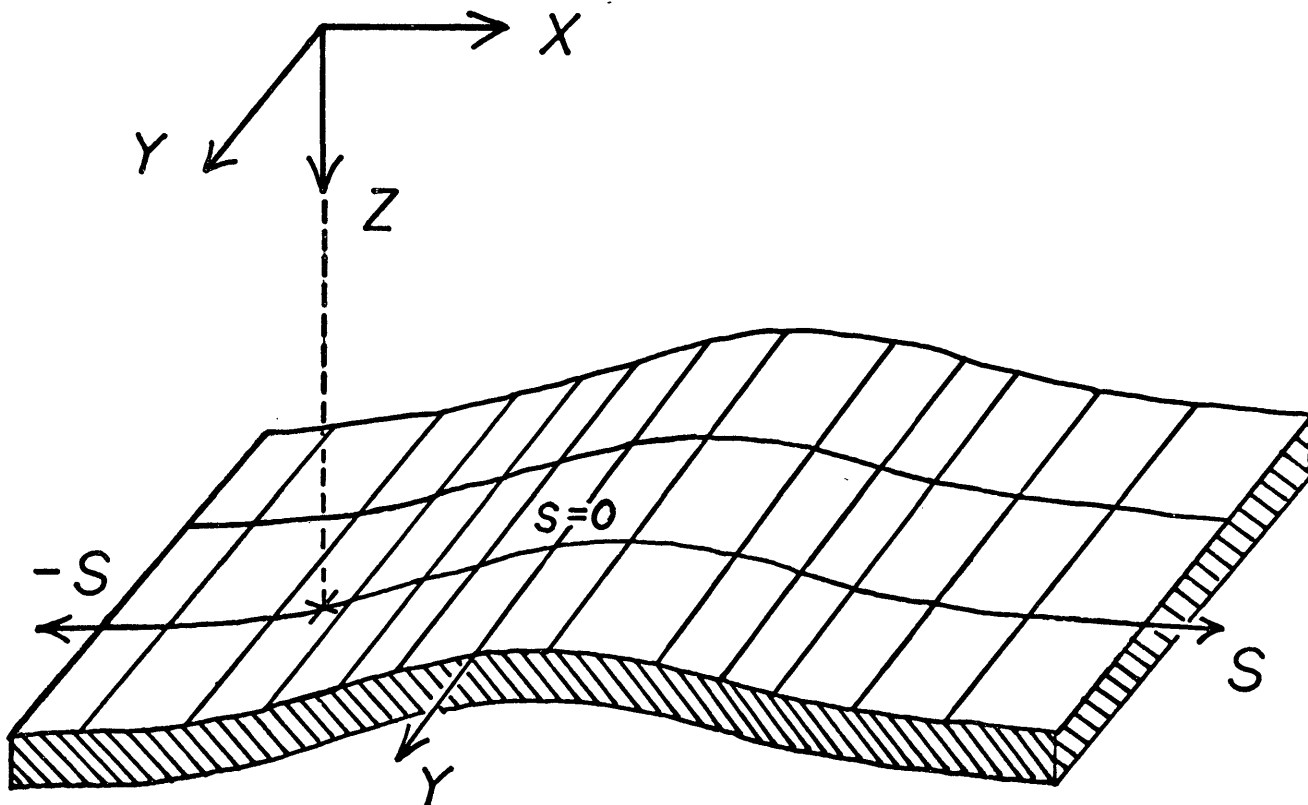


Figure 4. s - y coordinate system on S .

Using the parametric representation for S we can now transform equation 23 to

$$\begin{aligned}
 s(t) = & \frac{c}{2\pi} \int_{\frac{t_0}{c}}^{t_+} f(t') dt' \int_S \frac{\delta(c(t-t') - 2\sqrt{x^2(s)+y^2+z^2(s)})}{[x^2(s)+y^2+z^2(s)]^{3/2}} \frac{\partial R(s,y)}{\partial n'} \sqrt{EG-F^2} ds dy \\
 & + \frac{1}{2\pi} \int_{\frac{t_0}{c}}^{t_+} f(t') dt' \frac{d}{d(t-t')} \int_S \frac{\delta(c(t-t') - 2\sqrt{x^2(s)+y^2+z^2(s)})}{[x^2(s)+y^2+z^2(s)]} \frac{\partial R(s,y)}{\partial n'} \sqrt{EG-F^2} ds dy \quad (24)
 \end{aligned}$$

where $\sqrt{EG-F^2}$ is the Jacobian of the transformation

(Kaplan, 1959). More explicitly,

$$E = \left(\frac{\partial x}{\partial s}\right)^2 + \left(\frac{\partial y}{\partial s}\right)^2 + \left(\frac{\partial z}{\partial s}\right)^2,$$

$$F = \frac{\partial x}{\partial s} \frac{\partial x}{\partial y} + \frac{\partial y}{\partial s} \frac{\partial y}{\partial y} + \frac{\partial z}{\partial s} \frac{\partial z}{\partial y} \text{ and}$$

$$G = \left(\frac{\partial x}{\partial y}\right)^2 + \left(\frac{\partial y}{\partial y}\right)^2 + \left(\frac{\partial z}{\partial y}\right)^2.$$

Consequently,

$$E = x'(s) + 0 + z'(s) = 1$$

$$F = x'(s) \cdot 0 + 0 \cdot 1 + z'(s) \cdot 0 = 0$$

$$G = 0 + 1 + 0 = 1 \text{ or } \sqrt{EG-F^2} = 1.$$

E is equal to 1 because $ds = \sqrt{dx^2 + dy^2}$ or $1 = \sqrt{[x'(s)]^2 + [z'(s)]^2}$.

The $\frac{\partial R(s,y)}{\partial n'}$ term is just $\nabla R \cdot \vec{n}'$, and from

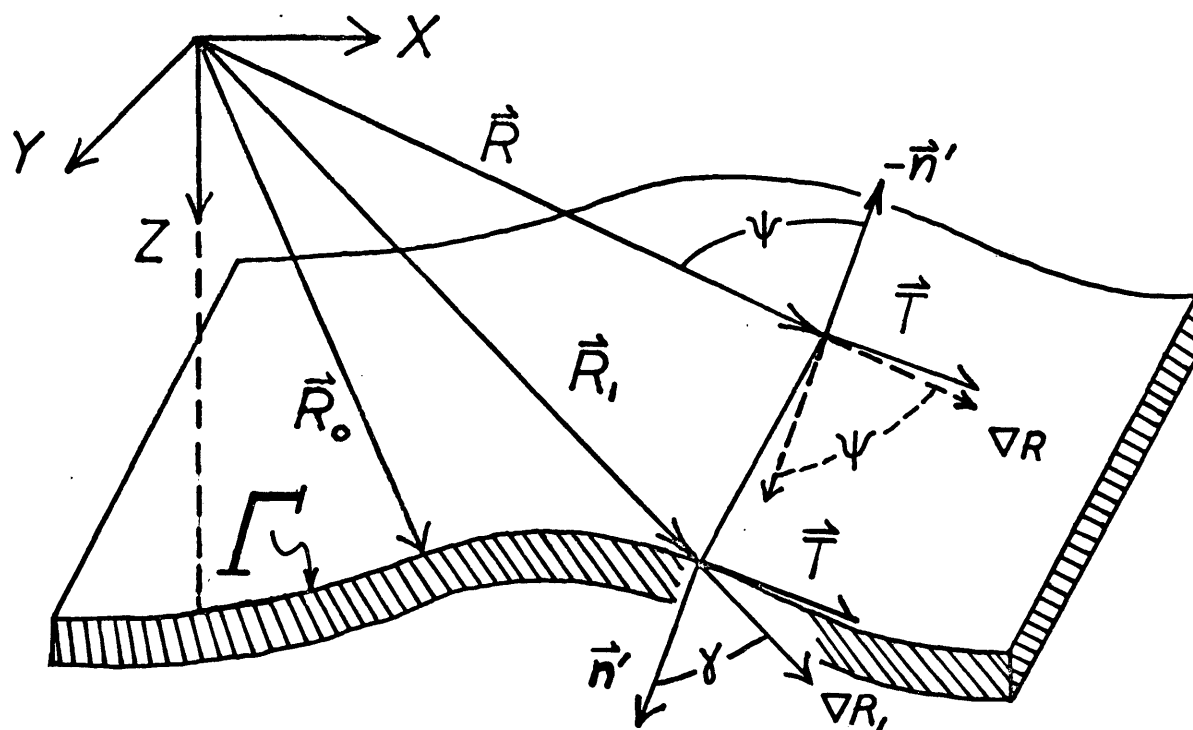


Figure 5. Angular relationship between ∇R and \vec{n}' .

Figure 5 we can see that $\nabla R \cdot \vec{n}' = \cos \psi$. The vector \vec{n}' , the unit normal vector to S , may be derived from the unit tangent vector to \int^2 — $\vec{T} = \frac{dx}{ds} \vec{i} + \frac{dz}{ds} \vec{k}$, or

$$\vec{n}' = \vec{T} \times \vec{j} = [x'(s)\vec{i} + z'(s)\vec{k}] \times \vec{j} = -z'(s)\vec{i} + x'(s)\vec{k}.$$

Since

$$\nabla R = \frac{\vec{R}}{|\vec{R}|} = \frac{x(s)\vec{i} + y\vec{j} + z(s)\vec{k}}{\sqrt{x^2(s) + y^2 + z^2(s)}}$$

then combining the above relationships we get

$$\frac{\partial R}{\partial n'} = \nabla R \cdot \vec{n}' = \frac{(x(s)\vec{i} + y\vec{j} + z(s)\vec{k}) \cdot (-z'(s)\vec{i} + x'(s)\vec{k})}{\sqrt{x^2(s) + y^2 + z^2(s)}}$$

or

$$\frac{\partial R}{\partial n'} = \frac{x'(s)z(s) - z'(s)x(s)}{\sqrt{x^2(s) + y^2 + z^2(s)}}.$$

Note that \vec{n}' is independent of y as would be expected from the symmetry assumed for S . Using this expression, (24)

can be written as

$$s(t) = \frac{c}{2\pi} \int_{\bar{t}_0}^{\bar{t}_+} f(t') dt' \int_{D_{sy}} \frac{\delta(c(t-t') - 2\sqrt{x^2(s) + y^2 + z^2(s)}) [x'(s)z(s) - z'(s)x(s)]}{[x^2(s) + y^2 + z^2(s)]^2} ds dy$$

(25)

$$+ \frac{1}{2\pi} \int_{\bar{t}_0}^{\bar{t}_+} f(t') dt' \frac{d}{d(t-t')} \int_{D_{sy}} \frac{\delta(c(t-t') - 2\sqrt{x^2(s) + y^2 + z^2(s)}) [x'(s)z(s) - z'(s)x(s)]}{[x^2(s) + y^2 + z^2(s)]^{3/2}} ds dy.$$

The arguments of the delta functions in (25) are functions of two variables s and y (t and t' are assumed as constants here). In Appendix B the general method of dealing with two-dimensional delta functions with functions as arguments is derived. Here we will simply say that in general

$$\iint_{D_{sy}} \delta(\alpha(s,y)) f(s,y) ds dy = \int_{C^*} \frac{f(s,y) dC^*}{\sqrt{\alpha_s^2 + \alpha_y^2}}$$

where α_s and α_y stand for $\frac{\partial \alpha}{\partial s}$ and $\frac{\partial \alpha}{\partial y}$.

C^* is a contour on the $s - y$ plane defined by $\alpha(s,y) = 0$ (Papoulis, 1968). The above line integral may be trans-

formed into a definite integral by solving $\alpha(s, y) = 0$ for $y = y(s)$, which yields

$$\int_{C^*} \frac{f(s, y) dc^*}{\sqrt{\alpha_s^2 + \alpha_y^2}} = \int_{s_0}^{s_1} \frac{f(s, y(s)) ds}{|\alpha_y|_{y=y(s)}}.$$

In equation 25, $\alpha(s, y)$ corresponds to

$$c(t-t') - 2\sqrt{x^2(s) + y^2 + z^2(s)} = 0$$

which in turn represents the intersection of the spherical wave (centered about the origin) with the surface S.

Solving the above equation for y yields

$$y = y(s) = \pm \sqrt{\frac{c^2(t-t')^2}{4} - x^2(s) - z^2(s)}$$

where the \pm indicates that C^* , represented by $y(s)$, is a symmetric contour about Γ^2 (Figure 6).

We can now evaluate $|\alpha_y|_{y=y(s)}$ as

$$\begin{aligned} \frac{\partial (2\sqrt{x^2(s) + y^2 + z^2(s)} - c(t-t'))}{\partial y} \Big|_{y=y(s)} &= \frac{2y}{[x^2(s) + y^2 + z^2(s)]^{1/2}} \Big|_{y=y(s)} \\ &= 2 \frac{\sqrt{\frac{c^2(t-t')^2}{4} - x^2(s) - z^2(s)}}{\left[x^2(s) + \frac{c^2(t-t')^2}{4} - x^2(s) - z^2(s) + z^2(s) \right]^{1/2}} = \frac{4\sqrt{\frac{c^2(t-t')^2}{4} - x^2(s) - z^2(s)}}{c(t-t')} \end{aligned}$$

and after carrying through all of the above steps, (25)

becomes

$$\begin{aligned} S(t) &= \frac{c}{2\pi} \int_{\tilde{t}_0}^{\tilde{t}_+} f(t') dt' \int_{D_S} \frac{[X'(s)Z(s) - Z'(s)X(s)] c(t-t') ds}{\left[x^2(s) + \frac{c^2(t-t')^2}{4} - x^2(s) - z^2(s) + z^2(s) \right]^{3/2}} \\ &= \frac{1}{\left[4\sqrt{\frac{c^2(t-t')^2}{4} - x^2(s) - z^2(s)} \right]} + \frac{1}{2\pi} \int_{\tilde{t}_0}^{\tilde{t}_+} f(t') dt' \int_{D_S} \frac{[X'(s)Z(s) - Z'(s)X(s)] c(t-t') ds}{\left[x^2(s) + \frac{c^2(t-t')^2}{4} - x^2(s) - z^2(s) + z^2(s) \right]^{3/2} \left[4\sqrt{\frac{c^2(t-t')^2}{4} - x^2(s) - z^2(s)} \right]} \end{aligned} \quad (26)$$

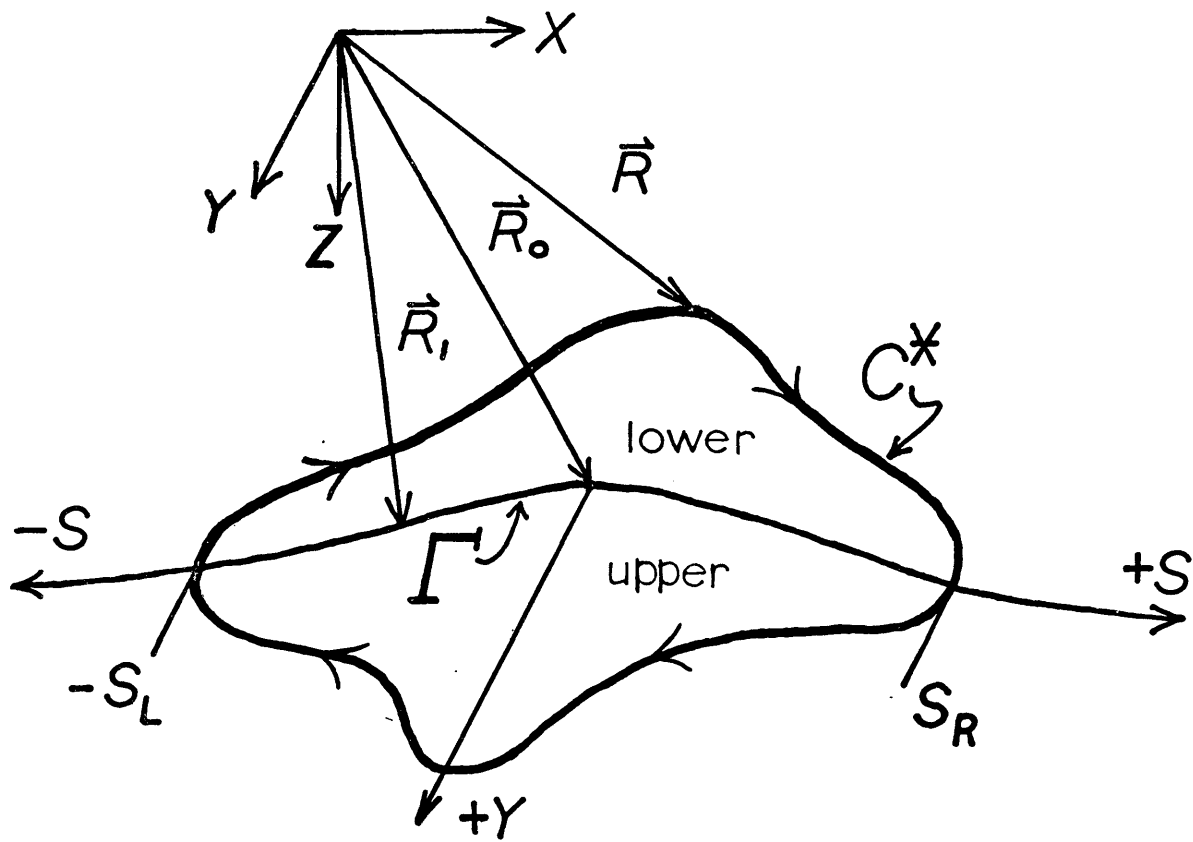


Figure 6. Intersection of spherical wave with S .

In (25) D_s denotes an interval on the s -axis.

Conventionally a closed line integral is integrated in a clockwise manner, and if transformed parametrically to a definite integral, the integration proceeds in the direction of the increasing parameter. From Figure 6 we can see that the positive y -axis points out of the page, and hence the right-hand sy -coordinate system must be viewed from below S . Consequently, the direction of integration around C^* appears as a clockwise direction when viewed from above S . Denoting the left and right-hand limits of s as $-s_L$ and s_R respectively and observing that a change in the direction of integration introduces a -1 multiplier, we can rewrite (26) as

$$\begin{aligned}
 s(t) &= \frac{-c}{2\pi} \int_{\bar{t}_0}^{\bar{t}_+} () dt' \underbrace{\int_{s_R}^{-s_L} () ds}_{\text{upper}} + \frac{c}{2\pi} \int_{\bar{t}_0}^{\bar{t}_+} () dt' \underbrace{\int_{-s_L}^{s_R} () ds}_{\text{lower}} \\
 &= -\frac{1}{2\pi} \int_{\bar{t}_0}^{\bar{t}_+} () dt' \underbrace{\frac{d}{d(t-t')} \int_{s_R}^{-s_L} () ds}_{\text{upper}} + \frac{1}{2\pi} \int_{\bar{t}_0}^{\bar{t}_+} () dt' \underbrace{\frac{d}{d(t-t')} \int_{-s_L}^{s_R} () ds}_{\text{lower}}.
 \end{aligned}$$

Exchanging limits on the negative terms and adding like expressions, as well as carrying the algebra through in (26), we get

$$s(t) = \frac{4c}{\pi} \int_{\bar{t}_0}^{\bar{t}_+} f(t') dt' \int_{-s_L}^{s_R} \frac{[X'(s)Z(s) - Z'(s)X(s)] ds}{c^3 (t-t')^3 \sqrt{\frac{c^2(t-t')^2}{4} - X^2(s) - Z^2(s)}} \\ + \frac{2}{\pi} \int_{\bar{t}_0}^{\bar{t}_+} f(t') dt' \frac{d}{d(t-t')} \int_{-s_L}^{s_R} \frac{[X'(s)Z(s) - Z'(s)X(s)] ds}{c^2 (t-t')^2 \sqrt{\frac{c^2(t-t')^2}{4} - X^2(s) - Z^2(s)}}$$

or

$$s(t) = \frac{4}{c^2 \pi} \int_{\bar{t}_0}^{\bar{t}_+} \frac{f(t') dt'}{(t-t')^3} \int_{-s_L}^{s_R} \frac{[X'(s)Z(s) - Z'(s)X(s)] ds}{\sqrt{\frac{c^2(t-t')^2}{4} - X^2(s) - Z^2(s)}} \\ + \frac{2}{c^2 \pi} \int_{\bar{t}_0}^{\bar{t}_+} f(t') dt' \frac{d}{d(t-t')} \left\{ \frac{1}{(t-t')^2} \int_{-s_L}^{s_R} \frac{[X'(s)Z(s) - Z'(s)X(s)] ds}{\sqrt{\frac{c^2(t-t')^2}{4} - X^2(s) - Z^2(s)}} \right\}. \quad (27)$$

Equation 27 may be further reduced by making a change of variables from s to t_1 . This is accomplished by allowing $x^2(s) + z^2(s) = R_1^2 = c^2 t_1^2$ where \vec{R}_1 is the position vector to any point on $\sqrt{\quad}$ (Figure 6). By taking the differential of this equation,

$$[X(s)X'(s) + Z(s)Z'(s)] ds = c^2 t_1 dt_1,$$

we may solve for ds in terms of t_1 and dt_1

$$ds = \frac{c^2 t_1 dt_1}{[X(s)X'(s) + Z(s)Z'(s)]}. \quad (28)$$

The initial point of contact with S is denoted by R_0 and as t_1 increases, R_1 will proceed along $\sqrt{\quad}$ in the negative and positive direction. Consequently, the R.H.S. (right hand side) of (28) will be negative for $s < 0$ and positive for $s > 0$. Each of the integrals of the form $\int_{-s_L}^{s_R}$ may be separated into the

form $-\int_0^{-s_L} + \int_0^{s_R}$. Making the above changes in (28),

we get

$$S(t) = \frac{4}{c^2 \pi} \int_{\frac{t_0}{c}}^{z_+} \frac{f(t') dt'}{(t-t')^3} \left\{ -\int_0^{-s_L} () ds + \int_0^{s_R} () ds \right\}$$

$$+ \frac{2}{c^2 \pi} \int_{\frac{t_0}{c}}^{z_+} f(t') dt' \frac{d}{d(t-t')} \left\{ \frac{1}{(t-t')^2} \left[-\int_0^{-s_L} () ds + \int_0^{s_R} () ds \right] \right\}$$

or

$$S(t) = \frac{4}{\pi} \int_{\frac{t_0}{c}}^{z_+} \frac{f(t') dt'}{(t-t')^3} \int_{\frac{t_0}{c}}^{\frac{(t-t')}{2}} \frac{t_1}{\sqrt{\frac{c^2(t-t')^2}{4} - c^2 t_1^2}} \left\{ \left(\frac{X'(s)Z(s) - X(s)Z'(s)}{X(s)X'(s) + Z(s)Z'(s)} \right) \Big|_{s=s(t_1)}^R \right.$$

$$\left. + \left(\frac{X'(s)Z(s) - X(s)Z'(s)}{X(s)X'(s) + Z(s)Z'(s)} \right) \Big|_{s=s(t_1)}^L \right\} dt_1 + \frac{2}{\pi} \int_{\frac{t_0}{c}}^{z_+} f(t') dt' \frac{d}{d(t-t')} \quad (29)$$

$$\cdot \left\{ \frac{1}{(t-t')^2} \int_{\frac{t_0}{c}}^{\frac{(t-t')}{2}} \frac{t_1}{\sqrt{\frac{c^2(t-t')^2}{4} - c^2 t_1^2}} \left[\left(\frac{X'(s)Z(s) - X(s)Z'(s)}{X(s)X'(s) + Z(s)Z'(s)} \right) \Big|_{s=s(t_1)}^R + \right.$$

$$\left. \left. \left(\frac{X'(s)Z(s) - X(s)Z'(s)}{X(s)X'(s) + Z(s)Z'(s)} \right) \Big|_{s=s(t_1)}^L \right] \right\} dt_1.$$

The one-way time variable, t , ranges between t_0 , the time of the initial contact with S, and $\frac{(t-t')}{2}$, the one-way time to C^* . However, t , cannot differentiate between the left-and right-hand side of $\sqrt{\quad}$; hence, both terms must be included in (29) as indicated by the R and L superscripts.

The upper limit in (29) is a variable, and as it increases the contours C^* will progress outwardly in all directions from the initial point of contact, $s = 0$ (Figure 7).

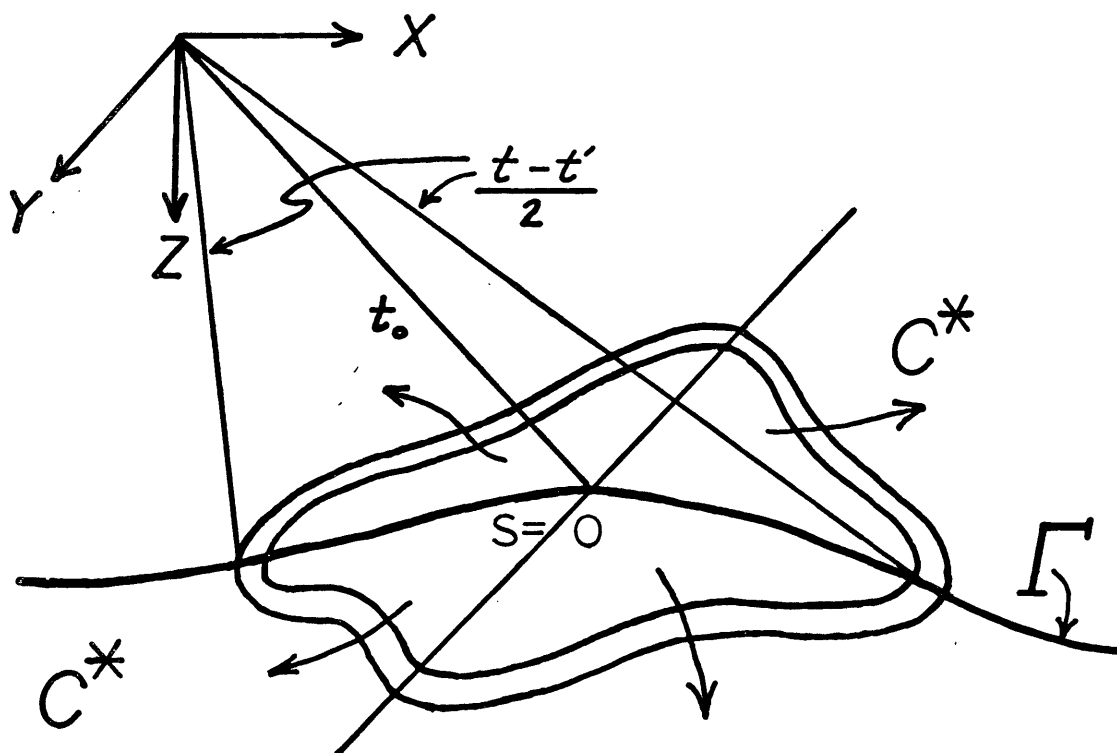


Figure 7. Description of progressing C^* and one-way time nomenclature.

From the definitions of \vec{n}' and \vec{T} on p. 28 we can see that $x'(s)z(s) - x(s)z'(s) = R\vec{n}' \cdot \vec{n}_s$ where \vec{n}_s is the unit vector perpendicular to the spherical wavefront and R is the radius of the sphere. Also, we have

$$x(s)x'(s) + z(s)z'(s) = R\vec{T} \cdot \vec{n}_s;$$

so from (29) and Figure 8, we get

$$\begin{aligned} \left. \frac{x'(s)z(s) - x(s)z'(s)}{x(s)x'(s) + z(s)z'(s)} \right|_R &= \left. \frac{R\vec{n}' \cdot \vec{n}_s}{R\vec{T} \cdot \vec{n}_s} \right|_R = \left. \frac{\vec{n}' \cdot \vec{n}_s}{\vec{T} \cdot \vec{n}_s} \right|_R = \left. \frac{\cos \gamma}{\cos \alpha} \right|_R \\ &= \left. \frac{\cos(\frac{3\pi}{2} + \alpha)}{\cos \alpha} \right|_R = \left. \frac{\sin \alpha}{\cos \alpha} \right|_R = \tan_R \alpha, \end{aligned} \quad (30)$$

and similarly for the left side

$$\begin{aligned} \left. \frac{x'(s)z(s) - x(s)z'(s)}{x(s)x'(s) + z(s)z'(s)} \right|_L &= \left. \frac{\vec{n}' \cdot \vec{n}_s}{\vec{T} \cdot \vec{n}_s} \right|_L = \left. \frac{\cos \gamma}{\cos \alpha} \right|_L = \left. \frac{\sin \alpha_c}{-\cos \alpha_c} \right|_L \\ &= -\tan_L \alpha_c. \end{aligned}$$

However, since the negative sign in the trigonometric identity for the L.H.S. of \int has already been incorporated through expression 28, (29) becomes

$$\begin{aligned} S(t) &= \frac{4}{\pi c} \int_{t_0}^{z_+} \frac{f(t') dt'}{(t-t')^3} \int_{t_0}^{\frac{(t-t')}{2}} \frac{t_1 [\tan_R \alpha(t_1) + \tan_L \alpha_c(t_1)] dt_1}{\sqrt{(t-t')^2 - t_1^2}} \\ &+ \frac{2}{\pi c} \int_{t_0}^{z_+} f(t') dt' \frac{d}{d(t-t')} \left\{ \frac{1}{(t-t')^2} \int_{t_0}^{\frac{(t-t')}{2}} \frac{t_1 [\tan_R \alpha(t_1) + \tan_L \alpha_c(t_1)] dt_1}{\sqrt{(t-t')^2 - t_1^2}} \right\}. \end{aligned} \quad (31)$$

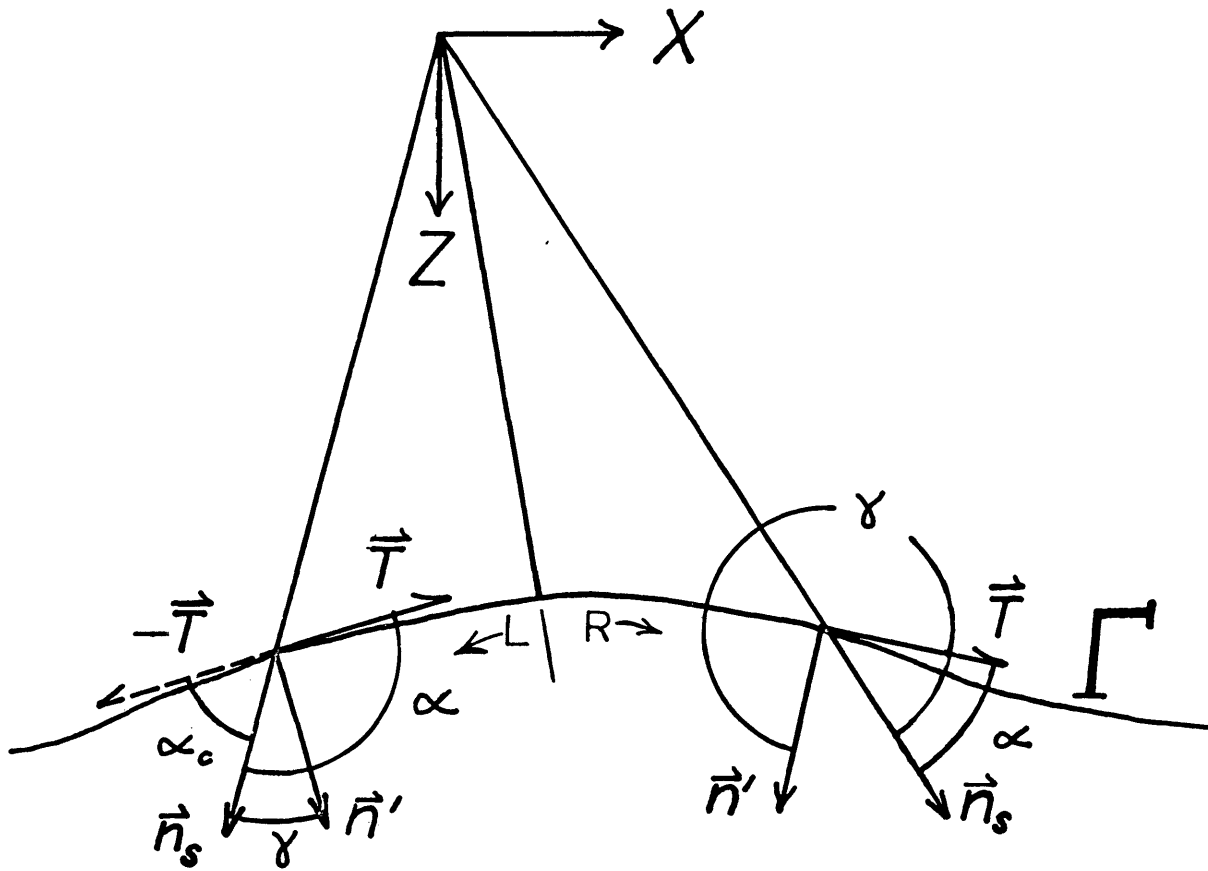


Figure 8. Trigonometric relationships of \vec{n}_s, \vec{n}' and \vec{T} .

Allowing $\tan_{\Sigma} \alpha(t)$ to stand for the sum of the tangents in (31) and dropping the subscript c in $\tan_{\Sigma} \alpha(t)$, (31) becomes

$$S(t) = \frac{4}{\pi c} \int_{\frac{t_0}{2}}^{z_+} \frac{f(t') dt'}{(t-t')^3} \int_{\frac{t_0}{2}}^{\frac{(t-t')}{2}} \frac{t, \tan_{\Sigma} \alpha(t_i) dt_i}{\sqrt{(\frac{t-t'}{2})^2 - t_i^2}} + \frac{2}{\pi c} \int_{\frac{t_0}{2}}^{z_+} \frac{f(t') dt' d}{d(t-t')} \left\{ \frac{1}{(t-t')^2} \int_{\frac{t_0}{2}}^{\frac{(t-t')}{2}} \frac{t, \tan_{\Sigma} \alpha(t_i) dt_i}{\sqrt{(\frac{t-t'}{2})^2 - t_i^2}} \right\},$$

and performing the differentiation in the last term yields

$$S(t) = \frac{4}{\pi c} \int_{\frac{t_0}{2}}^{z_+} \frac{f(t') dt'}{(t-t')^3} \int_{\frac{t_0}{2}}^{\frac{(t-t')}{2}} \frac{t, \tan_{\Sigma} \alpha(t_i) dt_i}{\sqrt{(\frac{t-t'}{2})^2 - t_i^2}} - \frac{4}{\pi c} \int_{\frac{t_0}{2}}^{z_+} \frac{f(t') dt'}{(t-t')^3} \int_{\frac{t_0}{2}}^{\frac{(t-t')}{2}} \frac{t, \tan_{\Sigma} \alpha(t_i) dt_i}{\sqrt{(\frac{t-t'}{2})^2 - t_i^2}} + \frac{2}{\pi c} \int_{\frac{t_0}{2}}^{z_+} \frac{f(t') dt' d}{(t-t')^2 d(t-t')} \int_{\frac{t_0}{2}}^{\frac{(t-t')}{2}} \frac{t, \tan_{\Sigma} \alpha(t_i) dt_i}{\sqrt{(\frac{t-t'}{2})^2 - t_i^2}}$$

or

$$S(t) = \frac{2}{\pi c} \int_{\frac{t_0}{2}}^{z_+} \frac{f(t') dt' d}{(t-t')^2 d(t-t')} \int_{\frac{t_0}{2}}^{\frac{(t-t')}{2}} \frac{t, \tan_{\Sigma} \alpha(t_i) dt_i}{\sqrt{(\frac{t-t'}{2})^2 - t_i^2}} \quad (32)$$

Since the shot pulse, $f(t')$, is finite in length and less than \mathcal{T}_+ we may change the upper limit from \mathcal{T}_+ to $\hat{\mathcal{T}}$ = length of $f(t')$. Furthermore, with no loss of generality, we may set the initial time \bar{t}_0 to 0 and (32)

becomes

$$S(t) = \frac{2}{\pi c} \int_0^{\hat{\mathcal{T}}} \frac{f(t') dt'}{(t-t')^2} \frac{d}{d(t-t')} \int_{t_0}^{\frac{(t-t')}{2}} \frac{t_1 \tan_{\Sigma} \alpha(t_1) dt_1}{\sqrt{(\frac{t-t'}{2})^2 - t_1^2}}. \quad (33)$$

This is the final expression of the diffraction integral and is in a form more amenable for inversion. In Appendix D starting with equation 20 and using the full-space Green's function, we derive the equation used by Hilterman (1970) to produce synthetic seismograms. Equation 33 is in the form of a convolution integral, with the down-going pulse convolved with the surface factor,

$$\frac{2}{\pi c} \frac{1}{t^2} \frac{d}{dt} \int_{t_0}^{t/2} \frac{t_1 \tan_{\Sigma} \alpha(t_1) dt_1}{\sqrt{(t/2)^2 - t_1^2}}. \quad (34)$$

Imbedded in the surface factor is information concerning the shape of \mathcal{F}' , namely the sum of the apparent slopes of \mathcal{F}' . The slopes are apparent because they represent the slope of \mathcal{F}' as seen by the normal to the wavefront. $\tan_{\Sigma} \alpha(t_1)$ must be extracted from the integro-differential equation represented by the surface factor in order to perform the inverse. The actual surface must, in turn, be extracted from the apparent slopes.

However, even if $\tan_{\Sigma}\alpha(t_1)$ can be extracted from (34), it still represents the sum of two unknown quantities -- $\tan_R\alpha(t_1)$ and $\tan_L\alpha(t_1)$. Therein lies the ambiguity of this particular inverse problem. There is no way to separate the two unless further assumptions are made.

Equation 34 is an improper integral at both the upper and lower limits. $\tan_{\Sigma}\alpha(t_1)$ approaches ∞ as $t_1 \rightarrow t_0$ and the denominator approaches zero at the upper limit giving us a second singularity. The weighting effect of the denominator causes more emphasis to be placed on those values of $\tan_{\Sigma}\alpha(t_1)$ closer to the upper limit than to those closer to t_0 . By itself equation 33 could be used to compute synthetic seismograms, but an algorithm based on equation D6 was considered more convenient. Lastly, the spatial symmetry of S, assumed for this problem, has allowed us to write (33) as two time integrals. The outside integral is in the form of a time convolution involving the shot pulse and the surface factor. The second time integral, part of the surface factor, contains the apparent slopes of \int' .

THE INVERSE PROCEDUREMathematical Development

Several assumptions must be made in order to perform the inverse problem:

- 1) $s(t)$ = the seismic trace is known,
- 2) $f(t)$ = the downgoing pulse is known,
- 3) the surface S is located with respect to the shot point in such a manner that the spherical wave never intersects S in more than one location,
- 4) the left-hand portion of S will be assumed known, and
- 5) the surface S must be cylindrically symmetrical with axis along the y -axis.

In 3) the assumption states implicitly that the curvature of S is always less than that of the spherical wave, or, stated another way, we may have only one point of spreading ($s = 0$ point) on S . This assumption precludes overhangs and vertical faults. Assumption 4 is necessary because, as stated earlier, $\tan_{\frac{1}{2}}\alpha(t)$ contains the sum of the apparent slopes at time t , from the left and right-hand side. Unless $\tan_{\frac{1}{2}}\alpha(t)$ is known a priori we cannot predict the surface to the right. All of the previous developments have made use of assumption 5.

For reference, equation 33 is written again as

$$s(t) = \frac{2}{\pi c} \int_0^{\hat{T}} \frac{f(t') dt'}{(t-t')^2} \frac{d}{d(t-t')} \int_{t_0}^{\frac{t-t'}{2}} \frac{t, \tan_{\Sigma} \alpha(t_1) dt_1}{\sqrt{(\frac{t-t'}{2})^2 - t_1^2}}. \quad (35)$$

Since $s(t)$ and $f(t)$ are known and since the R.H.S. of (35) is a convolution, we may Fourier transform both sides, yielding

$$\tilde{S}(\omega) = \frac{2}{\pi c} F(\omega) \mathcal{L} \left[\frac{1}{t^2} \frac{d}{dt} \int_{t_0}^{t/2} \frac{t, \tan_{\Sigma} \alpha(t_1) dt_1}{\sqrt{(t/2)^2 - t_1^2}} \right]$$

and dividing by $F(\omega)$, we get

$$\frac{\tilde{S}(\omega)}{F(\omega)} = \frac{2}{\pi c} \mathcal{L} \left[\frac{1}{t^2} \frac{d}{dt} \int_{t_0}^{t/2} \frac{t, \tan_{\Sigma} \alpha(t_1) dt_1}{\sqrt{(t/2)^2 - t_1^2}} \right]. \quad (36)$$

If we inverse Fourier transform (36), we obtain

$$\mathcal{L}^{-1} \left[\frac{\tilde{S}(\omega)}{F(\omega)} \right] \triangleq P(t) = \frac{2}{\pi c} \frac{1}{t^2} \frac{d}{dt} \int_{t_0}^{t/2} \frac{t, \tan_{\Sigma} \alpha(t_1) dt_1}{\sqrt{(t/2)^2 - t_1^2}} \quad (37)$$

where $P(t)$, the deconvolved trace, represents the impulse response of S .

Transposing the t^2 yields

$$t^2 P(t) = \frac{2}{\pi c} \frac{d}{dt} \int_{t_0}^{t/2} \frac{t, \tan_{\Sigma} \alpha(t_1) dt_1}{\sqrt{(t/2)^2 - t_1^2}} = \frac{1}{\pi c} \frac{d}{d(t/2)} \int_{t_0}^{t/2} \frac{t, \tan_{\Sigma} \alpha(t_1) dt_1}{\sqrt{(t/2)^2 - t_1^2}}$$

and integrating both sides with respect to $t/2$ from t_0 to $\hat{t}/2$ gives us

$$\int_{t_0}^{\hat{t}/2} t^2 P(t) d(t/2) = \frac{1}{\pi C} \int_{t_0}^{\hat{t}/2} \frac{t, \tan_2 \alpha(t)}{\sqrt{(\hat{t}/2)^2 - t^2}} dt.$$

Using an identity for π ,

$$\pi = 2 \int_{t/2}^{\hat{t}/2} \frac{t, dt}{\sqrt{-(t^4 - ((\hat{t}/2)^2 + (\frac{t}{2})^2)t^2 + (\frac{\hat{t}}{2})^2 t^2)}},$$

we can write (37) as

$$\left[\int_{t_0}^{\hat{t}/2} t^2 P(t) d(t/2) \right] \cdot \pi = \frac{1}{C} \int_{t_0}^{\hat{t}/2} \frac{t, \tan_2 \alpha(t) dt}{\sqrt{(\hat{t}/2)^2 - t^2}}$$

or

$$2C \int_{t_0}^{\hat{t}/2} t^2 P(t) d(t/2) \int_{t/2}^{\hat{t}/2} \frac{t, dt}{\sqrt{-(t^4 - ((\frac{\hat{t}}{2})^2 + (\frac{t}{2})^2)t^2 + (\frac{\hat{t}}{2})^2 (\frac{t}{2})^2)}} = \int_{t_0}^{\hat{t}/2} \frac{t, \tan_2 \alpha(t) dt}{\sqrt{(\hat{t}/2)^2 - t^2}}. \quad (38)$$

Proof of the identity for π may be found in Appendix C.

Factoring the denominator of the inner integral yields

$$2C \int_{t_0}^{\hat{t}/2} t^2 P(t) d(t/2) \int_{t/2}^{\hat{t}/2} \frac{t, dt}{\sqrt{(\hat{t}/2)^2 - t^2} \sqrt{t^2 - (t/2)^2}} = \int_{t_0}^{\hat{t}/2} \frac{t, \tan_2 \alpha(t) dt}{\sqrt{(\hat{t}/2)^2 - t^2}}$$

and exchanging the order of integration on the L.H.S.,

we obtain

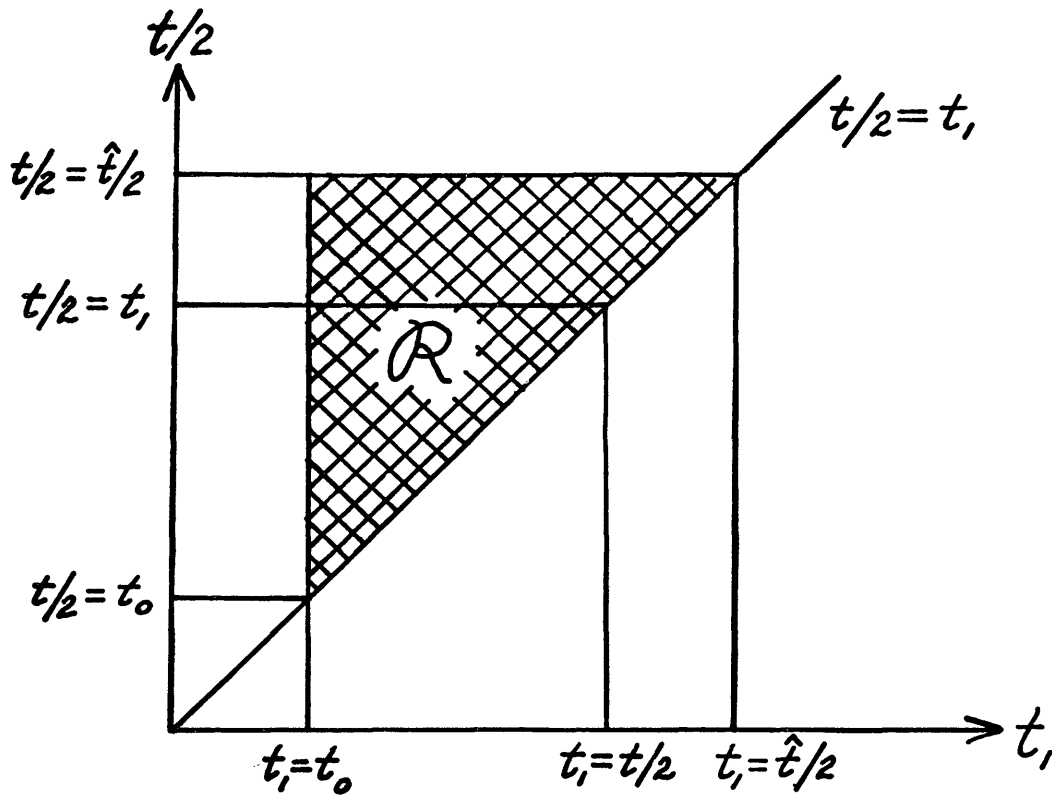


Figure 9. Region of integration in equation 39.

$$2c \int_{t_0}^{\hat{t}/2} \frac{t_1 dt_1}{\sqrt{(\hat{t}/2)^2 - t_1^2}} \int_{t_0}^{t_1} \frac{t^2 P(t) d(t/2)}{\sqrt{t_1^2 - (t/2)^2}} = \int_{t_0}^{\hat{t}/2} \frac{t_1 \tan_{\Sigma} \alpha(t_1) dt_1}{\sqrt{(\hat{t}/2)^2 - t_1^2}} \quad (39)$$

Interchanging the order of integration necessitates a change in the limits as can be seen from (38) and Figure

9. Comparison of both sides of (39) reveals that

$$\tan_{\Sigma} \alpha(t_1) = \tan_R \alpha(t_1) + \tan_L \alpha(t_1) = 2c \int_{t_0}^{t_1} \frac{t^2 P(t) d(t/2)}{\sqrt{t_1^2 - (t/2)^2}} \quad (40)$$

and therefore if $\tan_L \alpha(t_1)$ is known, we can solve for $\tan_R \alpha(t_1)$ -- the slope of the R.H.S. of \sqrt{z} as seen by the wavefront. Based on (40) we can extrapolate out from the initial point of contact and predict the R.H.S. of \sqrt{z} (i.e. S) from a single trace. The numerical calculations are discussed in Numerical Procedure.

P(t) For a Flat Plane

As a check on equation 37 the impulse response for a flat plane will be calculated. P(t) in this case should reduce to a delta function. For a flat plane

$$\tan_{R \text{ or } L} \alpha(t_1) = t_0 / \sqrt{t_1^2 - t_0^2}$$

as can be seen from Figure 10. Substituting this into

(37) and multiplying by two, since $\tan_S = \tan_R + \tan_L = \frac{2t_0}{\sqrt{t_1^2 - t_0^2}}$

we get

$$P(t) = \frac{4}{\pi c} \frac{1}{t^2} \frac{d}{dt} \int_{t_0}^{t/2} \frac{t_0 t_1 dt_1}{\sqrt{t_1^2 - t_0^2} \sqrt{(t/2)^2 - t_1^2}}$$

$$= \frac{4t_0}{\pi c t^2} \frac{d}{dt} \int_{t_0}^{t/2} \frac{t_1 dt_1}{\sqrt{-(t_1^4 - (t_0^2 + (t/2)^2)t_1^2 + t_0^2(t/2)^2)}} \quad (41)$$

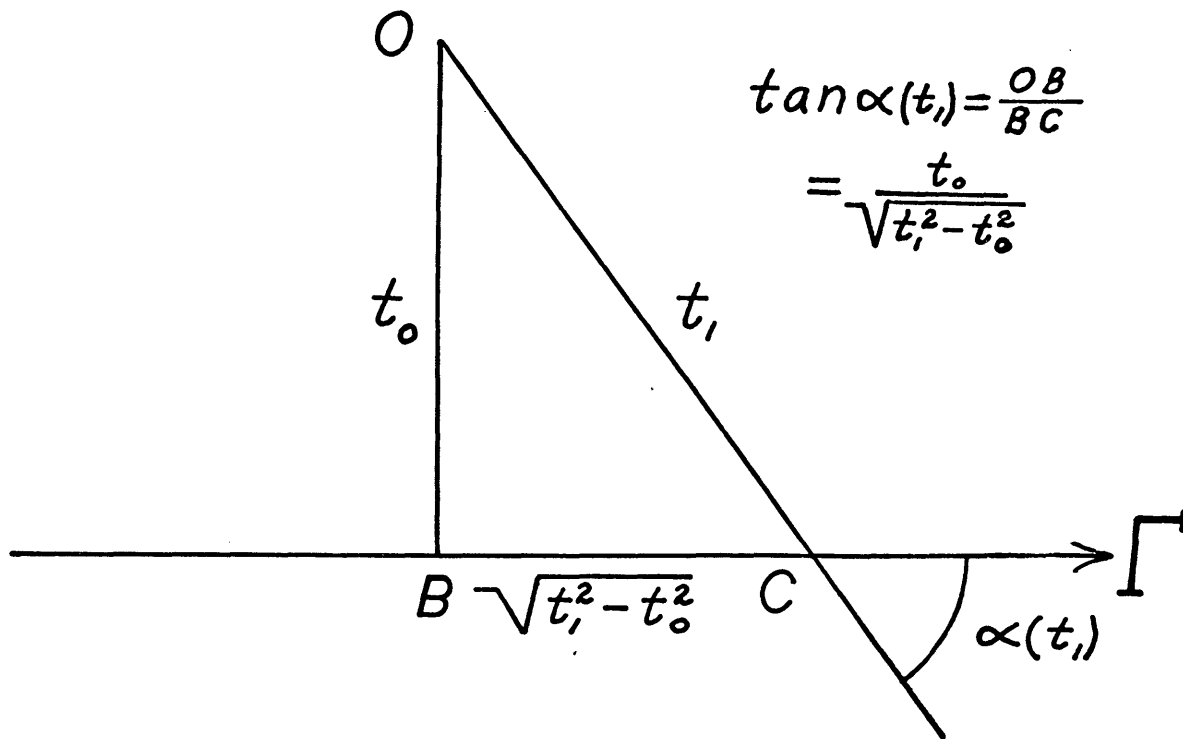


Figure 10. Angular relationships for a flat plane.

This integral is identical to that encountered previously and is simply equal to $\pi/2$ — independent of the upper limit. In other words, it is equal to

$$\pi/2 \delta^{-1}(t/2 - t_0)$$

where $\delta^{-1}(\quad)$ denotes the step function. Hence (41)

becomes

$$P(t) = \frac{2t_0}{\pi c t^2} \frac{d}{dt} \left(\pi \delta^{-1}(t/2 - t_0) \right) = \frac{2t_0}{c t^2} \frac{d \delta^{-1}(t/2 - t_0)}{dt}$$

and the derivative is just

$$\frac{d\delta^{-1}(t/2 - t_0)}{dt} = \frac{d\delta^{-1}(t/2 - t_0)}{d(t/2 - t_0)} \frac{d(t/2 - t_0)}{dt} = \frac{1}{2} \delta(t/2 - t_0) = \delta(t - 2t_0);$$

consequently,

$$P(t) = \frac{2t_0}{c t^2} \delta(t - 2t_0). \quad \text{However, } h(t)\delta(t) = h(0)\delta(t)$$

so that we may write this as

$$P(t) = \frac{2t_0}{c(2t_0)^2} \delta(t - 2t_0) = \frac{2t_0}{4c t_0^2} \delta(t - 2t_0) = \frac{\delta(t - 2t_0)}{2R_0} \quad (42)$$

where R_0 is the distance to the first point of contact. Therefore, the impulse response for a flat plane reduces to a delta function with a spherical divergence multiplier. Hence, any pulse sent out from 0 will return $2t_0$ later with exactly the same shape but with the amplitude diminished by $1/2R_0$.

Exact Inverse For a Flat Plane

As a proof that (40) will indeed produce the apparent slopes of S, the simple case for a flat plane will be undertaken. The impulse response, $P(t)$, for a flat plane is given by equation 42. From the last section

$$\tan \Sigma \alpha(t_1) = \frac{2t_0}{\sqrt{t_1^2 - t_0^2}}, \quad \text{hence}$$

$$\frac{2t_0}{\sqrt{t_1^2 - t_0^2}} = 2c \int_{t_0}^{t_1} \frac{t^2 P(t) d(t/2)}{\sqrt{t_1^2 - (t/2)^2}} = \frac{2c}{2ct_0} \int_{t_0}^{t_1} \frac{t^2 \delta(t-2t_0) d(t/2)}{\sqrt{t_1^2 - (t/2)^2}}$$

or

$$= \frac{1}{2t_0} \int_{2t_0}^{2t_1} \frac{t^2 \delta(t-2t_0) dt}{\sqrt{t_1^2 - (t/2)^2}} = \frac{4t_0^2}{2t_0 \sqrt{t_1^2 - t_0^2}} = \frac{2t_0}{\sqrt{t_1^2 - t_0^2}}$$

With the values of $\tan \alpha(t_1)$ known exactly, the shape of a flat plane may be reconstructed as outlined in the next section.

NUMERICAL PROCEDURENumerical Integration

The first step in the inversion process, the deconvolution, was actually performed by allowing $f(t) = \delta(t)$ = forcing function. Thus, the computed synthetic trace automatically became the deconvolved trace. However since Hilterman's routine was used to calculate the synthetic traces, the numerical approximation to the doublet $\delta'(t)$ was also needed. A short account of the numerical procedure may be found in Appendix D.

From equation 40 the determination of $\tan_{\alpha}(t_1)$ is basically a matter of integrating the R.H.S. If the L.H.S. of S is assumed to be a flat plane, then from (40) and (42) its impulse response must be $\frac{1}{4}R_0\delta(t - 2t_0)$; that is one-half of the initial impulse of P(t). Subtracting this portion of the initial impulse from P(t) removes the effect of the L.H.S., which from (40) yields

$$\tan_{\alpha}(t_1) = 2c \int_{t_0}^{t_1} \frac{t^2 \bar{P}(t) d(t/2)}{\sqrt{t_1^2 - (t/2)^2}} \quad (43)$$

where

$$\bar{P}(t) = P(t) - \frac{1}{4R_0} \delta(t - 2t_0).$$

Despite the singularity at the upper limit, (43) may be numerically evaluated through a Chebysheff-Gauss

quadrature. The Chebysheff-Gauss quadrature may be used effectively to evaluate integrals of the form,

$$\int_{-1}^1 \frac{f(x) dx}{\sqrt{1-x^2}},$$

because the denominator is the weighting function of the orthogonal Chebysheff polynomials. Selection of the abscissas for the quadrature summation at the zeros of the Chebysheff polynomials removes the denominator from the summation (Kopal, 1961), and hence the singularity is also removed.

The Chebysheff-Gauss quadrature has the form

(Ralston, 1965)

$$\int_{-1}^1 \frac{f(x) dx}{\sqrt{1-x^2}} = \sum_{j=1}^n H_j f(a_j) + E \quad (44)$$

where the a_j 's are the unequally spaced abscissas of f , the H_j 's are the weighting coefficients (all equal to π/n), and E is the error of the numerical approximation. The a_j 's are determined from

$$a_j = \cos\left(\frac{2j-1}{2n}\pi\right), \quad j = 1, 2, 3, \dots, n, \quad (45)$$

and are densely crowded toward the ends of the interval -1 to 1 (Hamming, 1962). Equation 44 will integrate a $(2n - 1)$ th degree polynomial exactly (Ralston and Wilf, 1967).

In order to put (43) in a form suitable for quadrature, we multiply and divide the denominator by t_1 , yielding

$$\tan_R \alpha(t_i) = zc \int_{t_0}^{t_i} \frac{t^2 \bar{P}(t) d(t/2t_1)}{t_1 \sqrt{1 - (t/2t_1)^2}}.$$

The change of variable $x = t/2t_1$ transforms this to

$$\tan_R \alpha(t_i) = zc \int_{t_0/t_1}^1 \frac{(2t_1 x)^2 \bar{P}(2t_1 x) dx}{\sqrt{1-x^2}}, \quad (46)$$

and since $\bar{P}(2t_1 x) = 0$ for $x < t_0/t_1$, the bottom limit may be extended to -1 if desired. Equation 46 can now be integrated via (44) as follows

$$\begin{aligned} \tan_R \alpha(t_i^i) &= zc \int_{t_0/t_1^i}^1 \frac{(2t_1^i x)^2 \bar{P}(2t_1^i x) dx}{\sqrt{1-x^2}} \\ &\approx \frac{2\pi c}{n} \sum_{j=1}^n (2t_1^i a_j)^2 \bar{P}(2t_1^i a_j) \end{aligned} \quad (47)$$

$i = 1, 2, \dots, M$, where M is the desired number of $\tan_R \alpha(t_1^i)$ values commensurate with the length of \bar{P} . Equation 47 must be repeated for each value of t_1^i , the one-way time to S. It was incremented in units of $5\Delta t$, where Δt was the sample interval of $\bar{P}(t)$. The initial time $t_1 = t_0$ was avoided since $\tan_R \alpha(t_0) = \infty$ but the location and true slope of S at this time were assumed as given.

Prediction of S

Introduction -- Knowing the apparent slopes of the R.H.S. of S from (47), an extrapolation procedure is necessary to project from one time increment to the next. The initial point of contact as well as the true slope of \sqrt{r} at this point is given. The procedure of this study was to extrapolate linearly from the initial point using the initial slope until the linear extension intersected a circle of radius $t_1 = t_0 + 5\Delta t$. \sqrt{r} is known to lie on this circle. Having solved for the intersection point, we now call this the predicted location of \sqrt{r} . Moreover, the apparent slope of \sqrt{r} is known at this point, but since we now know its true spatial location, we may convert the apparent slope to a true slope in the xz-coordinate system. This procedure is performed again by using the true slope, just determined, to project to the next circle of radius $t_1 = t_0 + 10\Delta t$ and so on.

A piece-wise linear extrapolator tends to diverge from a curved surface (Hamming, 1962); hence an iterative scheme was implemented to counter this trend. After the estimated location and estimated slope were computed for a predicted point, the slope was averaged with the slope of the previous point and a new predicted location and slope were computed. Two iterations were found to yield sufficiently accurate results.

In essence the above procedure is nothing more than the numerical solution of a first order differential equation with given initial conditions. The extrapolation technique discussed above is one of the predictor-corrector methods used to solve numerically a differential equation. The particular technique employed was an iterative scheme using the Modified Euler Method (Stark, 1970). The only difference between the ordinary numerical solution of a differential equation using the predictor-corrector methods and the technique used for this study is that an intermediate step of converting the apparent slopes to true slopes is necessary. Figure 11 displays the reconstruction of a syncline using the above method. The apparent slopes were computed directly.

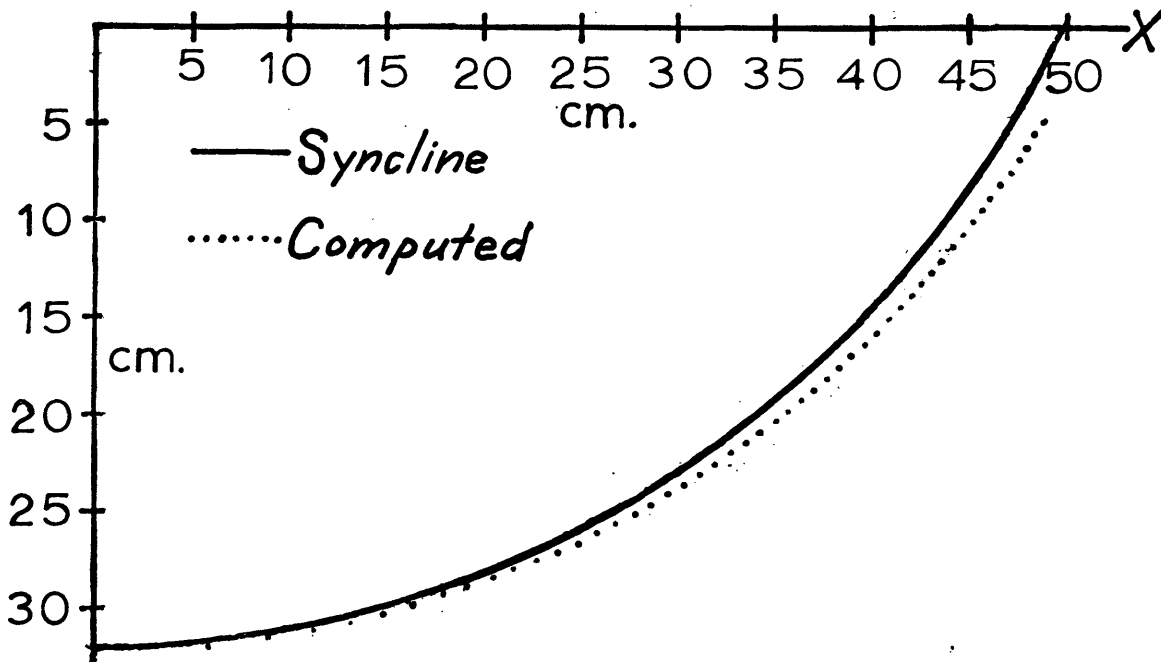
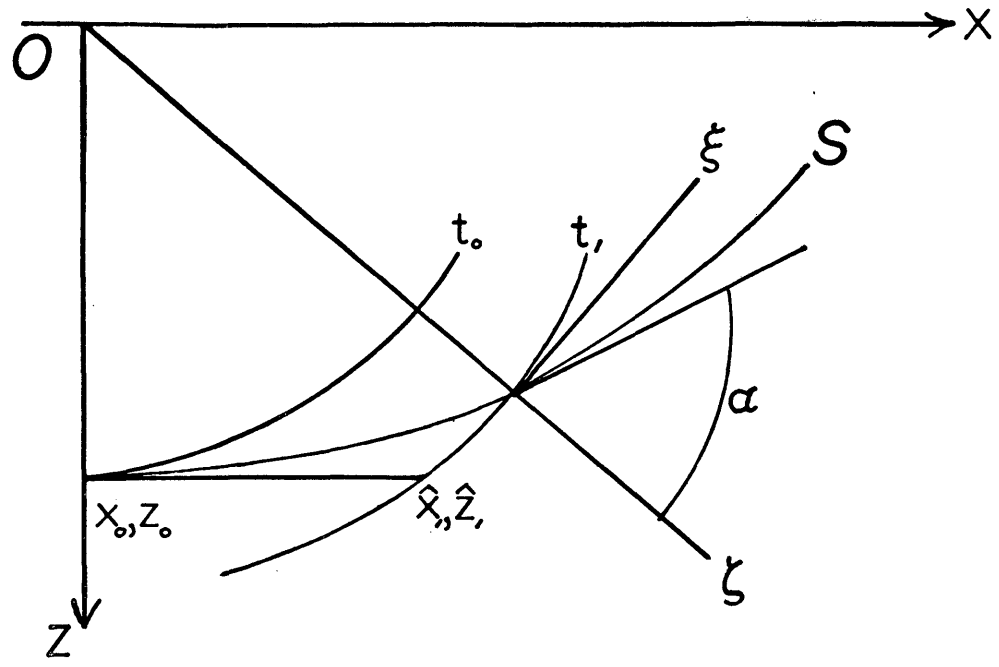
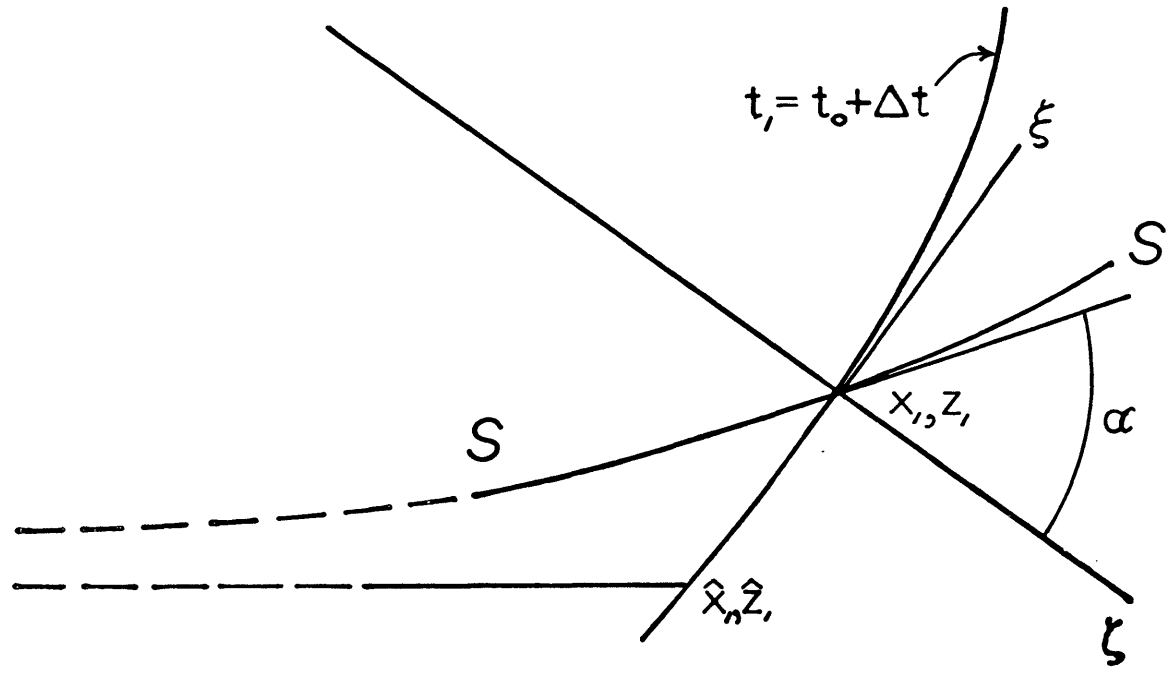


Figure 11. Reconstruction of S using the Modified Euler Method.



(a)



(b)

Figure 12. (a) Geometry of initial prediction.
 (b) Expansion of 12a.

Prediction of the First Point -- Figures 12 a and b indicate the geometry involved in the initial prediction. Since the initial slope, m_0 , is equal to 0, the initial linear extension must be a horizontal line. Hence, the first predicted location must be $z_1 = z_0$ and $x_1 = \sqrt{c^2 t_{(1)}^2 - z_1^2}$. However, if S is a curved surface, then x_1, z_1 will differ from the true location; consequently, we denote these predicted values as \hat{x}_1, \hat{z}_1 (Figure 12a,b). From Figure 13 and the estimated location \hat{x}_1, \hat{z}_1 we can convert the apparent slope, $\tan_R \alpha_1$, to an estimated true slope, \hat{m}_1 .

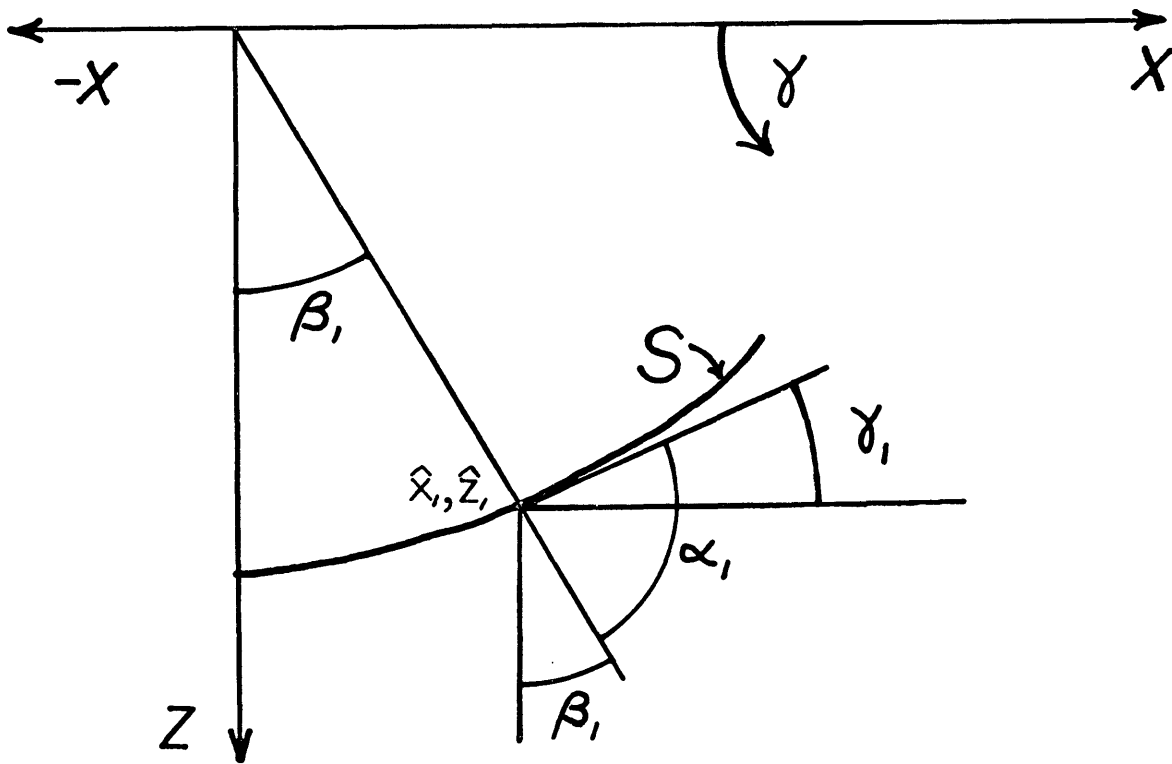


Figure 13. Determination of \hat{m}_1 .

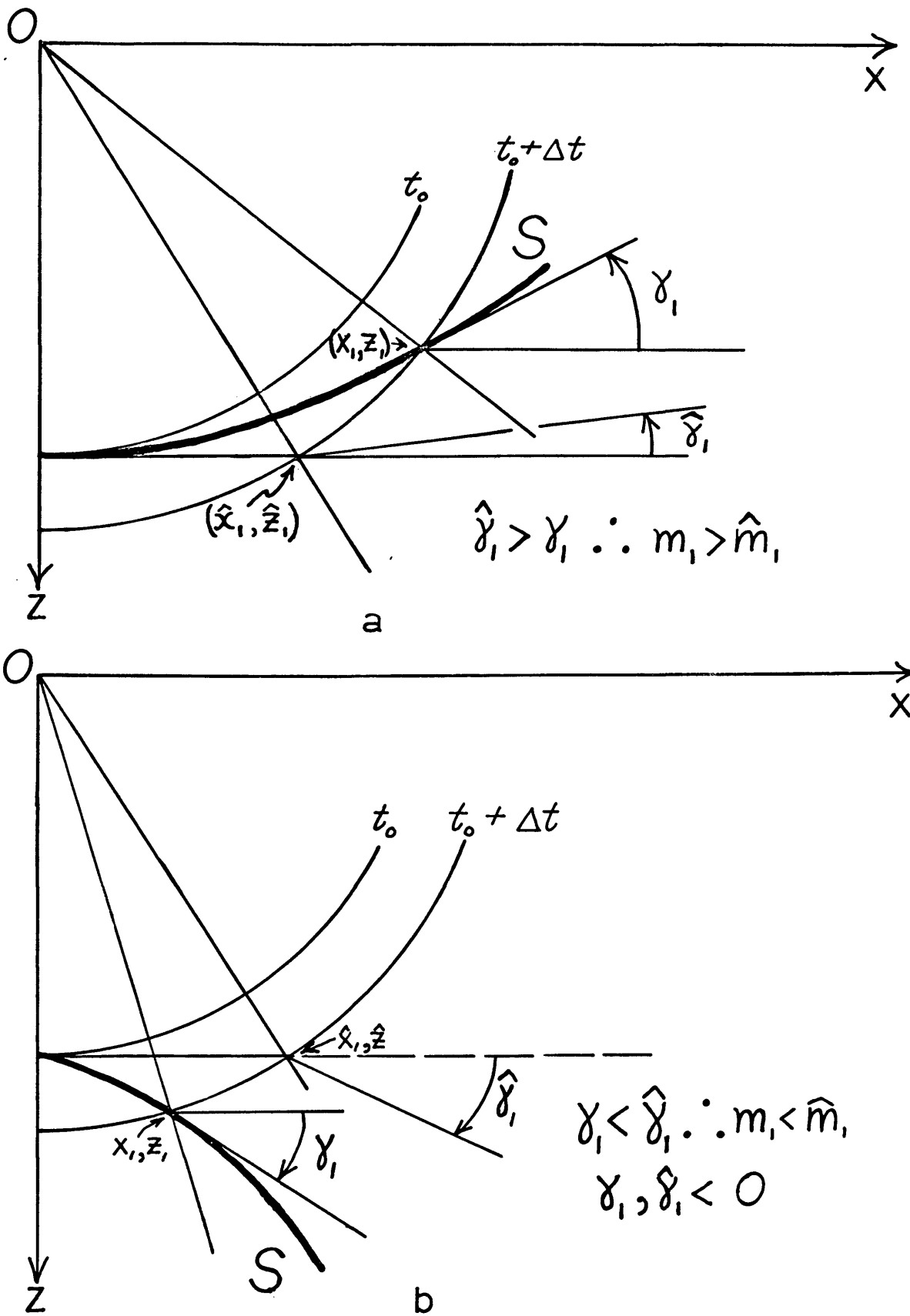


Figure 14. (a) Estimated versus true slope for a concave surface.
 (b) Estimated versus true slope for a convex surface.

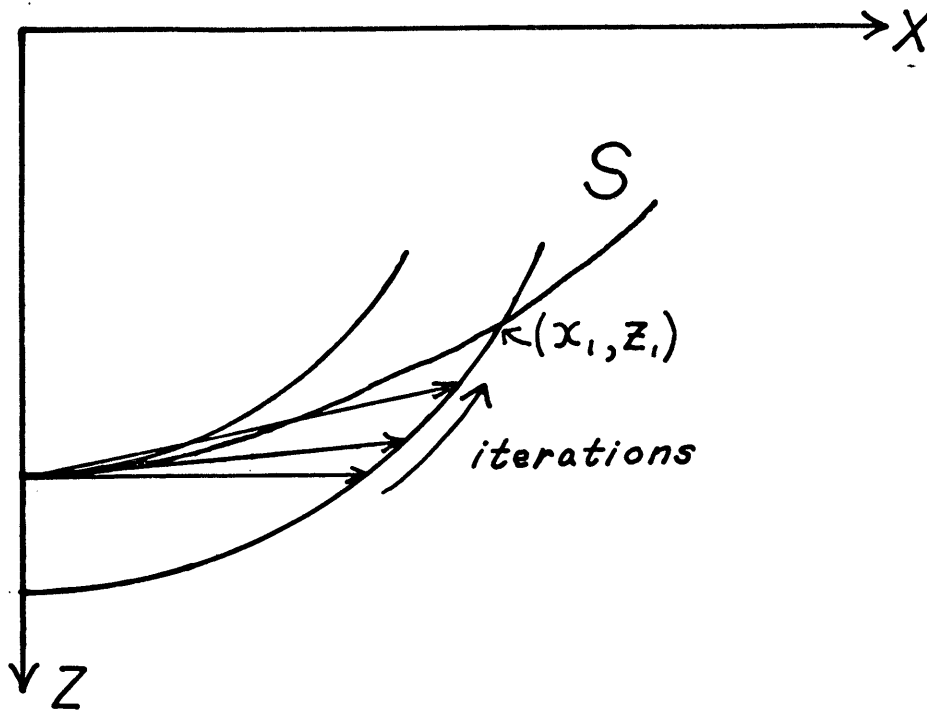


Figure 15. Iterative improvement of x_1, z_1 .

We have $\alpha_1 + \hat{\beta}_1 - \pi/2 = \hat{\gamma}_1$, hence, $\tan \hat{\gamma}_1 = \tan((\alpha_1 + \hat{\beta}_1) - \pi/2) = -\text{ctn}(\alpha_1 + \hat{\beta}_1)$ where $\alpha_1 = \tan^{-1}(\tan \alpha_1)$ and $\hat{\beta}_1 = \tan^{-1}(\frac{\hat{x}_1}{\hat{z}_1})$. The angle $\hat{\gamma}_1$ is measured from the negative x-axis in a counter-clockwise manner so that concave surfaces will have a positive slope when looking down the +z-axis.

The estimated true slope, \hat{m}_1 , will be less than the true slope m_1 for a concave surface (Figure 14a) and greater than the true slope for a convex surface (Figure 14b). However, averaging the estimated slope \hat{m}_1 with $m_0 = 0$ will yield a slightly better slope to project from x_0, z_0 . Each iteration will move the linear extension progressively closer to x_1, z_1 as shown in Figure 15 for a concave surface.

Prediction For the General Case -- Assuming the prediction process has proceeded to the point x_i, z_i , we wish to predict the point x_{i+1}, z_{i+1} . Writing the linear extension from the point x_i, z_i in the point-slope form, $(z_{i+1} - z_i) = m_i(x_{i+1} - x_i)$, and the equation of the circle as $x_{i+1}^2 + z_{i+1}^2 = c^2 t_{1(i+1)}^2$, we may solve for z_{i+1} from the equation for the circle. Substituting this expression into the linear equation yields

$$\left(\sqrt{c^2 t_{1(i+1)}^2 - x_{i+1}^2} - z_i \right) = m_i (x_{i+1} - x_i).$$

Squaring both sides and collecting terms we arrive at

$$(1+m_i^2)x_{i+1}^2 - 2m_i(m_i x_i - z_i)x_{i+1} - (c^2 t_{1(i+1)}^2 + 2z_i m_i x_i + m_i^2 x_i^2) = 0,$$

and solving for x_{i+1} (using the positive square root), we get

$$x_{i+1} = \frac{m_i(m_i x_i - z_i) + \sqrt{m_i^2(m_i x_i - z_i)^2 + (1+m_i^2)(c^2 t_{1(i+1)}^2 + 2m_i x_i z_i + m_i^2 x_i^2)}}{(1+m_i^2)}.$$

The z_{i+1} may be determined by substituting this value of x_{i+1} into the equation for the circle.

RESULTS OF NUMERICAL PREDICTION

Two types of surfaces were predicted: 1) symmetrical surfaces with the observation-source point directly over the axis of symmetry and 2) one-sided surfaces where the L.H.S. of S was a flat-plane. Both concave and convex models were run. In addition, a normal fault model was tested to determine the effects of kinky surfaces.

Table 1. Summary of experimental scale factors and units. (After Hilterman, 1970)

$$\text{Time scale factor} = \text{time}_p / \text{time}_m^1 = 1,000$$

$$\text{Length scale factor} = \text{length}_p / \text{length}_m = 12,000$$

<u>Quantity</u>	<u>Model</u>	<u>Prototype</u>
Length	1 in	1000 ft
	1 cm	394 ft
Time	1 μ sec	1 msec
Velocity	1120 fps	13440 fps
Peak Frequency	40 kHz	40 Hz

¹Subscript "p" represents prototype and subscript "m" represents model

All of the models had dimensions of centimeters and microseconds. The scaling factors needed to simulate earth-size models are indicated in Table 1. A Δt of 2 μsec and a velocity, c , of $.0342\text{cm}/\mu\text{sec}$ were used for all models.

Since the deconvolution was performed directly, p. 49, the synthetic trace was generated by convolving a 99 point Ricker wavelet (Figure 16) with the deconvolved trace. The amplitude spectrum of the Ricker wavelet is shown in Figure 17. The phase is zero since the wavelet is symmetric.

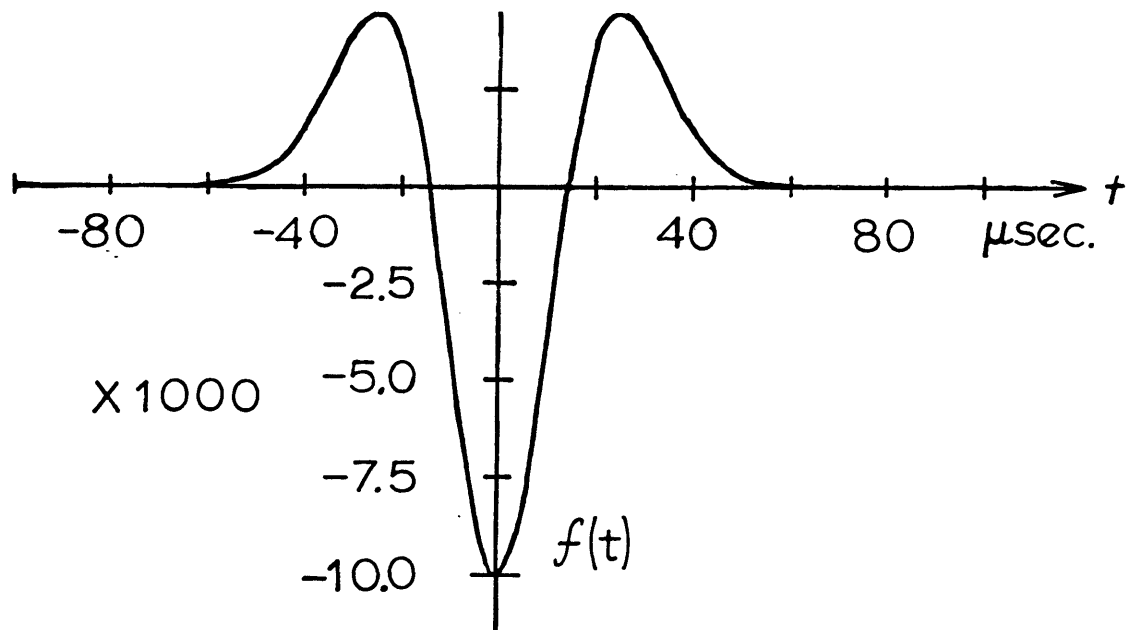


Figure 16. Ricker wavelet.

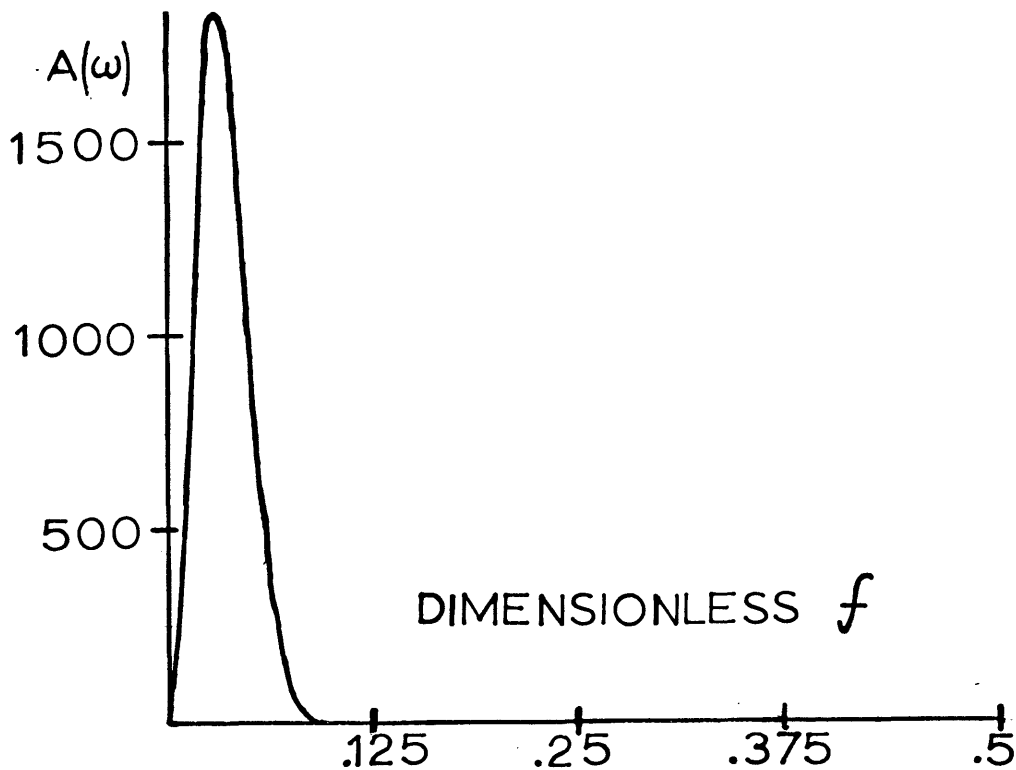


Figure 17. Amplitude spectrum of the Ricker wavelet.

Model A--Flat Plane

A flat plane with infinite lateral extent was run to determine the effects of round-off errors and drift in the prediction routine. The depth to the surface was 32 cm (Figure 18). As stated on page 47, the impulse response $P(t)$ is equal to $\frac{1}{2R_0} \delta(t - 2t_0) = \frac{1}{64} \delta(t - 2t_0)$ and, consequently, the weight of the impulse should be $1/64 = .015625$. The actual weight was computed as $.0156584$. This slight discrepancy is due to

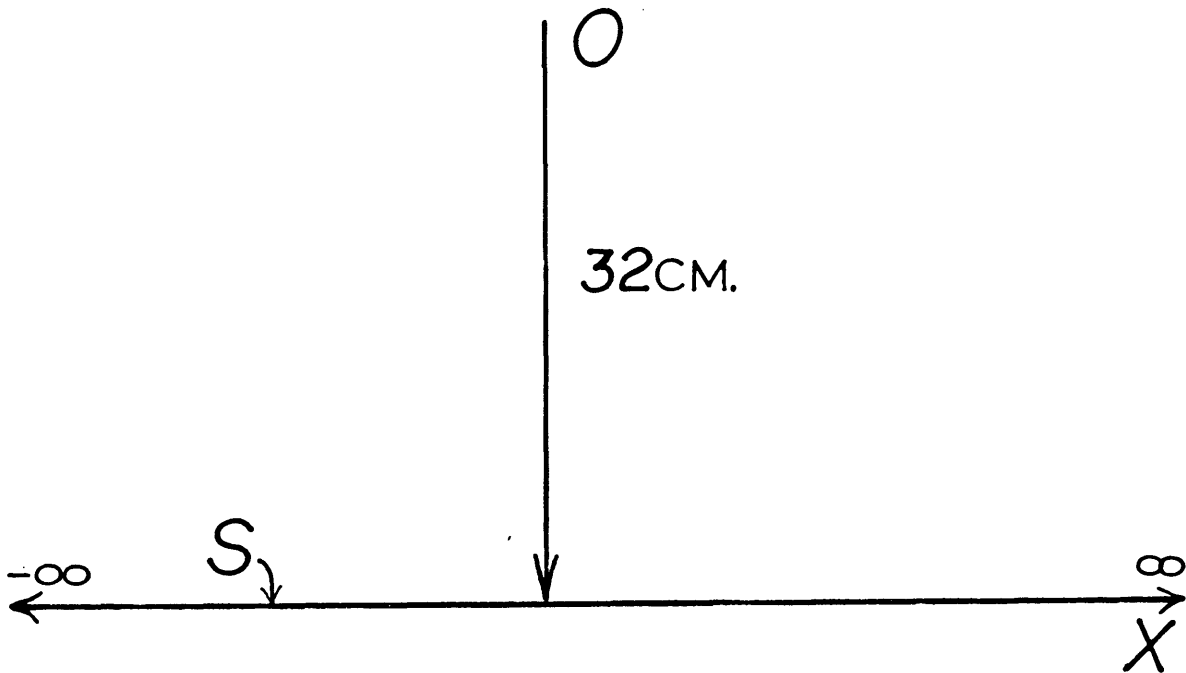


Figure 18. Dimensions of model A.

round-off errors in calculating $d\Omega$ and in the convolution process, as well as inherent difficulties in approximating the delta and doublet functions.

Following the initial pulse a small negative tail with values on the order of 10^{-7} were computed. This is a good indication of error magnitude since, for a flat plane, the values following the initial pulse should be identically zero. However, the magnitude difference between the pulse and the tail was on the order of 10^6 which was considered a remarkably good representation of a delta function.

The initial weight of $P(t)$ was included in all

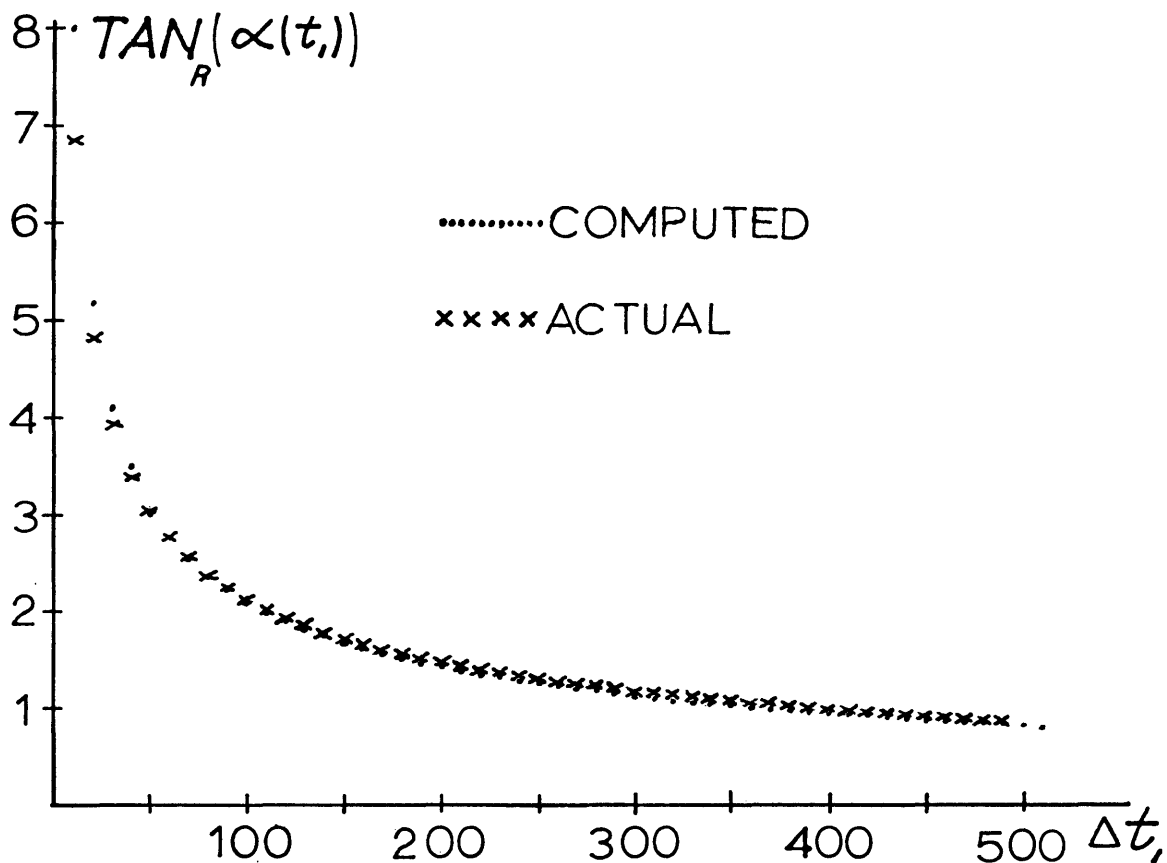


Figure 19. Comparison of computed versus true $\tan_R(\alpha(t_1))$ for model A.

integrations of (40) and hence, the small positive error mentioned above would tend to make the values of $\tan_R \alpha_i$ slightly larger than their true values. A comparison of true versus computed $\tan_R \alpha_i$ is shown in Figure 19. Equation 40 reveals that the values of \bar{P} are multiplied by t^2 , and consequently any noise on the trace such as the small negative tail of this model will eventually be built up as more values are added to the summation of equation 44. The results of the prediction process are shown in Figure 20.

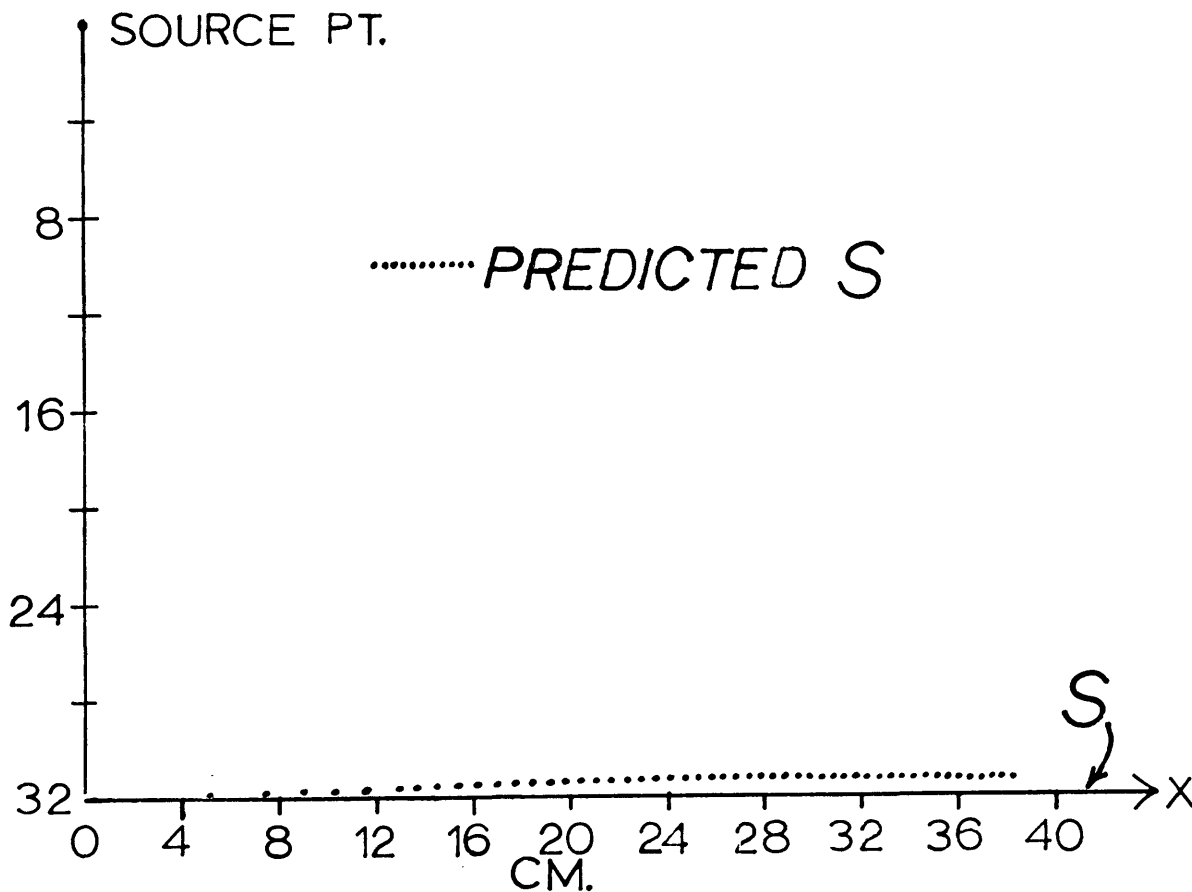


Figure 20. Inverse of model A.

Model B--Anticline

Two models were run where the observation-source point was directly overlying the axis of symmetry. In this anticlinal model the depth to the nearest point was 32 cm and the radius was 36 cm (Figure 21). Due to symmetry, the distinction between left and right values of $\tan \alpha_i$ was unnecessary. The initial pulse has a weight of .01141497 which is followed by a small negative tail with magnitudes on the order of 10^{-5} (Fig-

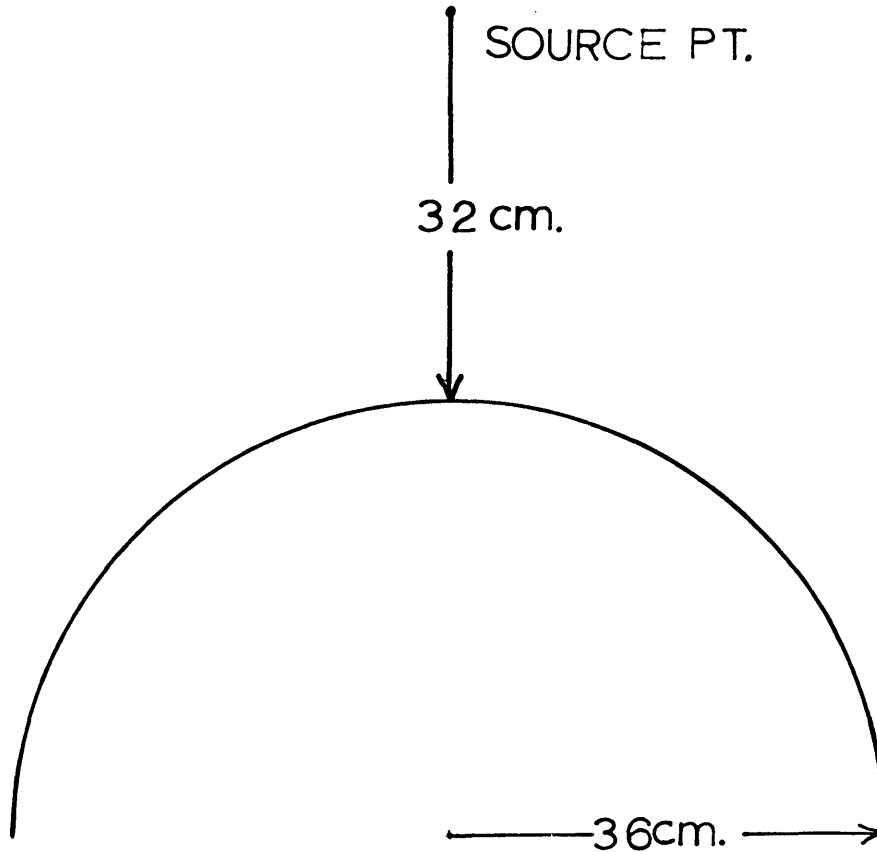


Figure 21. Dimensions of model B.

ure 22). Note that the pulse weight is smaller than that of the flat plane, and the negative tail is 100 times larger even though $R_0=32$ is the same in both cases. The magnitude difference of the pulse and the tail is of the order of 10^4 . The smaller pulse weight and the negative tail are needed in equation 40 to reduce the values of $\tan\alpha_i$ as required by the geometry of the problem.

In Figure 23 the computed $\tan\alpha_i$ versus the true

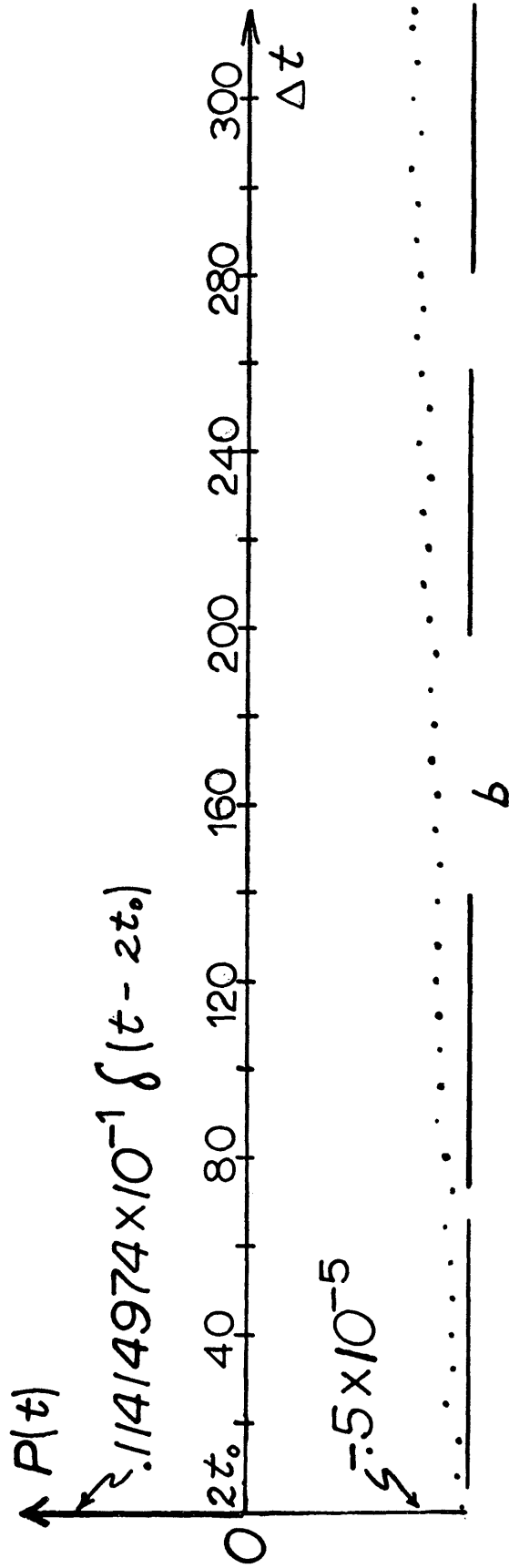
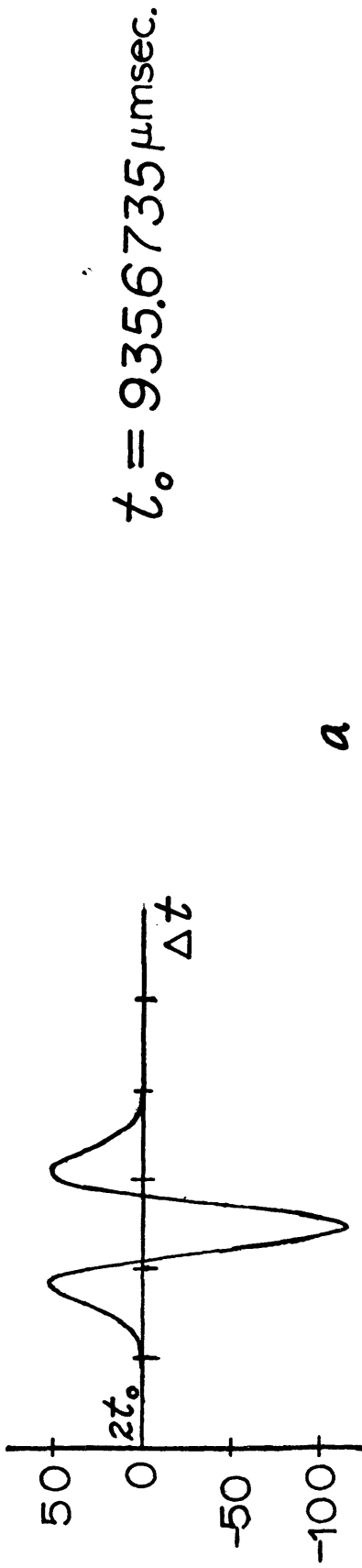


Figure 22. (a) Synthetic trace of model B.
 (b) Deconvolved trace of model B.

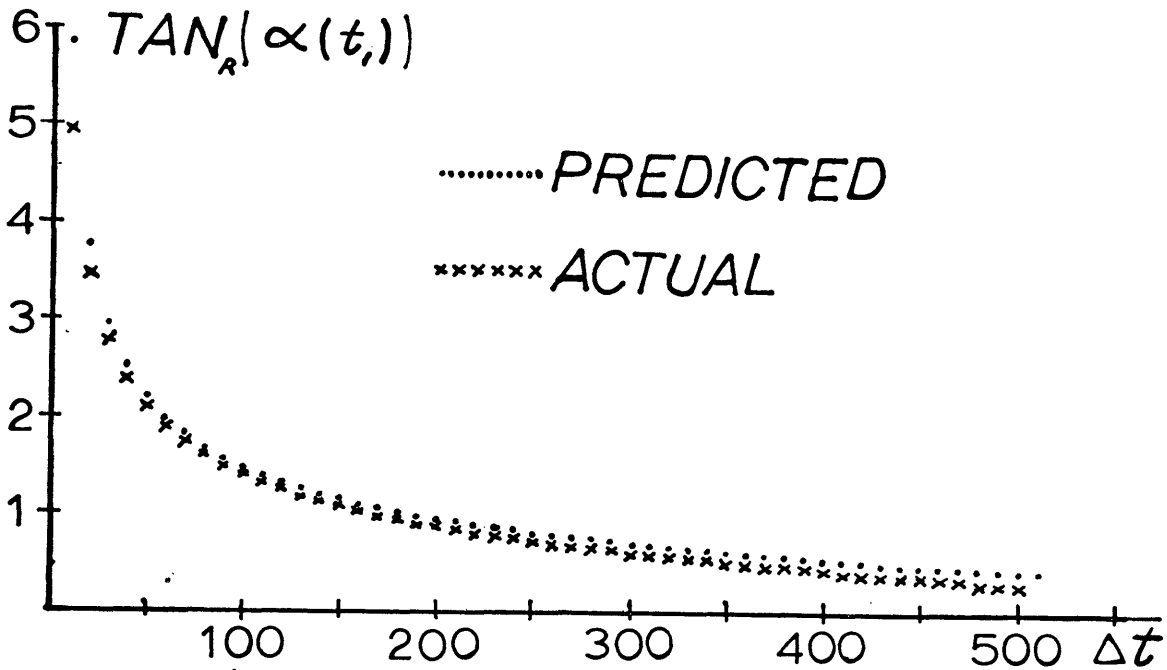


Figure 23. Computed versus true $\tan_R(\alpha(t))$ for model B.

values are displayed. The computed values are slightly larger than the true values which accounts for most of the discrepancy between the predicted S of Figure 24 and the actual surface. This is a severe test for the prediction process since the curvature of the anticline is pronounced. Nevertheless, the reconstruction process indicates the general shape.

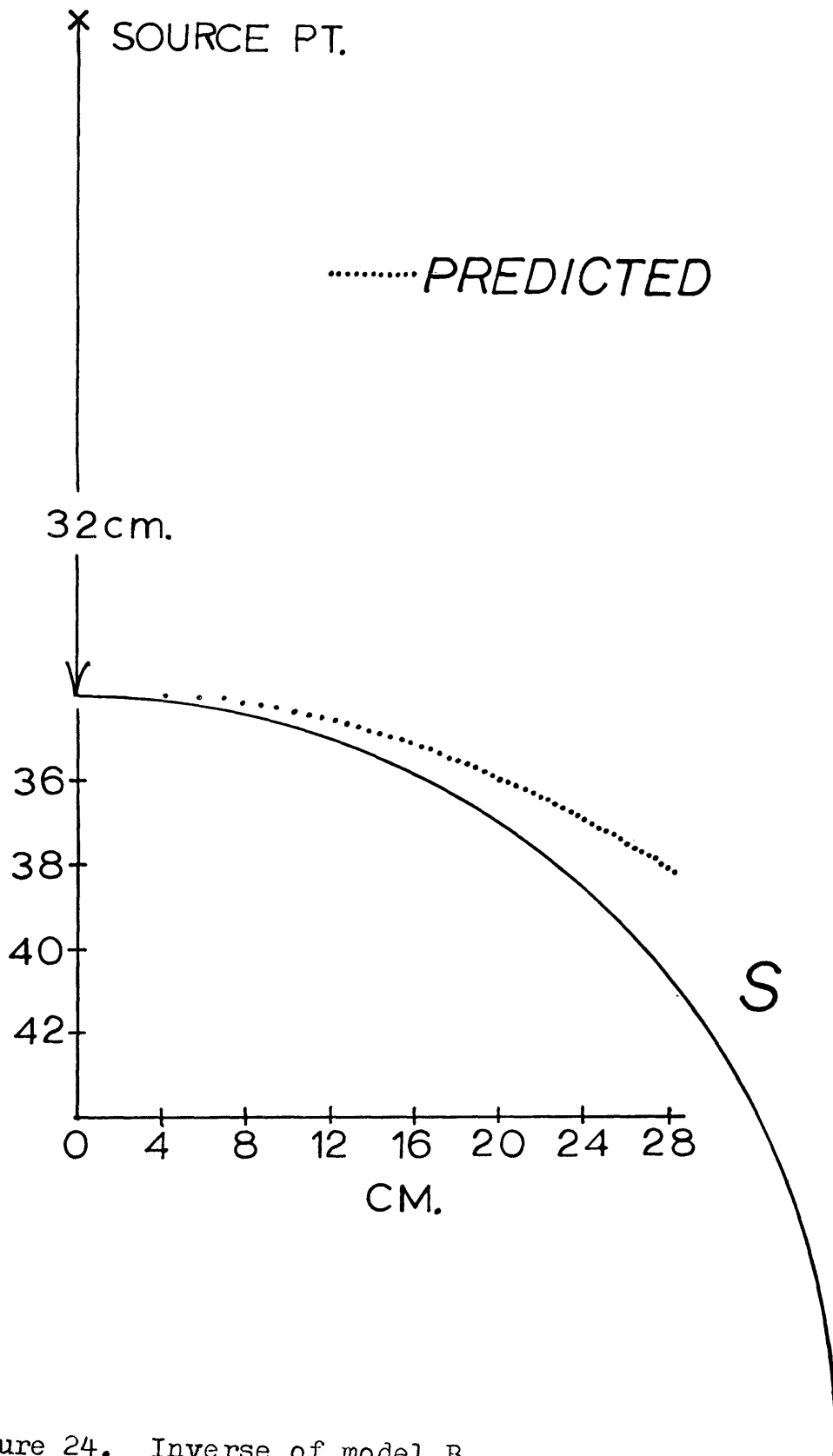


Figure 24. Inverse of model B.

Model C--Syncline

The second symmetric surface was a synclinal structure of radius 56 cm with an R_0 distance of 32 cm (Figure 25). The focal line was 24 cm above the observation-source point. The initial pulse weight was .02395408 or nearly two times greater than that of the anticline. Furthermore, the pulse is followed by a small positive tail with $.975 \times 10^{-5}$ as its largest value (Figure 26b). The magnitude difference between the pulse and the tail's largest value was 2.4568×10^3 .

Once again, the positive values of the tail are necessary in equation 40 because the geometry of the

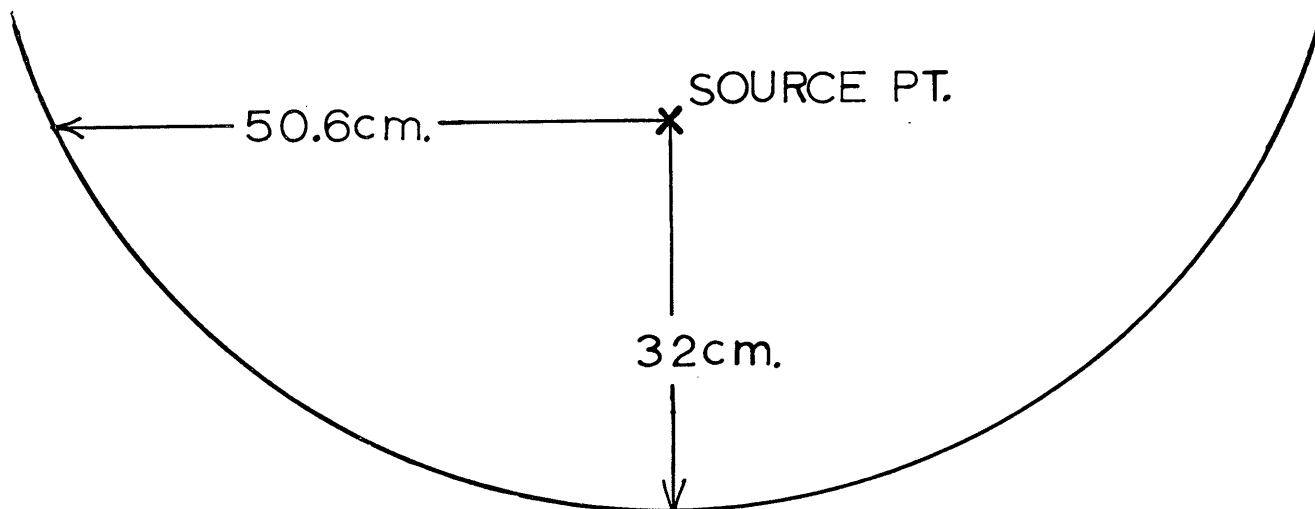


Figure 25. Dimensions of model C.

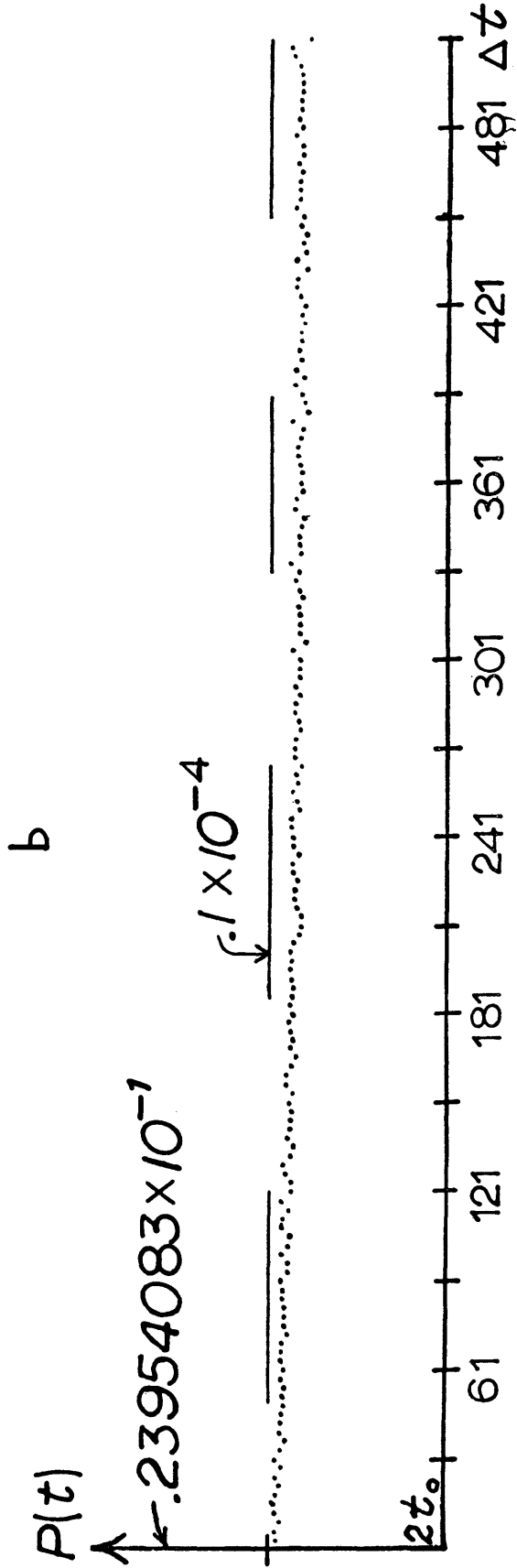
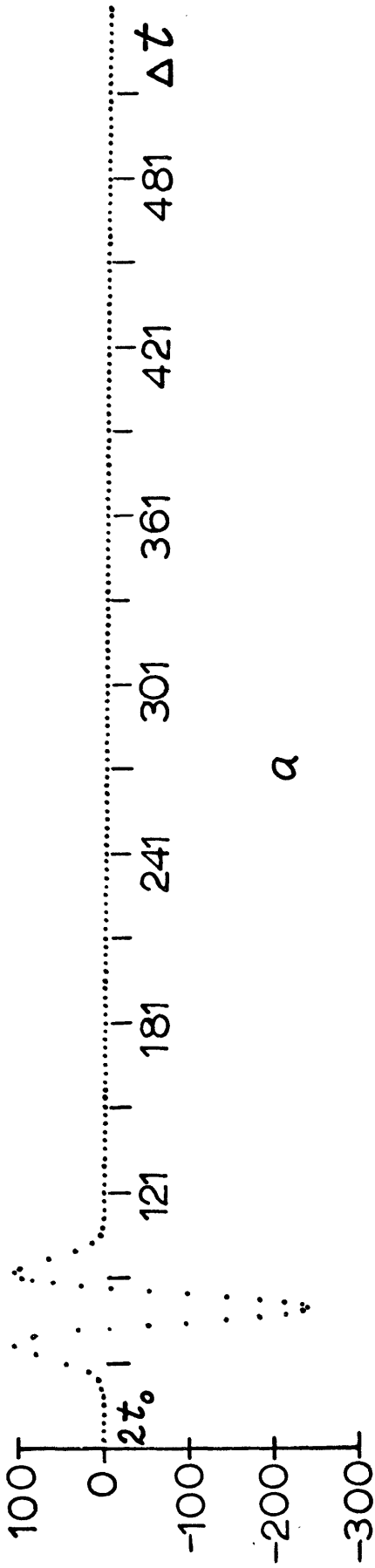


Figure 26. (a) Synthetic trace of model C. (b) Deconvolved trace of model C.

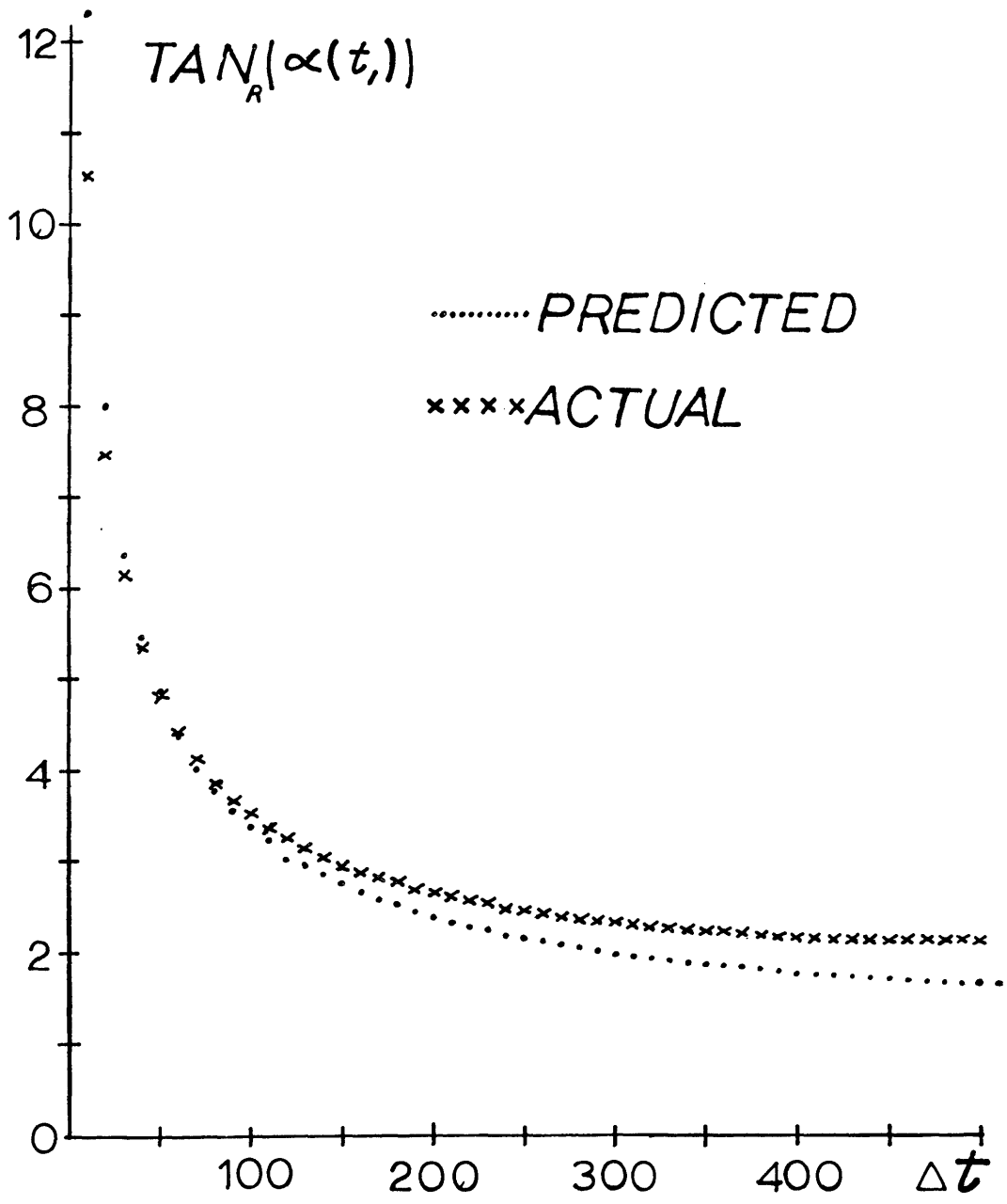


Figure 27. Computed versus true $\tan_R(\alpha(t_1))$ for model C.

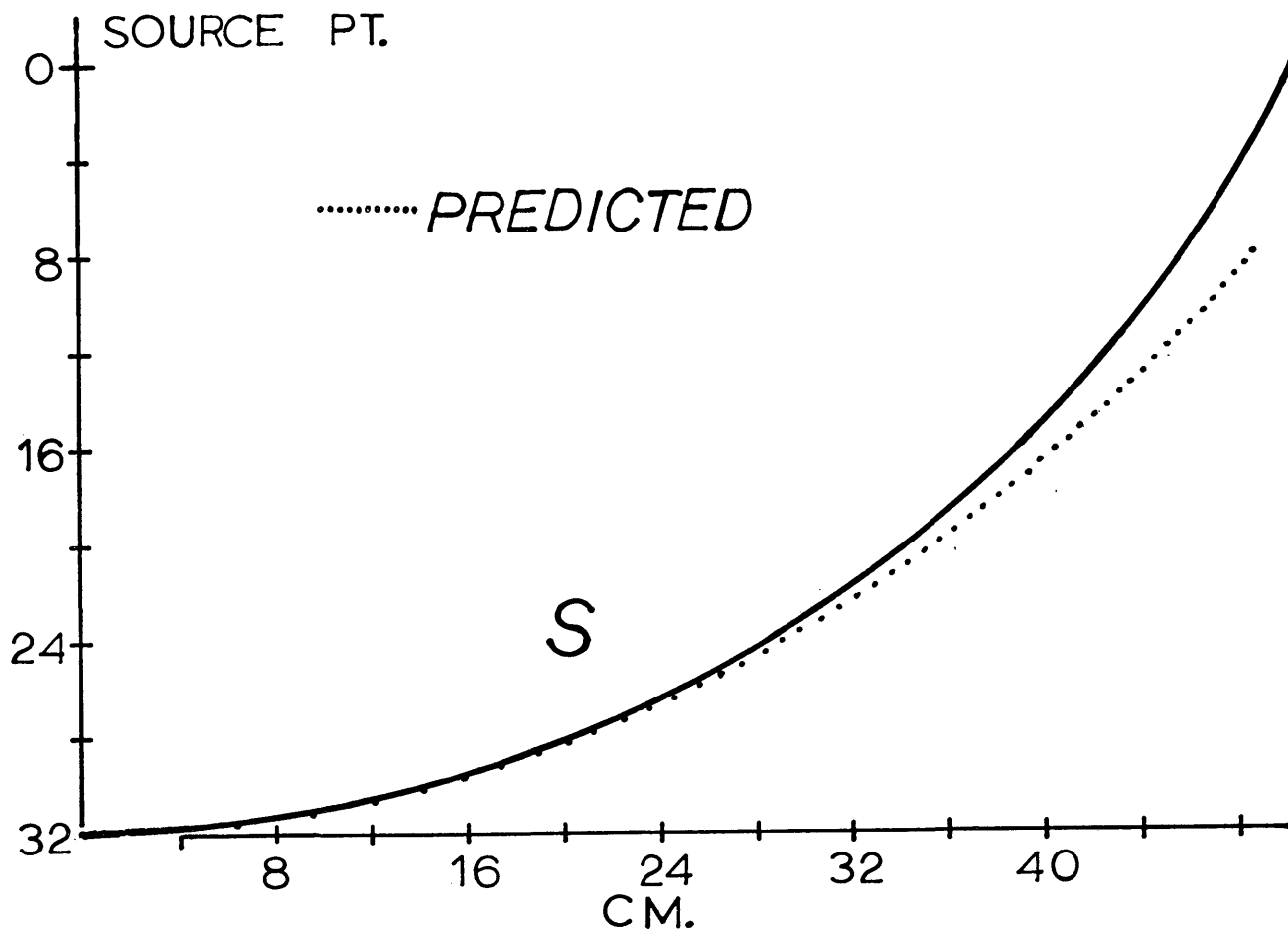


Figure 28. Inverse of model C.

syncline requires that the values of $\tan \alpha_i$ decay more slowly than those of either the anticline or the flat plane. In Figure 27 the difference between the actual versus the computed values of $\tan \alpha_i$ are shown. At first the computed values are larger than the true values, but gradually they become smaller. Results of the inversion are shown in Figure 28. The effect of double reflections have not been taken into account for this model.

Model D--Normal Fault

A normal fault with sharp corners was tested to determine the effects of kinks on the inversion process. The model dimensions are displayed in Figure 29 with the synthetic trace shown in Figure 30a. The deconvolved trace is shown in Figure 30b. Note that the response due to the first kink point (with a one-way time of \hat{t}_1) yields a small positive event following the initial pulse. Later at time $2\hat{t}_2$ a small negative response is produced.

Since the inversion process is basically an integration procedure, the effects of jump discontinuities in $\tan_R \alpha_i$ will tend to be smoothed. Hence the predicted S of Figure 31 is a smoothed version of the true S.

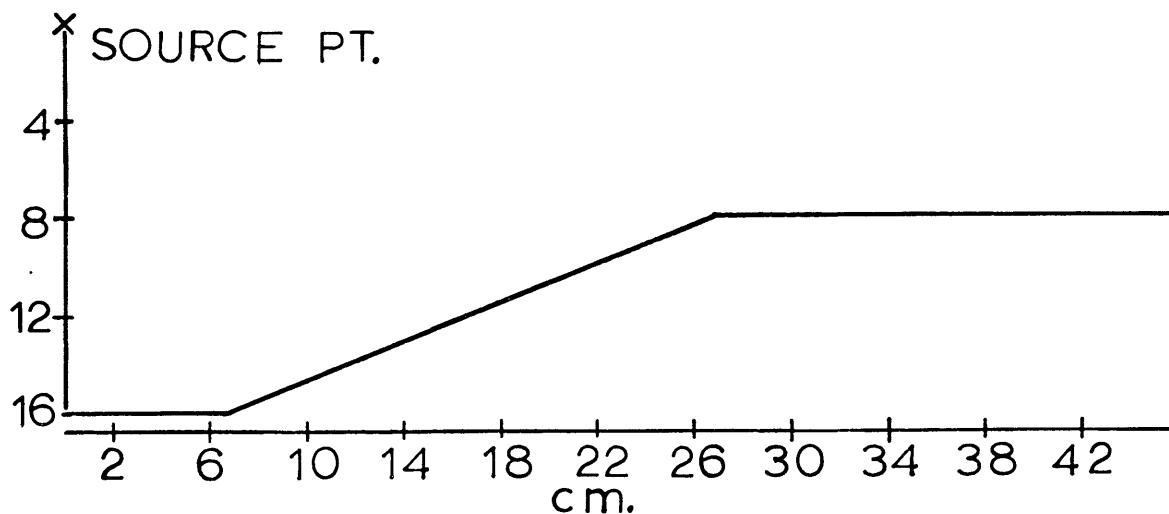


Figure 29. Dimensions of model D.

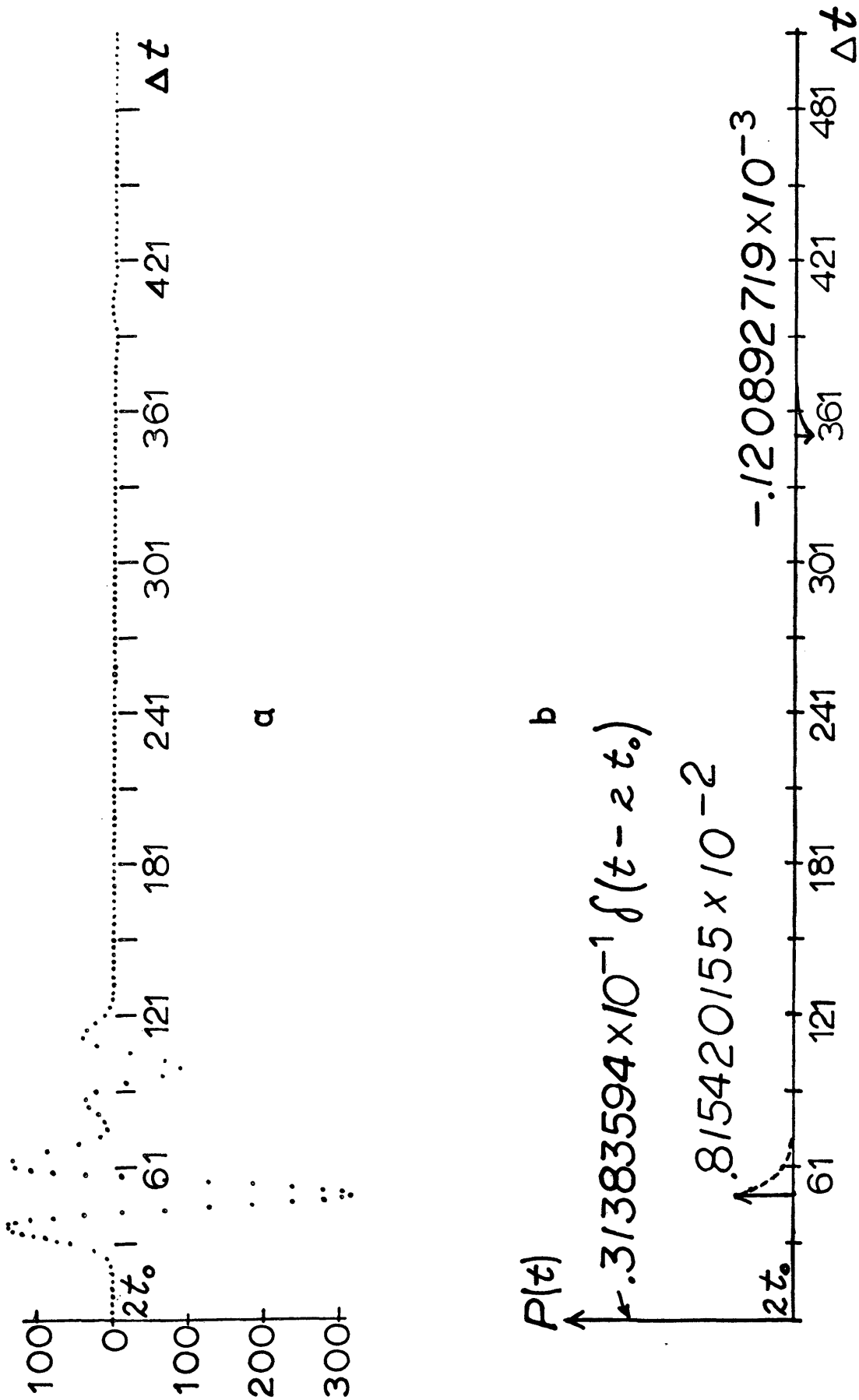


Figure 30. (a) Synthetic trace of model D.
 (b) Deconvolved trace of model D.

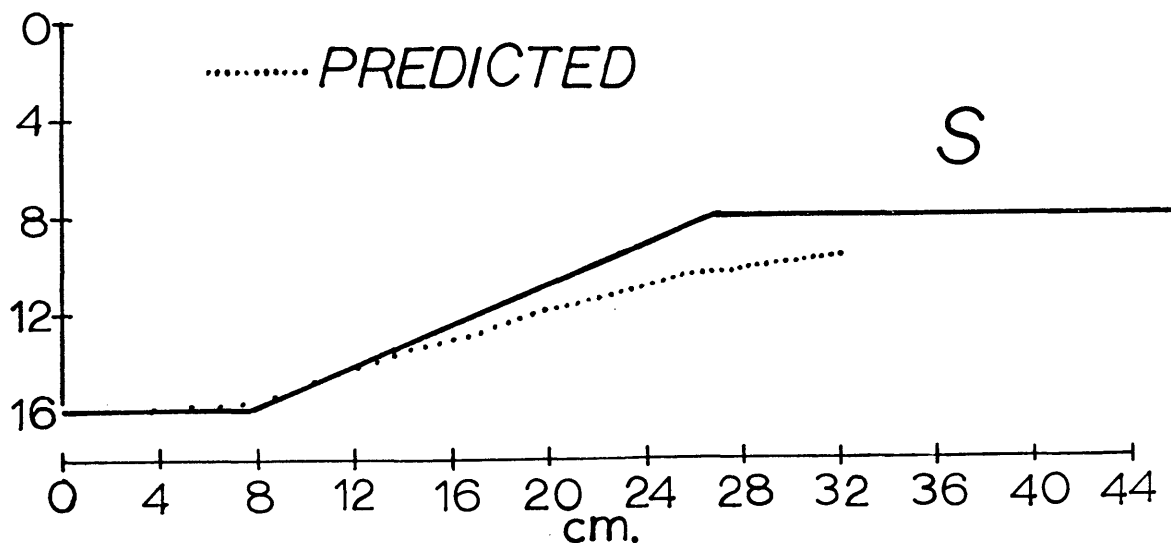


Figure 31. Inverse of model D.

Model E--Composite

The effects of lateral displacement of the observation-source point with respect to a fixed S are tested in this model. Figure 32 displays the dimensions of this model as well as the three shot points involved. In Figure 33 the three synthetic traces are shown. There is apparently very little difference in the response for all three shot points. However, the three deconvolved traces shown in Figure 34 reveal the differences in the tails. As one might expect, shot point 3 has a smaller tail than shot point 1, with the trailing tail of shot point 2 falling in between. Figure 35 shows the reconstructed surface, S, for all three shot

points. The predictions become progressively worse as the lateral separation increases. However, all of the reconstructions reveal the general trend of S.

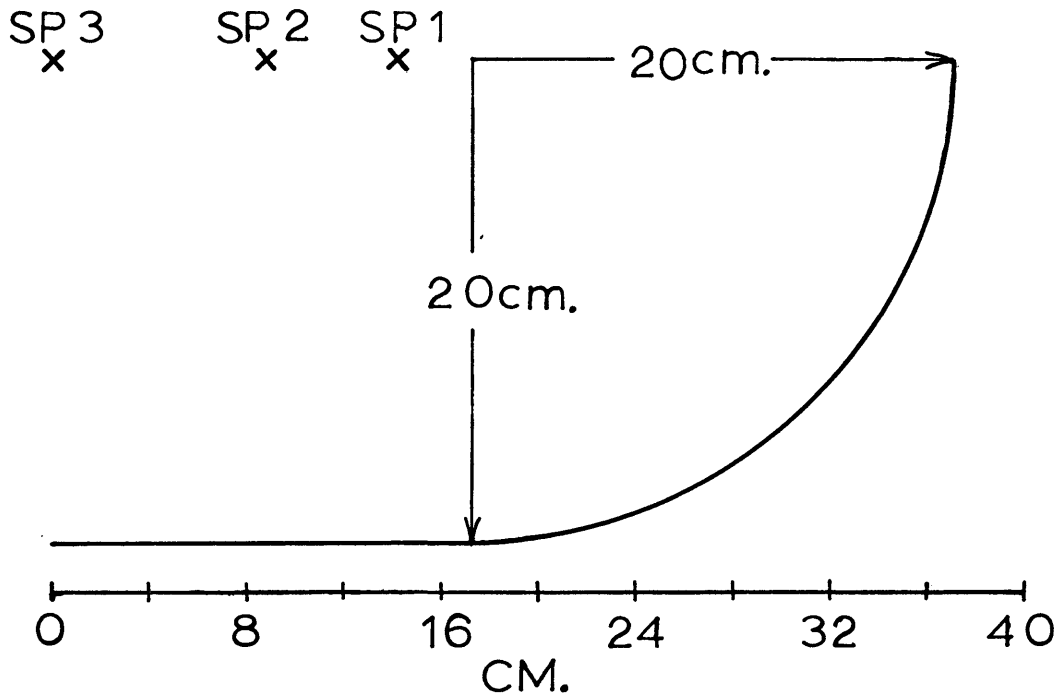


Figure 32. Dimensions of model E.

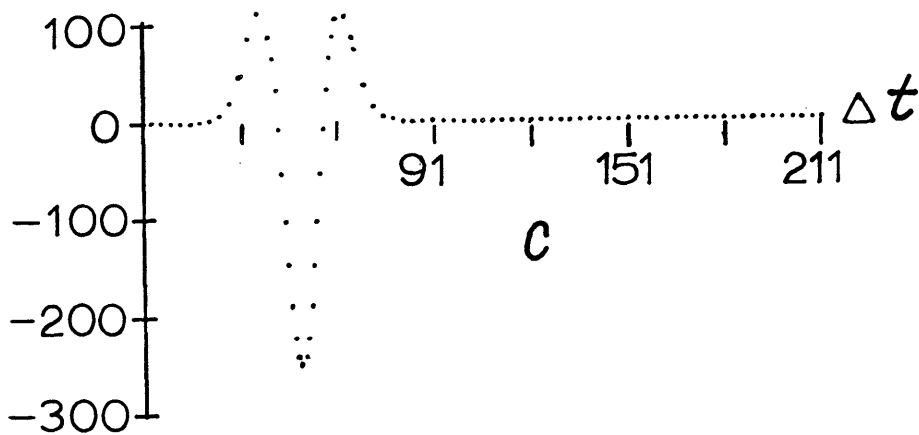
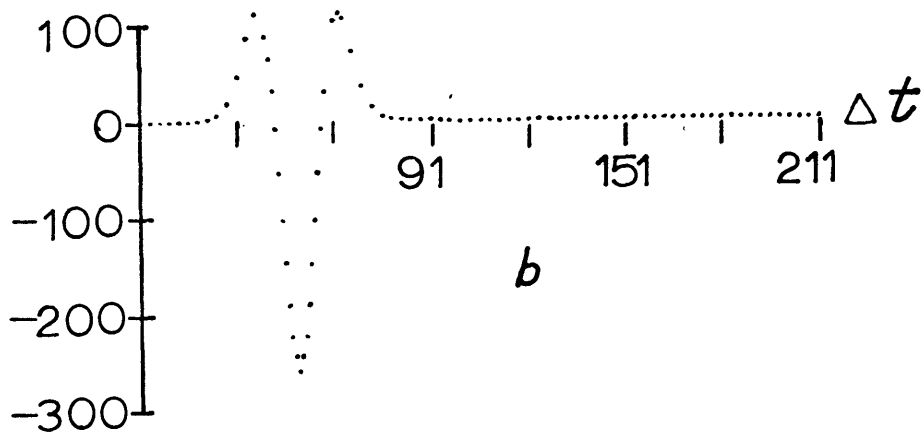
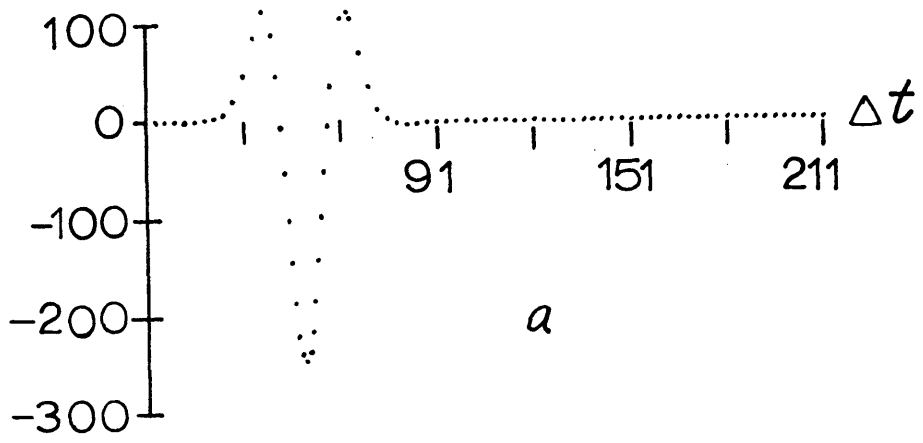


Figure 33. (a) Synthetic trace for shot point 1.
(b) Synthetic trace for shot point 2.
(c) Synthetic trace for shot point 3.

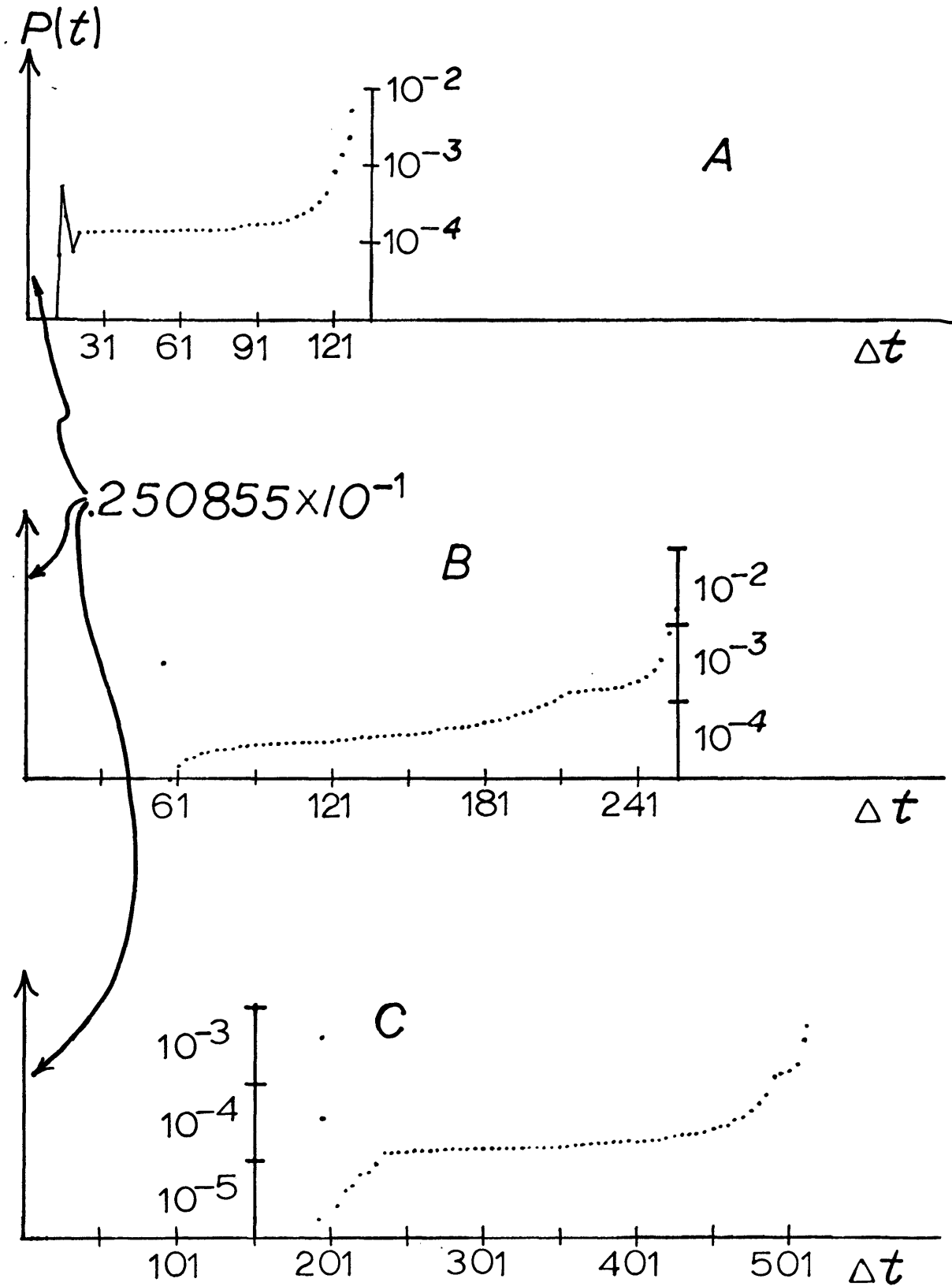


Figure 34. (a) Deconvolved trace for shot point 1.
 (b) Deconvolved trace for shot point 2.
 (c) Deconvolved trace for shot point 3.

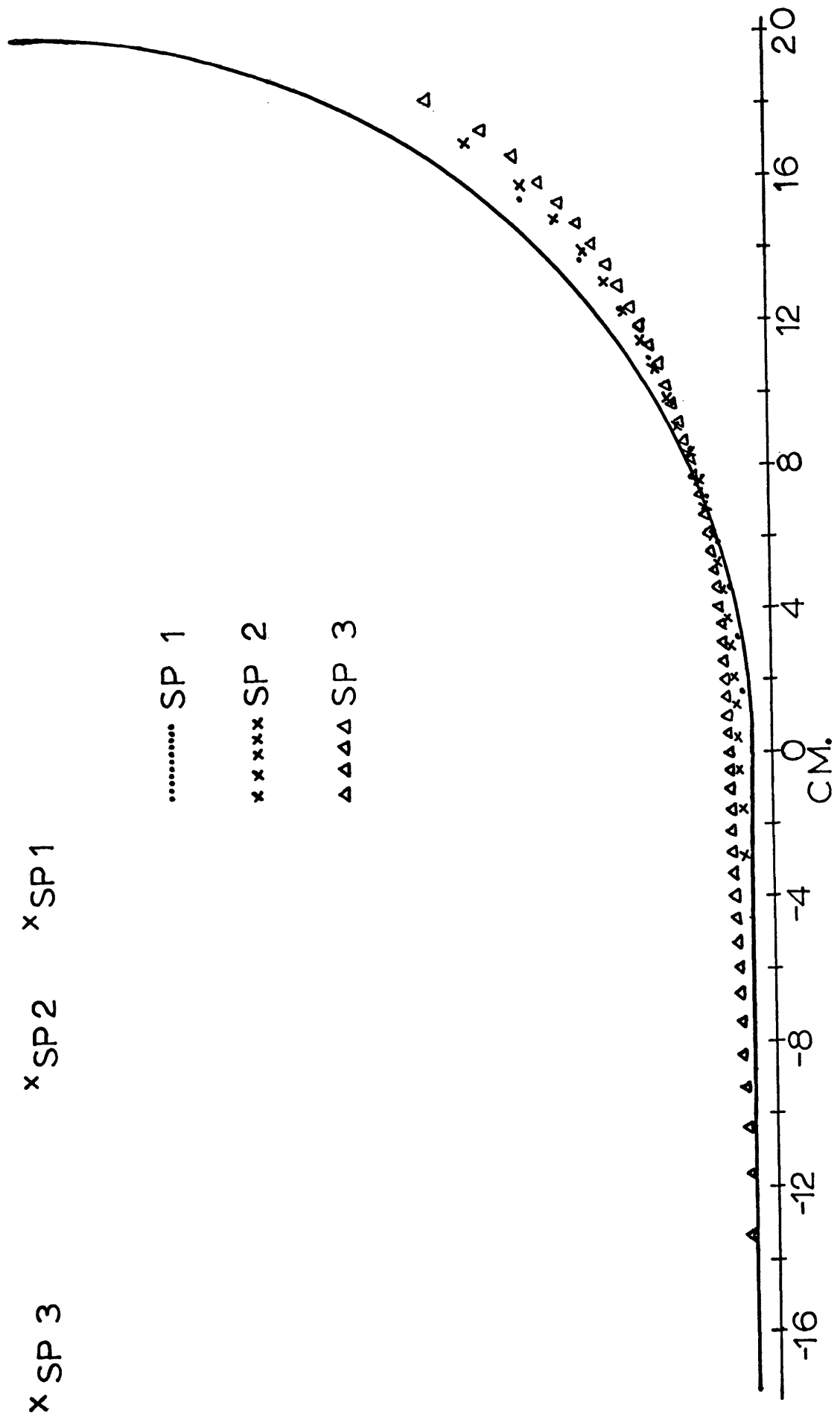


Figure 35. Inverse of model E.

COMPOSITION OF $P(t)$

As can be seen from the results of the previous section, the impulse response, $P(t)$, contains several features of merit. First, a leading impulse was encountered in all models as a result of the initial contact of the spherical wave with S . Secondly, for a non-planar surface, either a small positive or negative tail followed the impulse. Finally, sharp changes in the slope of S resulted in observable effects in the synthetic trace.

The weight of the initial pulse depends on the surface shape. The largest value was produced by the concave surface of model C with the smallest value observed for the convex surface of model B. The weight for the flat plane of model A fell between these two values. This indicates that the weight of the initial impulse provides some information about the surface shape in the vicinity of the first point of contact.

The sign of the tail is also an indication of the surface type: a positive tail for a concave surface and a negative tail for a convex surface. However, in all cases, the magnitude of the tail is small.

A surface with sharp corners will produce jump discontinuities in $\tan_R(\alpha(t_1))$. These jumps, after

proper weighting (equation 40), produce the observed diffraction arrivals in model D. The simple surface of Figure 36a was investigated to determine the response, $P(t)$, due to the sharp corners. The response $t^2P(t) =$

$$d/dt \int_{t_0}^{t/2} \frac{t_1 \tan_R \alpha(t_1) dt_1}{\sqrt{(t/2)^2 - t_1^2}} \quad \text{is shown in Figure 36b.}$$

At time \hat{t}_1 , the apparent slope $\tan_R \alpha(t_1)$ suddenly de-

creases. This results in the sharp negative jump in

$t^2P(t) \Big|_{t/2 = \hat{t}_1}$. Note also the exponential-like decay after the initial jump. Conversely, at time $t/2 = \hat{t}_2$,

the apparent slope suddenly increases resulting in a similar but positive jump, also with an associated decay-curve.

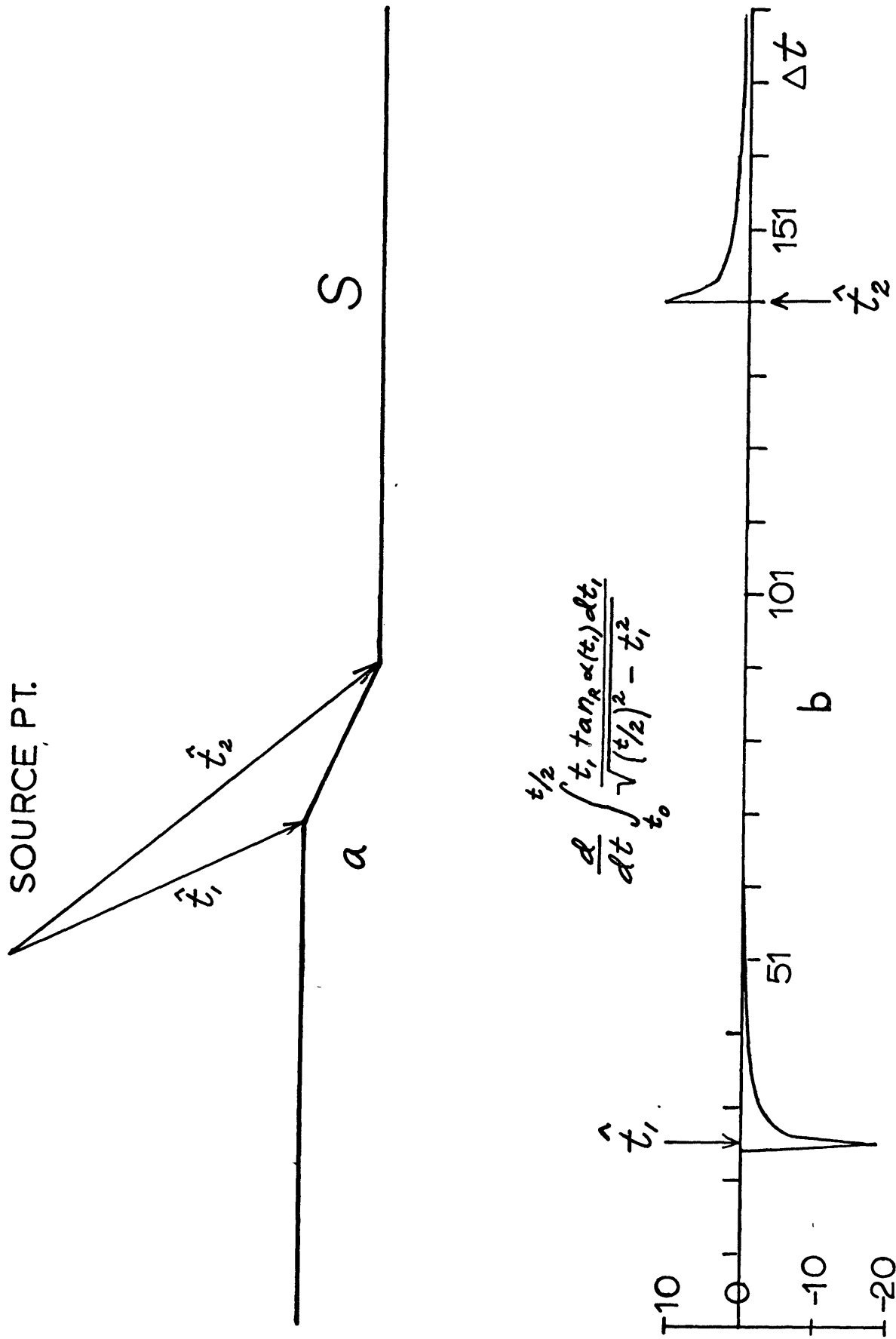


Figure 36. (a) Faulted surface. (b) Surface factor-- $t^2 P(t)$.

CONCLUSIONS

A single, consistent, and closed-form solution to the diffraction integral has been derived. Furthermore, any surface adhering to the assumptions made may be uniquely predicted from a single seismic trace.

The diffraction integral is put into a convolutional form where the shot pulse is convolved with an unknown surface factor. Cylindrical symmetry of the surfaces involved allows the surface factor to be expressed in terms of time. Surface dependence appears directly in the surface factor in the form of apparent slopes. Therefore, the effects of surface shape may be deduced from the form of the equation and the manner in which it operates on the apparent slopes. In the case of a flat plane, the surface factor reduces, as it should, to a delta function.

For smooth non-planar models the surface factor consists of an impulse followed by either a small negative or positive tail. The sign of the tail depends on whether the surface is convex or concave respectively. The magnitude of the initial impulse provides information on the surface curvature in the vicinity of the first point of contact. Kinky surfaces provide sharp jumps in the surface factor, the polarity of which depends on

whether the apparent slopes increase or decrease at the kink point. The jump is followed by an exponential-like decay. Both the initial pulse and the subsequent tail are used to predict the surface.

Attempts to apply the procedure of this study to seismic field data would be difficult. For example, an acoustic model represents the earth only approximately and features such as mode conversion, attenuation, anisotropy and variable velocity have been omitted. Moreover the tails of $P(t)$ are on the order of 60 db down from the impulse weight and would be difficult to detect.

Although the acoustic model of this study differs from the true earth, valuable insight may be gained from the reflection-diffraction process. Indeed, just the knowledge of their existence and surface-dependent form helps to complete the composition of a single trace and suggests additional processing techniques. For example, the weight of the initial impulse is a parameter which may be estimated from seismic data. Since this value depends on surface curvature, comparison with similar values of nearby traces could yield knowledge of curvature changes quite apart from the reflection times.

APPENDIX ADERIVATION OF THE FULL-SPACE GREEN'S FUNCTION

Green's function for a full-space may be derived by solving (Jackson, 1962)

$$\nabla^2 G(\vec{R}, t | \vec{R}', t') - \frac{1}{c^2} \frac{\partial^2 G(\vec{R}, t | \vec{R}', t')}{\partial t^2} = -4\pi \delta(\vec{R} - \vec{R}') \delta(t - t') \quad (\text{A1})$$

for G using a Fourier transform method. The delta functions may be represented with a Fourier integral as

$$-4\pi \delta(\vec{R} - \vec{R}') \delta(t - t') = \frac{-4\pi}{(2\pi)^4} \int_{-\infty}^{\infty} d^3k \int_{-\infty}^{\infty} d\omega e^{i\vec{k} \cdot (\vec{R} - \vec{R}')} e^{-i\omega(t - t')} \quad (\text{A2})$$

where $\vec{k} = k_x \vec{i} + k_y \vec{j} + k_z \vec{k}$. The sign of the time exponential has been reversed from its normal form. Likewise the unknown G can be written as a Fourier integral,

$$G(\vec{R}, t | \vec{R}', t') = \int_{-\infty}^{\infty} d^3k \int_{-\infty}^{\infty} d\omega g(\vec{k}, \omega) e^{i\vec{k} \cdot (\vec{R} - \vec{R}')} e^{-i\omega(t - t')} \quad (\text{A3})$$

where $g(\vec{k}, \omega)$ is also unknown and has the 2π -terms

incorporated. Performing the derivative indicated in (A1) on both sides of (A3) yields

$$\nabla^2 G - \frac{1}{c^2} \frac{\partial^2 G}{\partial t^2} = \int_{-\infty}^{\infty} d^3 k \int_{-\infty}^{\infty} d\omega g(\vec{k}, \omega) \left(\nabla^2 - \frac{1}{c^2} \frac{\partial^2}{\partial t^2} \right) \cdot \left[e^{i\vec{k} \cdot (\vec{R} - \vec{R}')} e^{-i\omega(t-t')} \right]$$

or, looking just at the x expression, we get

$$\frac{\partial^2}{\partial x^2} \left[e^{i\vec{k} \cdot (\vec{R} - \vec{R}')} \right] = i^2 k_x^2 = -k_x^2.$$

Similar terms evolve for y, z and t, yielding

$$\nabla^2 G - \frac{1}{c^2} \frac{\partial^2 G}{\partial t^2} = \int_{-\infty}^{\infty} d^3 k \int_{-\infty}^{\infty} d\omega g(\vec{k}, \omega) \left[-k^2 + \frac{\omega^2}{c^2} \right] e^{i\vec{k} \cdot (\vec{R} - \vec{R}')} e^{-i\omega(t-t')} \quad (A4)$$

Comparing (A4) with (A2), we get the following algebraic equation for $g(\vec{k}, \omega)$

$$\left(-k^2 + \frac{\omega^2}{c^2} \right) g(\vec{k}, \omega) = \frac{-4\pi}{(2\pi)^4}$$

or

$$g(\vec{k}, \omega) = \frac{-4\pi}{(2\pi)^4} \frac{1}{\left(-k^2 + \frac{\omega^2}{c^2} \right)} = \frac{1}{4\pi^3 \left(k^2 - \frac{\omega^2}{c^2} \right)} \quad (A5)$$

Substituting this result into (A3) yields

$$G(\vec{R}, t | \vec{R}', t') = \frac{1}{4\pi^3} \int_{-\infty}^{\infty} d^3 k \int_{-\infty}^{\infty} d\omega \left(\frac{1}{k^2 - \frac{\omega^2}{c^2}} \right) e^{i\vec{k} \cdot (\vec{R} - \vec{R}')} e^{-i\omega(t-t')} \quad (A6)$$

If we allow ω to be complex, $\omega = \alpha + i\beta$, then (A6) has two poles at $\omega = ck$ and $\omega = -ck$. Equation A6 may now be integrated using the residue theorem. The solution G will be the disturbance (wave) for a point source at $\vec{R} = \vec{R}'$ and at $t = t'$. We require that this wave be causal, i.e. $G = 0$ for $t < t'$ (no wave before the source excitation has begun) and G must be an outward traveling wave from the point \vec{R}' .

Since $\omega = \alpha + i\beta$, the exponential involving ω becomes

$$e^{-i\omega(t-t')} = e^{-i(\alpha+i\beta)(t-t')} = e^{-i\alpha(t-t')} e^{\beta(t-t')}$$

If $\beta < 0$, then since $t - t' > 0$, the last exponential will approach zero as $\rho \rightarrow \infty$ in Figure A1.

If we pick the closed path, C of Figure A1, the path of integration will go through the poles at $\omega = \pm ck$; consequently, both are displaced a small amount,

ϵ , in the negative β direction. Therefore, the ω -integration becomes

$$-c^2 \oint_C \frac{e^{-i\omega(t-t')}}{(\omega - ck - i\epsilon)(\omega + ck - i\epsilon)} = -c^2 2\pi i \sum \text{residues, or}$$

$\epsilon \rightarrow 0$

$$\begin{aligned}
 & -c^2 2\pi i \left\{ \lim_{\epsilon \rightarrow 0} \frac{(\omega - ck - i\epsilon) e^{-i\omega(t-t')}}{\omega \rightarrow ck (\omega - ck - i\epsilon)(\omega + ck - i\epsilon)} + \lim_{\epsilon \rightarrow 0} \frac{(\omega + ck - i\epsilon) e^{-i\omega(t-t')}}{\omega \rightarrow -ck (\omega - ck - i\epsilon)(\omega + ck - i\epsilon)} \right\} \\
 & = -2\pi i c^2 \left(\frac{e^{-ick(t-t')} - e^{ick(t-t')}}{2ck} \right) = \frac{2\pi c}{k} \sin ck(t-t').
 \end{aligned}$$

Substituting this result into (A6) yields

$$G(\vec{R}, t / \vec{R}', t') = \frac{2\pi c}{4\pi^3} \int_{-\infty}^{\infty} d^3 k \frac{\sin ck(t-t')}{k} e^{i\vec{k} \cdot (\vec{R} - \vec{R}')} \quad (\text{A7})$$

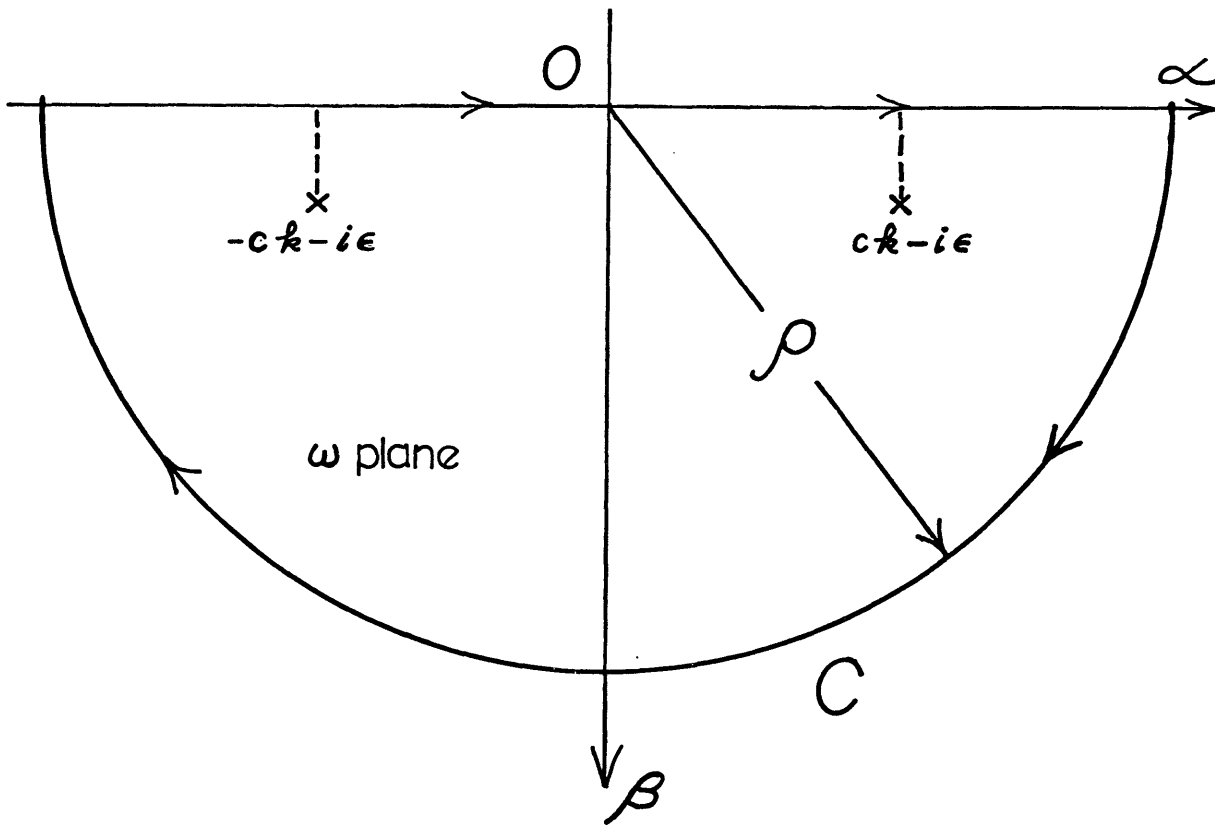


Figure A1. The complex path of integration.

and switching to spherical coordinates, where the polar axis is chosen along $(\vec{R} - \vec{R}')$ yields

$$= \frac{c}{2\pi^2} \int_0^\infty k^2 dk \int_0^\pi \sin\theta d\theta \int_0^{2\pi} d\varphi e^{ik|\vec{R}-\vec{R}'|\cos\theta} \frac{\sin ckt}{k}.$$

Integrating with respect to φ yields

$$= \frac{c}{\pi} \int_0^\infty k \sin ck(t-t') dk \int_0^\pi \sin\theta e^{ik|\vec{R}-\vec{R}'|\cos\theta} d\theta$$

and making the change of variables,

$$w = ik|\vec{R}-\vec{R}'|\cos\theta \text{ or, } dw = -ik|\vec{R}-\vec{R}'|\sin\theta d\theta$$

we get

$$\begin{aligned} G &= \frac{c}{\pi} \int_0^\infty k \sin ck(t-t') dk \int \frac{e^w dw}{-ik|\vec{R}-\vec{R}'|} \\ &= \frac{c}{\pi} \int_0^\infty k \sin ck(t-t') \left[\frac{e^{ik|\vec{R}-\vec{R}'|\cos\theta}}{-ik|\vec{R}-\vec{R}'|} \right] \Bigg|_{\theta=0}^{\theta=2\pi} \quad (\text{A8}) \end{aligned}$$

Evaluating the limits of this expression, we get

$$\begin{aligned} G &= \frac{2c}{\pi} \int_0^\infty \frac{\sin ck(t-t') \sin(k|\vec{R}-\vec{R}'|) dk}{|\vec{R}-\vec{R}'|} \\ &= \frac{2c}{\pi|\vec{R}-\vec{R}'|} \int_0^\infty \sin(ck(t-t')) \sin(k|\vec{R}-\vec{R}'|) dk. \quad (\text{A9}) \end{aligned}$$

Using the trigonometric identity,

$$\sin x \sin y = 1/2(\cos(x - y) - \cos(x + y)),$$

equation A9 becomes

$$G = \frac{c}{\pi |\vec{R} - \vec{R}'|} \int_0^{\infty} \left\{ \cos(c k(t-t') - k|\vec{R} - \vec{R}'|) - \cos(c k(t-t') + k|\vec{R} - \vec{R}'|) \right\} dk$$

or

$$G = \frac{c}{2\pi |\vec{R} - \vec{R}'|} \int_{-\infty}^{\infty} \left\{ e^{i k(c(t-t') - |\vec{R} - \vec{R}'|)} - e^{i k(c(t-t') + |\vec{R} - \vec{R}'|)} \right\} dk. \quad (\text{A10})$$

The limits have been extended in (A10) to $-\infty$, since cosine is an even function. The result is divided by two.

(A10) is the Fourier representation of a delta function, namely,

$$\delta(t) \triangleq \frac{1}{2\pi} \int_{-\infty}^{\infty} e^{i\omega t} d\omega$$

so (A10) becomes

$$G = \frac{c}{|\vec{R} - \vec{R}'|} \left[\delta(c(t-t') - |\vec{R} - \vec{R}'|) - \delta(c(t-t') + |\vec{R} - \vec{R}'|) \right].$$

The argument of the last delta function never vanishes, since $t > t'$. Hence,

$$G = \frac{c}{|\vec{R} - \vec{R}'|} \delta(c(t-t') - |\vec{R} - \vec{R}'|).$$

APPENDIX BDELTA FUNCTION RELATIONSHIPSCase I--Two One-Dimensional Delta Functions

Equation 21 in the text had the expression

$$\int_{t_0}^{t^*} \delta(c(\tau - t') - R) \delta(c(t - \tau) - R) d\tau \quad (\text{B1})$$

where $R = \sqrt{x^2 + y^2 + z^2}$. This expression will be evaluated. For this case we may consider R , t' and t as constants and defining $g(\tau; t') \triangleq c(\tau - t') - R$ and $h(\tau) \triangleq c(t - \tau) - R$ we rewrite (B1) as

$$\int_{-\infty}^{\infty} \delta(g(\tau; t')) \delta(h(\tau)) \varphi(\tau) d\tau$$

where $\varphi(\tau)$ is a testing function and the limits have been extended to infinity. Calling $u = h(\tau)$ we can make the change of variables,

$$\int_{-\infty}^{\infty} \frac{\delta(u) \delta(g(\tau; t'))}{|h'(\tau)|} du.$$

Assuming we can solve for the inverse function $\tau = w(u)$

we can rewrite the above as

$$\int_{-\infty}^{\infty} \frac{\delta(u) \delta(g(w(u); t'))}{|h'(w(u))|} du. \quad (\text{B2})$$

The first delta will have a value when $u = 0 = h(\tau)$.

Then,

$$\int_{-\infty}^{\infty} \frac{\delta(u) \delta(g(w(u); t')) du}{|h'(w(u))|} = \frac{\delta(g(w(0); t'))}{|h'(w(0))|}. \quad (B3)$$

If $\tau = w(u) \Big|_{u=0}$ has more than one root, this must be written as

$$\frac{\delta(g(w(0); t'))}{|h'(w(0))|} = \sum_i \frac{\delta(g(\tau_i; t'))}{|h'(\tau_i)|} \quad (B4)$$

where the τ_i are the locations of the roots of $\tau = w(u)$. If none of the $g(\tau_i; t') = 0$, then the entire expression (B3) is equal to zero. If at some of the τ_i 's, $g(\tau_i; t') = 0$; then B(3) condenses to the sum of $\delta(g(\tau_i; t')) / |h'(\tau_i)|$ at these points.

For the expression (B1) this procedure reduces to

$$\int_{\tau_0}^{\tau_1} \delta(c(\tau - t') - R) \delta(c(t - \tau) - R) d\tau = \frac{\delta(c(t - t') - 2R)}{c}.$$

Case II--Two-Dimensional Delta Functions

After a transformation of variables, equation 25 in the main text has the form

$$\int_{D_{sy}} \frac{\delta(c(t - t') - 2\sqrt{x^2(s) + y^2 + z^2(s)}) [x'(s)z(s) - x(s)z'(s)] ds dy}{[x^2(s) + y^2 + z^2(s)]^2}. \quad (B5)$$

This is an example of the general relation

$$\int_{D_{sy}} \delta(\alpha(s, y)) F(s, y) ds dy. \quad (B6)$$

Making the change of variables,

$$\left\{ \begin{array}{l} u = \alpha(s, y) = c(t-t') - 2\sqrt{x^2(s) + y^2 + z^2(s)} \\ v = \beta(s, y) = s \end{array} \right\}$$

and solving for the inverse functions (if possible)

$$y = y(u, v) = y(u, s)$$

$$s = s(u, v) = v$$

we can write (B6) as

$$\int_{D_{uv}} \delta(u) F(s(u, v), y(u, v)) |J| du dv = \int_{D_{uv}} \frac{\delta(u) F(s(u, v), y(u, v)) du dv}{|J^{-1}|} \quad (\text{B7})$$

where $J = \frac{\partial(s, y)}{\partial(u, v)}$ and $J^{-1} = \frac{\partial(u, v)}{\partial(s, y)}$

are the Jacobian and inverse Jacobian respectively.

Integrating the last expression with respect to u yields

$$\int_{D_{uv}} \frac{\delta(u) F(s(u, v), y(u, v)) du dv}{|J^{-1}|} = \int_{D_v} \frac{F(s(0, v), y(0, v)) dv}{|J^{-1}|_{\substack{s=s(0, v) \\ y=y(0, v)}}} ;$$

however, since $v = s$ we get

$$= \int_{D_s} \frac{F(s, y(s)) ds}{\left| \left\{ \alpha_s \beta_y - \alpha_y \beta_s \right\} \right|_{\substack{s=s \\ y=y(s)}}} \quad (\text{B8})$$

In equation B5 $\alpha(s, y) = c(t-t') - 2\sqrt{x^2(s) + y^2 + z^2(s)}$

so that

$$\alpha_s = \frac{-2(x(s)x'(s) + z(s)z'(s))}{\sqrt{x^2(s) + y^2 + z^2(s)}}, \beta_y = 0, \alpha_y = \frac{2y}{\sqrt{x^2(s) + y^2 + z^2(s)}}$$

and $\beta_s = 1$. Solving $\alpha(s, y) = 0$ for y as a function of s yields

$$y(s) = \pm \sqrt{\frac{c^2(t-t')^2}{4} - x^2(s) - z^2(s)}.$$

Substituting these specific expressions into (B8) yields

$$\oint_{C^*} \frac{[x'(s)z(s) - x(s)z'(s)] \sqrt{x^2(s) + \frac{c^2(t-t')^2}{4} - x^2(s) - z^2(s) + z^2(s)} ds}{\left[x^2(s) + \frac{c^2(t-t')^2}{4} - x^2(s) - z^2(s) + z^2(s) \right]^2 \sqrt{\frac{c^2(t-t')^2}{4} - x^2(s) - z^2(s)}}$$

$$= \frac{16}{c^3(t-t')^3} \int_{-S_L}^{S_R} \frac{[x'(s)z(s) - x(s)z'(s)] ds}{\sqrt{\frac{c^2(t-t')^2}{4} - x^2(s) - z^2(s)}}.$$

APPENDIX CPROOF OF THE π IDENTITY

The integral in equation 38 of the main text was said to be equal to π ; in the following appears the proof. Equation 38 is rewritten for convenience as

$$2 \int_{t/2}^{\hat{t}/2} \frac{t, dt,}{\sqrt{-(t,^4 - ((\hat{t}/2)^2 + (t/2)^2) t,^2 + (\hat{t}/2)^2 (t/2)^2}} = \pi. \quad (C1)$$

Making the transformation of variables, $u = t_1^2$, we get $du = 2t_1 dt_1$ and $t_1 dt_1 = \frac{du}{2}$. Also, the upper and lower limits become $u_L = t^2$ and $u_u = (t/2)^2$ respectively.

Consequently, equation C1 becomes

$$= \int_{(t/2)^2}^{(\hat{t}/2)^2} \frac{du}{\sqrt{-[u^2 - ((\hat{t}/2)^2 + (t/2)^2)u + (\hat{t}/2)^2 (t/2)^2]}} \quad (C2)$$

and completing the square of the quadratic in the denominator as follows

$$u^2 - \left(\left(\frac{\hat{t}}{2} \right)^2 + \left(\frac{t}{2} \right)^2 \right) u - \frac{\left[\left(\frac{\hat{t}}{2} \right)^2 + \left(\frac{t}{2} \right)^2 \right]^2}{4} + \frac{\left[\left(\frac{\hat{t}}{2} \right)^2 + \left(\frac{t}{2} \right)^2 \right]^2}{4} + \left(\frac{\hat{t}}{2} \right)^2 \left(\frac{t}{2} \right)^2$$

and factoring, this can be written as

$$\left[u - \frac{\left(\frac{\hat{t}}{2} \right)^2 + \left(\frac{t}{2} \right)^2}{2} \right]^2 - \frac{\left[\left(\frac{\hat{t}}{2} \right)^2 + \left(\frac{t}{2} \right)^2 \right]^2}{4} + \left(\frac{\hat{t}}{2} \right)^2 \left(\frac{t}{2} \right)^2.$$

Hence, (C2) becomes

$$= \int_{(t/z)^2}^{(\hat{t}/z)^2} \frac{du}{\sqrt{\left[u - \frac{(\hat{t}/z)^2 + (t/z)^2}{2} \right]^2 - \frac{\left[\frac{(\hat{t}/z)^2 + (t/z)^2}{2} \right]^2 + \left(\frac{\hat{t}}{z} \right)^2 \left(\frac{t}{z} \right)^2}}}. \quad (C3)$$

Expanding the last two terms of the denominator yields

$$\begin{aligned} - \frac{\left[\frac{(\hat{t}}{z})^2 + (t/z)^2 \right]^2}{4} + \left(\frac{\hat{t}}{z} \right)^2 \left(\frac{t}{z} \right)^2 &= - \frac{\left[\left(\frac{\hat{t}}{z} \right)^4 + 2 \left(\frac{\hat{t}}{z} \right) \left(\frac{t}{z} \right)^2 + \left(\frac{t}{z} \right)^4 \right]}{4} + \frac{4 \left(\frac{\hat{t}}{z} \right)^2 \left(\frac{t}{z} \right)^2}{4} \\ &= - \frac{\left(\frac{\hat{t}}{z} \right)^4 + 2 \left(\frac{\hat{t}}{z} \right)^2 \left(\frac{t}{z} \right)^2 + \left(\frac{t}{z} \right)^4}{4} + \frac{4 \left(\frac{\hat{t}}{z} \right)^2 \left(\frac{t}{z} \right)^2}{4} \\ &= - \frac{\left(\frac{\hat{t}}{z} \right)^4 + 2 \left(\frac{\hat{t}}{z} \right)^2 \left(\frac{t}{z} \right)^2 + \left(\frac{t}{z} \right)^4}{4} = - \frac{\left[\left(\frac{\hat{t}}{z} \right)^2 + \left(\frac{t}{z} \right)^2 \right]^2}{2} \end{aligned}$$

and

substitution into (C3) yields

$$\int_{(t/z)^2}^{(\hat{t}/z)^2} \frac{du}{\sqrt{\left[\frac{(\hat{t}/z)^2 - (t/z)^2}{2} \right]^2 - \left[u - \frac{(\hat{t}/z)^2 + (t/z)^2}{2} \right]^2}}}. \quad (C4)$$

Allowing $w = \left[u - \frac{(\hat{t}/z)^2 + (t/z)^2}{2} \right]$, then $dw = du$ with the

limits becoming $w_L = \frac{(t/z)^2 - (\hat{t}/z)^2}{2}$ and $w_U = \frac{(\hat{t}/z)^2 - (t/z)^2}{2}$.

Equation C4 becomes

$$\int_{-\frac{[(\hat{t}/2)^2 - (t/2)^2]}{2}}^{\frac{[(\hat{t}/2)^2 - (t/2)^2]}{2}} \frac{dW}{\sqrt{\left(\frac{(\hat{t}/2)^2 - (t/2)^2}{2}\right)^2 - W^2}} = \sin^{-1} \left(\frac{W}{\frac{[(\hat{t}/2)^2 - (t/2)^2]}{2}} \right) \Bigg|_{W = -\frac{[(\hat{t}/2)^2 - (t/2)^2]}{2}}^{W = \frac{[(\hat{t}/2)^2 - (t/2)^2]}{2}} \quad (C5)$$

After evaluating the limits, we get

$$= \sin^{-1} \left[\frac{(\hat{t}/2)^2 - (t/2)^2}{\frac{[(\hat{t}/2)^2 - (t/2)^2]}{2}} \right] - \sin^{-1} \left[\frac{-\frac{[(\hat{t}/2)^2 - (t/2)^2]}{2}}{\frac{[(\hat{t}/2)^2 - (t/2)^2]}{2}} \right] \quad (C6)$$

$$= \sin^{-1}(1) - \sin^{-1}(-1) = 2 \sin^{-1}(1) = \frac{2\pi}{2} = \pi.$$

Therefore, assertion C1 is proven.

Note that even with the upper limit as a variable, the integral is such that it is independent of this limit.

Hence, we can write

$$2 \int_{t/2}^{\hat{t}/2} \frac{t, dt,}{\sqrt{-\left[t^4 - \left(\left(\frac{\hat{t}}{2}\right)^2 + \left(\frac{t}{2}\right)^2\right)t^2 + \left(\frac{\hat{t}}{2}\right)^2 \left(\frac{t}{2}\right)^2\right]}} = \pi \int (\hat{t}/2 - t/2).$$

APPENDIX DDERIVATION OF HILTERMAN'S DIFFRACTION ALGORITHM

Using the same nomenclature as the text and starting with equation 20, rewritten below,

$$S(t) = \frac{-c^2}{2\pi} \int_{\bar{z}_0}^{z_+} d\tau \left\{ \int_S \left\{ \frac{f(\tau') \delta(c(\tau' - t) - R)}{R} d\tau' \right\} \left\{ \delta(c(t - \tau) - R) \frac{\partial(R)}{\partial n'} + \frac{1}{R} \frac{\partial \delta(c(t - \tau) - R)}{\partial n'} \right\} dS \right\} \quad (D1)$$

we will derive Hilterman's algorithm (1970) since it was used to compute synthetic traces. Performing the τ' -integration and expanding the last term yields

$$S(t) = \frac{1}{2\pi} \int_{\bar{z}_0}^{z_+} d\tau \int_S \left\{ -f(\tau' - R/c) \frac{\partial \delta(c(t - \tau) - R/c)}{\partial n'} + \frac{f(\tau' - R/c) \delta((t - \tau) - R/c) \partial R}{R^3 \partial n'} \right\} dS. \quad (D2)$$

However,

$$\frac{\partial \delta((t - \tau) - R/c)}{\partial n'} = \frac{\partial \delta((t - \tau) - R/c)}{\partial((t - \tau) - R/c)} \frac{\partial((t - \tau) - R/c)}{\partial n'} = -\frac{\delta'((t - \tau) - R/c) \partial R}{c \partial n'} ;$$

hence, (D2) can be written as

$$S(t) = \frac{1}{2\pi} \int_{\bar{z}_0}^{z_+} d\tau \int_S \left\{ \frac{f(\tau' - R/c) \delta'((t - \tau) - R/c) \partial R}{c R^2 \partial n'} + \frac{f(\tau' - R/c) \delta((t - \tau) - R/c) \partial R}{R^3 \partial n'} \right\} dS. \quad (D3)$$

Allowing $\tau' = \tau$, because the arrival time at S equals the departure time, and switching integrations,

(D3) becomes

$$S(t) = \frac{1}{2\pi} \int_S \frac{1}{cR^2} \frac{\partial R}{\partial n'} dS \int_{\tau_0}^{\tau_+} f(\tau - R/c) \delta'((t-\tau) - R/c) d\tau$$

$$+ \frac{1}{2\pi} \int_S \frac{1}{R^3} \frac{\partial R}{\partial n'} dS \int_{\tau_0}^{\tau_+} f(\tau - R/c) \delta((t-\tau) - R/c) d\tau. \quad (D4)$$

Using

$$\frac{\partial \delta((t-\tau) - R/c)}{\partial t} = \frac{\partial \delta((t-\tau) - R/c)}{\partial ((t-\tau) - R/c)} \frac{\partial ((t-\tau) - R/c)}{\partial t} = \delta'((t-\tau) - R/c)$$

in (D4), we get

$$S(t) = \frac{1}{2\pi} \int_S \frac{1}{cR^2} \frac{\partial R}{\partial n'} dS \left\{ \frac{\partial}{\partial t} \int_{\tau_0}^{\tau_+} f(\tau - R/c) \delta((t-\tau) - R/c) d\tau \right\}$$

$$+ \frac{1}{2\pi} \int_S \frac{1}{R^3} \frac{\partial R}{\partial n'} dS \int_{\tau_0}^{\tau_+} f(\tau - R/c) \delta((t-\tau) - R/c) d\tau \quad (D5)$$

or

$$S(t) = \frac{1}{2\pi} \int_S \frac{1}{R^2} \frac{\partial R}{\partial n'} \left\{ \frac{f'(t - 2R/c)}{c} + \frac{f(t - 2R/c)}{R} \right\} dS. \quad (D6)$$

Equation D6 is the central expression used by Hilterman (1970) to compute synthetic seismograms. Since $d\Omega = 1/R^2 \frac{\partial R}{\partial n'} dS =$ differential solid angle, (D6) may be rewritten as

$$S(t) = \frac{1}{2\pi} \int_{\Omega(S)} \left\{ t f'(t - 2R/c) + f(t - 2R/c) \right\} \frac{d\Omega}{R}. \quad (D7)$$

Knowing the shape and location of S, one can compute the differential solid angle subtended by the expanding the wavefront as it intersects S. Each value of R will have one differential solid angle associated with it. Consequently, (D7) may be written as a convolution

$$S(t) = \frac{1}{2\pi} \left\{ f(t) + t f'(t) \right\} * d\Omega' \quad (D8)$$

where $d\Omega' = d\Omega/R$.

This was the formulation used to compute the synthetic traces of this study. To determine the deconvolved trace directly, $f(t) = \delta(t)$ and $f'(t) = \delta'(t)$ were used as input functions. The R's were incremented in units of $\Delta R = c\Delta t/2$, and f and f' were sampled in units of Δt . $d\Omega$ was incremented at half the Δt interval because the one-way time necessary to reach a

particular ring was doubled upon its return trip. Hence, an incremented time of $\Delta t/2$ between rings becomes a total total time delay of Δt upon its arrival at the observation point.

(D8) may be written in a discrete form as

$$S(2t_0 + (m+1)\Delta t) \cong \frac{1}{2\pi} \sum_{k=L}^m \Delta\Omega'(k) \left[f(m-k) + t_k f'(m-k) \right] \quad (D9)$$

where $m = 0, 1, 2, \dots$; and with N the number of samples of f and f' , the lower limit L becomes

$$\left\{ \begin{array}{l} k = 0 \quad m < N \\ k = m - N, \quad m > N \end{array} \right\}.$$

BIBLIOGRAPHY

- Carpenter, W. T., Wozny, M. J., and Goodson, R. E., 1971, Distributed parameter identification using the method of characteristics: *Journal of Dynamic Systems, Measurement, and Control*, v. 93, p. 73-78.
- Collins, R. L., and Khatri, H. C., 1969, Identification of distributed parameter systems using finite differences: *Journal of Basic Engineering*, v. 91, p. 239-245.
- Duff, G. F. D., and Naylor, D., 1966, *Differential equations of applied mathematics*: New York, John Wiley and Sons, 423 p.
- Fontanel, A., and Grau, G., 1969, Application of impulse seismic holography: 39'th Annual International Meeting of the Society of Exploration Geophysics, Calgary, Alberta.
- Good, R. H., and Nelson, T. J., 1971, *Classical theory of electric and magnetic fields*: New York, Academic Press, 637 p.
- Goodman, J. W., 1969, *Introduction to Fourier optics*: New York, McGraw-Hill, 287 p.
- Hamming, R. W., 1962, *Numerical methods for scientists and engineers*: New York, McGraw-Hill, 411 p.
- Hilterman, F. J., 1970, Three-dimensional seismic modeling: Colorado School of Mines Ph.D. Thesis, 93 p.
- Hilterman, F. J., 1970, Three-dimensional seismic modeling: *Geophysics*, v. 35, no. 6, p. 1020-1037.
- Jackson, J. D., 1962, *Classical electrodynamics*: New York, John Wiley and Sons, 641 p.
- Kaplan, W., 1952, *Advanced calculus*: Reading, Mass., Addison-Wesley, 679 p.
- Kopal, Z., 1961, *Numerical analysis*: New York, John Wiley and Sons, 594 p.

- Morse, P. M., and Feshbach, H., 1953, Methods of theoretical physics, Vol. 1: New York, McGraw-Hill, 997 p.
- Papoulis, A., 1968, Systems and transforms with applications in optics: New York, McGraw-Hill, 474 p.
- Perdreauville, F. J., and Goodson, R. E., 1966, Identification of systems described by partial differential equations: Journal of Basic Engineering, v. 88, p. 463-468.
- Peterson, R. A., 1969, Seismography 1970: the writing of the earth waves: United Geophysical Company.
- Ralston, A., 1965, A first course in numerical analysis: New York, McGraw-Hill, 578 p.
- Ralston, A., and Wilf, H. S., 1967, Mathematical methods for digital computers, Vol. 2: New York, John Wiley and Sons, 287 p.
- Roy, A., 1962, Ambiguity in geophysical interpretation: Geophysics, v. 27, no. 1, p. 90-99.
- Schneider, W. A., 1971, Developments in seismic data processing and analysis (1968-1970): Geophysics, v. 36, no. 6, p. 1043-1073.
- Seinfeld, J. H., and Chen, W. H., 1971, Estimation of parameters in partial differential equations from noisy experimental data: Chemical Engineering Science, v. 26, p. 753-766.
- Stark, P. A., 1970, Introduction to numerical methods: London, Macmillan, 334 p.
- Trorey, A. W., 1970, A simple theory for seismic diffraction: Geophysics, v. 35, no. 5, p. 762-784.